AD-A053 254 PENNSYLVANIA STATE UNIV UNIVERSITY PARK APPLIED RESE--ETC F/G 20/4
PREDICTION OF BODY TEMPERATURE DISTRIBUTION, LAMINAR SEPARATION--ETC(U)
FEB 78 J J EISENHUTH N00017-73-C-1418
UNCLASSIFIED TM-78-39 NL

| OF |
AD
A053254

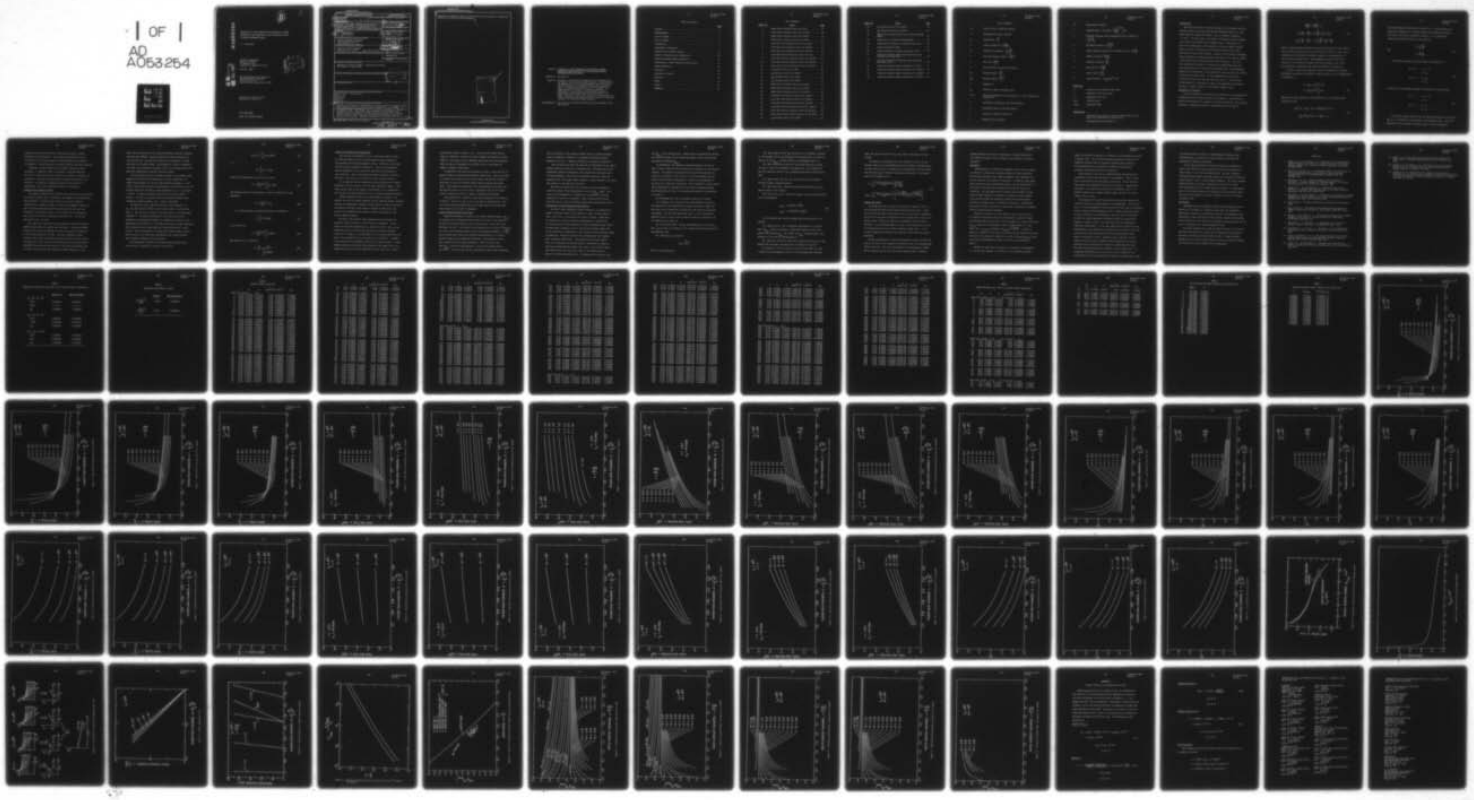

END
DATE
FILMED
6-78
DDC

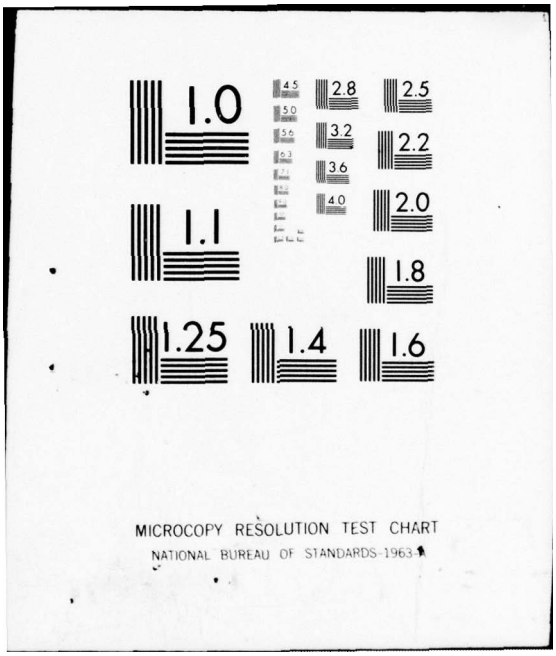
1.0
1.1
1.25
1.4
1.6
1.8
2.0
2.2
2.5
2.8
3.2
3.6
4.0
4.5
5.0
5.6
6.3
MICROCOPY RESOLUTION TEST CHART
NATIONAL BUREAU OF STANDARDS-1963-A

PREDICTION OF BODY TEMPERATURE DISTRIBUTION, LAMINAR SEPARATION, AND TRANSITION IN THE PRELIMINARY DESIGN OF HEATED UNDERWATER BODIES

J. J. Eisenhuth

Technical Memorandum
File No. TM 78-39
22 February 1978
Contract No. N00017-73-C-1418

Copy No. 23

The Pennsylvania State University
APPLIED RESEARCH LABORATORY
Post Office Box 30
State College, Pennsylvania 16801

NAVY DEPARTMENT

NAVAL SEA SYSTEMS COMMAND

UNCLASSIFIED

SECURITY CLASSIFICATION OF THIS PAGE *(When Data Entered)*

REPORT DOCUMENTATION PAGE

READ INSTRUCTIONS BEFORE COMPLETING FORM

1. REPORT NUMBER: TM-78-39	2. GOVT ACCESSION NO.
3. RECIPIENT'S CATALOG NUMBER	
4. TITLE *(and Subtitle)*: PREDICTION OF BODY TEMPERATURE DISTRIBUTION, LAMINAR SEPARATION, AND TRANSITION IN THE PRELIMINARY DESIGN OF HEATED UNDERWATER BODIES.	5. TYPE OF REPORT & PERIOD COVERED: Technical Memorandum
	6. PERFORMING ORG. REPORT NUMBER
7. AUTHOR(s): J. J. Eisenhuth	8. CONTRACT OR GRANT NUMBER(s): N00017-73-C-1418
9. PERFORMING ORGANIZATION NAME AND ADDRESS: APPLIED RESEARCH LABORATORY, Post Office Box 30, State College, PA 16801	10. PROGRAM ELEMENT, PROJECT, TASK AREA & WORK UNIT NUMBERS: 79p.
11. CONTROLLING OFFICE NAME AND ADDRESS: Naval Sea Systems Command, Washington, DC 20362 Codes 031 and 035	12. REPORT DATE: 22 Feb 1978
	13. NUMBER OF PAGES: 76
14. MONITORING AGENCY NAME & ADDRESS *(if different from Controlling Office)*	15. SECURITY CLASS. *(of this report)*: UNCLASSIFIED
	15a. DECLASSIFICATION/DOWNGRADING SCHEDULE

16. DISTRIBUTION STATEMENT *(of this Report)*

Approved for public release. Distribution unlimited.
Per NAVSEA - 11 April 1978.

17. DISTRIBUTION STATEMENT *(of the abstract entered in Block 20, if different from Report)*

18. SUPPLEMENTARY NOTES

19. KEY WORDS *(Continue on reverse side if necessary and identify by block number)*

boundary layer
laminar flow
heated body
separation
transition
hydrodynamics

20. ABSTRACT *(Continue on reverse side if necessary and identify by block number)*

Because of the interest in predicting the characteristics of laminar, heated, water boundary layers, an existing code was adapted for use on ~~The~~ an ~~Pennsylvania State University's~~ IBM 370 computer and extended to include the axisymmetric case. The similar type solutions of the boundary layer equations made it possible to perform a parametric study and to use the results in developing a means for specifying a stabilizing temperature distribution on a body. Additional studies into the effect of → next page

DD FORM 1 JAN 73 1473 EDITION OF 1 NOV 65 IS OBSOLETE

UNCLASSIFIED

SECURITY CLASSIFICATION OF THIS PAGE *(When Data Entered)*

391 007

temperature on laminar separation and transition have resulted in simplified criteria for predicting these phenomena.

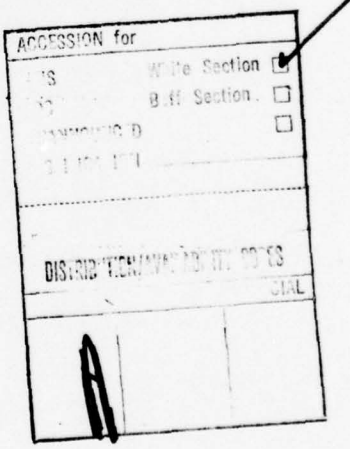

Subject: Prediction of Body Temperature Distribution, Laminar Separation, and Transition in the Preliminary Design of Heated Underwater Bodies

References: See page 22.

Abstract: Because of the interest in predicting the characteristics of laminar, heated, water boundary layers, an existing code was adapted for use on The Pennsylvania State University's IBM 370 computer and extended to include the axisymmetric case. The similar type solutions of the boundary layer equations made it possible to perform a parametric study and to use the results in developing a means for specifying a stabilizing temperature distribution on a body. Additional studies into the effect of temperature on laminar separation and transition have resulted in simplified criteria for predicting these phenomena.

Acknowledgment: This work was sponsored by Naval Sea Systems Command, Codes 031 and 035.

Table of Contents

List of Figures

List of Symbols

C_p	specific heat at constant pressure
f	nondimensional stream function
H	shape factor = $\frac{\delta^*}{\theta}$
k	thermal conductivity, $\frac{\text{watts}}{\text{ft } ^\circ\text{R}}$
M	Falkner-Skan parameter = $\frac{x}{U_e}\frac{dU_e}{dx}$
P	free-steam Prandtl number = $\frac{C_{p_\infty}\,\mu_\infty}{k_\infty}$
q	heat flux, $\frac{\text{watts}}{\text{ft}^2}$
r	section radius for body of revolution
R_x	Reynolds number = $\frac{U_e x}{\nu_\infty}$
R_{δ^*}	Reynolds number = $\frac{U_e\,\delta^*}{\nu_\infty}$
T	temperature
U_e	velocity at edge of boundary layer
u,v,w	velocity components in the orthogonal x, y, and z directions, respectively
x	curvilinear coordinate in the flow direction
y	coordinate normal to the body surface
z	transverse coordinate direction
δ	boundary layer thickness

δ^* displacement thickness

η nondimensional y coordinate = $\left(\frac{U_e}{\nu_\infty x}\right)^{1/2} \int_o^y \bar{\rho} dy$

θ momentum thickness; also nondimensional mean temperature $= \frac{T - T_\infty}{T_\delta - T_\infty}$

Λ Pohlhausen parameter = $\frac{\delta^2}{\nu_\infty} \frac{dU_e}{dx}$

λ radius gradient parameter for axisymmetric flow = $\frac{2x}{r} \frac{dr}{dx}$

μ dynamic viscosity, $\frac{\text{lb sec}}{\text{ft}^2}$

ν kinematic viscosity, $\frac{\text{ft}^2}{\text{sec}}$

ρ mass density in $\frac{\text{slugs}}{\text{ft}^3}$

τ shear stress in $\frac{\text{lb}}{\text{ft}^2}$

ψ stream function = $(\rho_\infty \mu_\infty x U_e)^{1/2} f(\eta)$

Subscripts

e evaluated at the boundary layer edge

∞ evaluated in the free stream

w evaluated at the wall

crit critical value

trans transition value

Superscripts

$\bar{}$ normalized with respect to the free-stream value; in the case of $\bar{u}$, normalized with respect to U_e

' differentiation with respect to η

Introduction

Effective calculation of laminar boundary layer properties has been possible either by the approximate Karman-Pohlhausen method or by more exact numerical integration methods. See, for example, References 1, 2 and 3. In recent years, this kind of calculation has been extended to the case of the heated, water boundary layer. In Reference 4, as part of the computations of the stability of heated, laminar boundary layers in water, the solution of the mean-flow equations was coded and specific results were presented. Because of the interest in applying these predictions to design techniques, this part of the code was adapted to The Pennsylvania State University's IBM 370 computer. The code, as it appeared in Reference 4, treated the two-dimensional flow case and therefore had to be altered for axisymmetric flow. This memorandum summarizes the development of the altered code and the results of calculations using the code to date. It also summarizes some of the uses to which the output data from the code have been put. This includes the development of a procedure to predict the temperature distribution necessary to insure stability of the laminar boundary layer.

Development of Equations

The basic boundary layer equations were derived for an incompressible, axisymmetric flow with heat addition at the boundary. Such effects as buoyancy and dissipation of energy by friction were ignored. The resulting equations, including an equation of energy balance are as follows:

$$\frac{\partial(\rho r u)}{\partial x} + \frac{\partial(\rho r v)}{\partial y} = 0$$

$$\rho\left(u \frac{\partial u}{\partial x} + v \frac{\partial u}{\partial y}\right) = \rho U_e \frac{dU_e}{dx} + \frac{\partial}{\partial y}\left(\mu \frac{\partial u}{\partial y}\right) \tag{1}$$

$$\rho C_p\left(u \frac{\partial T}{\partial x} + v \frac{\partial T}{\partial y}\right) = -\rho u U_e \frac{dU_e}{dx} + \frac{\partial}{\partial y}\left(k \frac{\partial T}{\partial y}\right) \quad .$$

There is another momentum equation in the z direction which is not coupled with the above and, of course, in the y direction, $\partial p/\partial y = 0$. The x and y coordinates are curvilinear coordinates tangent to and perpendicular to the body surface respectively. The axisymmetric nature of the flow is reflected in the continuity equation with the inclusion of the r term. This represents a departure from Lowell and Reshotko in Reference 4.

In order to solve these equations, they are transformed to ordinary differential equations by defining a stream function, ψ, and a nondimensional y coordinate, η.

$$\psi = (\rho_\infty \mu_\infty \times U_e)^{1/2} f(\eta)$$

$$\eta = (U_e/\nu_\infty x)^{1/2} \int_0^y \bar{\rho}\, dy \quad . \tag{2}$$

Making use of these definitions and Equations (1), the following final equations result:

$$(\bar{\rho}\,\bar{\mu}\, f'')' + M\left(\frac{1}{\bar{\rho}} - f'^2\right) + \left(\frac{M + \lambda + 1}{2}\right) ff'' = 0$$

$$\bar{P}\bar{C}_p \left(\frac{M + \lambda + 1}{2}\right) f\theta' + (\overline{\rho k}\theta')' = 0 \quad . \tag{3}$$

The primes indicate derivatives with respect to η. These equations are explicitly independent of x and the velocity and temperature profiles that result are given by similarity solutions. θ is a normalized temperature difference and M and λ are given by:

$$M = \frac{x}{U_e}\frac{dU_e}{dx}$$

and (4)

$$\lambda = \frac{2x}{r}\frac{dr}{dx} \quad .$$

The following boundary conditions apply for Equations (1):

$$\begin{aligned} &\text{at } y = 0 && u = v = 0 \\ & && T = T_w \\ &\text{as } y \to \infty && u \to U_e \\ & && T \to T_\infty \quad . \end{aligned} \tag{5}$$

In terms of the transformed variables in Equations (3), these become:

$$\begin{aligned} &\text{at } \eta = 0 && f' = f = 0 \\ & && \theta = 1 \\ &\text{as } \eta \to \infty && f' \to 1 \\ & && \theta \to 0 \quad . \end{aligned} \tag{6}$$

The solution process requires that the physical properties of the water (C_p, ρ, μ, k) be known at each location in the boundary layer. Since the temperature varies through the boundary layer, so will the physical

properties and one must know their values and the values of their derivatives with temperature. The formulas (from Reference 4) for the variation of the water properties with temperature are presented in Appendix A. The derivatives are obtained directly from these equations.

Equations (3) are nonlinear and are coupled through the fluid properties. In addition, there are problems of initial conditions (f'' and θ' at the wall) and of the value of η at which to terminate the integration. The method of Nachtscheim and Swigert (Reference 5) was adopted for the numerical integration process and was found to be satisfactory. All this is discussed in detail in Reference 4.

Boundary Layer Computer Program

The computer program for the boundary layer calculations was extracted from the more general code of Reference 4 and adapted to the University's IBM 370 computer. Besides being altered to account for computer idiosyncracies, changes were made to include the axisymmetric body case and to calculate additional boundary layer quantities that were not available in the original program. The inclusion of the axisymmetric case results in the term λ appearing in Equations (3). For the two-dimensional case, λ is zero.

The total code consists of a Main program and a Mean-Flow Equation (MFEQN) program plus three additional subroutines. The Main and MFEQN programs could have been combined, but were left separate in deference to the original makeup of the code. The code originally included stability calculations and the Main program was used to control overall execution and as such, was used in conjunction with eleven subroutines. The MFEQN routine controls the solution of the mean-flow equations and to do this calls upon the DIFF, TEMVAR, and ADAMS subroutines. The

DIFF routine evaluates the first order differential mean-flow equations and calls upon TEMVAR to evaluate required mean-flow properties and their derivatives. The mean-flow equations are integrated in double precision by the ADAMS routine. The integration routine is designed to use single step Runge-Kutta procedures alone or in combination with the multi-step Adams-Moulton predictor-corrector scheme.

The key quantities that are needed as inputs to the boundary layer program are the free-stream temperature, the wall temperature, the Falkner-Skan parameter, M, and the radius gradient parameter, λ. The M and λ values could have been input directly or been calculated from the provided quantities that make up these parameters (i.e., x, U_e, dU_e/dx, r, dr/dx). The latter quantities were the ones that were used in practice. By their use, actual values of the various boundary layer thicknesses, Reynolds numbers, etc., could be calculated.

The important output quantities include a term referred to as η_{δ^*}, the shape factor, $H=\delta^*/\theta$, the wall shear stress, τ, and the heat flux, q. The term η_{δ^*} is derived in the evaluation of the displacement thickness δ^*. It should be mentioned at this time that both the displacement and momentum thicknesses are defined in the sense of two-dimensional flow definitions. This leads eventually to slight differences when comparing with the same quantities defined differently in other sources. Little difference in the shape factor should result, however, when the point on the body under consideration has a small boundary layer thickness compared to the body radius.

The displacement thickness for the heated water boundary layer is here used to represent the decrease in mass flow:

$$\rho_\infty U_e \delta^* = \int_0^\infty (\rho_\infty U_e - \rho u)dy \tag{7}$$

or

$$\delta^* = \int_0^\infty (1 - \bar{\rho}\,\bar{u})dy \quad . \tag{8}$$

This can be transformed in terms of $d\eta$, so that

$$\delta^* = \left(\frac{\nu_\infty x}{U_e}\right)^{1/2} \int_0^\infty \left(\frac{1}{\bar{\rho}} - \bar{u}\right)d\eta \quad . \tag{9}$$

The integral portion of this equation is what is referred to as η_{δ^*}. Therefore,

$$\delta^* = \left(\frac{\nu_\infty x}{U_e}\right)^{1/2} \eta_{\delta^*} \quad . \tag{10}$$

In a similar manner, the momentum thickness is defined as

$$\theta = \int_0^\infty \bar{\rho}\,\bar{u}\,(1-\bar{u})dy \quad , \tag{11}$$

or in terms of $d\eta$

$$\theta = \left(\frac{\nu_\infty x}{U_e}\right)^{1/2} \int_0^\infty \bar{u}(1-\bar{u})d\eta \quad . \tag{12}$$

The shape factor is, therefore:

$$H = \frac{\delta^*}{\theta} = \frac{\eta_{\delta^*}}{\int_0^\infty \bar{u}(1-\bar{u})d\eta} \quad . \tag{13}$$

Results of Boundary Layer Computations

The code was used primarily to run a sufficient number of cases of varied parameters so that one could generate design information and procedures for heated axisymmetric bodies. Checks were first made with the results presented in Reference 4. Much of the information shown in Reference 4 is in the form of plots which are difficult to read accurately. Some of the quantities which are listed in tables in Reference 4 and which can be compared are those listed in Table 1.

It is apparent that the comparisons are quite good and the largest difference is of the order of 2 in the sixth significant figure. Since these are key terms in the scheme of calculations, it is assumed that all the other calculated quantities are of a similar comparative accuracy.

Another comparison (Table 2) is made between the results of the unheated case with no pressure gradient and the classical Blasius solution. Although the displacement thickness results appear to check very closely, the momentum thickness results appear to differ by about 0.5%. The results were considered close enough to verify the operation of the present computer program.

The bulk of the boundary layer computations were performed as a parametric study in which M, λ, and ΔT were the parameters. In all cases the free-stream temperature, T_∞, was kept at 60°F. Also, so that comparative values of shear stress and heat flux could be obtained, a value of arc length, x, was made equal to 4 ft and the velocity at the edge of the boundary layer, U_e, was chosen to be 50 ft/sec. A summary of the results of this parameter study is to be found in Table 3. Other computed quantities could have been included in this table, but it was thought that these are the more important ones for later use. Plots of

these data are shown in Figures 1-15. As can be seen, within certain ranges of parameters, the data are fairly abundant and amenable to interpolation. The ranges in which seemingly sparse data exist were generally found to show up infrequently in practical cases or were beyond the computer program's capabilities.

An additional side study was performed in order to learn some of the general effects of having elevated ambient temperatures. This is the kind of situation that would occur in a water tunnel test where an attempt is being made to extend the Reynolds number range by heating the tunnel water. This study was performed for the two-dimensional case (λ=0) only. The implication here is that at least a qualitative idea of the effect could be learned and serve as a guide in designing an experiment.

Data generated for a number of free-stream temperatures is presented in Table 4. Plots of H, η_{δ}*, q, and τ are shown in Figures 16-27. Data for a 60°F free-stream temperature are included again in this table and these figures for the sake of comparison.

Critical Reynolds Number Correlation

Stability information in terms of the critical Reynolds number, $R_{\delta^*_{crit}}$, is available for two-dimensional flow both for the case of the unheated boundary with pressure gradient and for the flow over a flat plate with heating at the wall. The results of the unheated case are found in Reference 6 as the critical Reynolds number versus the Pohlhausen parameter $\Lambda = \frac{\delta}{\nu}\frac{dU_e}{dx}$, and the heated case results were obtained from Reference 4 as critical Reynolds number versus temperature difference. The parameter Λ and ΔT were translated into the shape parameter $H = \delta^*/\theta$ so that in each case $R_{\delta^*_{crit}}$ could be plotted against H. The curves in Figure 28 are the result. It can be seen that the correlation is quite good, indicating

that the stability of the laminar boundary layer is strongly dependent upon H, regardless of whether it is obtained by favorable pressure gradient or by heat. A similar correlation is reported in Reference 7.

This correlation provides the basis for the development of the type of design information which will be presented here. Although based on two-dimensional stability information, the correlation is considered valid for the axisymmetric case because the stability equations, under the assumption that the boundary layer thickness is small compared to the local body radius, are the same for both cases.

The curve in Figure 28 for the variation in pressure gradient is repeated in Figure 29 and extrapolated in the low $R_{\delta^*_{crit}}$ range. This curve is used subsequently to represent the variation of H with R_{δ^*} regardless of how the H is obtained. Table 5 gives specific values from this curve for ease in effecting computations involving this curve.

Determination of Body Temperature Distribution

In order to make preliminary design estimates of the temperatures needed to maintain stable flow at points on a body, the data shown in Table 3 were used in conjunction with certain criteria. Essentially two criteria were chosen to insure the maintenance of laminar flow: (1) the provision of just enough heat to keep the Reynolds number (based on displacement thickness) equal to the critical Reynolds number and, (2) the provision of enough heat so that the peak critical Reynolds number is maintained. These are referred to as "minimum heat" and "maximum heat" conditions respectively. The minimum heat criterion implies that, for a particular free-stream velocity, enough heat is added to make the operating Reynolds number, R_{δ^*}, equal to the critical value. This should insure that there will never be any amplification of waves in the laminar boundary layer. The maximum heat criterion fixes

the R_{δ^*} at its maximum value. Whether there is amplification depends upon the free-stream velocity being high enough to have the operating R_{δ^*} exceed the maximum $R_{\delta^*_{crit}}$.

In implementing the temperature hunting procedure, the data in Table 3 can be filed and then recovered by the computer for interpolation purposes. The geometry and potential flow pressure distribution for a body will be known so that an M and a λ can be determined for each point on the body under consideration. These will be designated as M_o and λ_o for a particular body point. The ΔT required at a body station can be determined by applying one of the criteria already mentioned and interpolating the data to get appropriate quantities corresponding to M_o and λ_o.

In the minimum heat case the procedure would be as follows:

(1) Determine an H_o versus ΔT curve corresponding to M_o and λ_o as illustrated by the interpolation procedure pictured in Figure 30. The curves can be represented by spline fits and values are extracted accordingly. All the other quantities (η_{δ^*}, q, τ) can be similarly handled so that a curve of each of these is known as a function of ΔT for particular M_o's and λ_o's.

(2) First choose $\Delta T=0$. The η_{δ^*} corresponding then to $\Delta T=0$, M_o, and λ_o can be used to determine δ^* for a particular free-stream velocity using Equation (10).

(3) Calculate R_{δ^*} by means of

$$R_{\delta^*} = \frac{\delta^* U_e}{\nu_\infty} \quad .$$

This is the operating R_{δ^*}.

(4) Enter Figure 29 with $R_{\delta}*$ from step (3) to determine a required H. By entering with the operating $R_{\delta}*$ we are saying that, in order for this to be the $R_{\delta}*_{crit}$, we must produce a corresponding value of H.

(5) The H required from step (4) can be used with the H_o versus ΔT curve of step (1) to determine the required ΔT. This required ΔT now will change the value of $\eta_{\delta}*$, originally determined in step (2) for $\Delta T=0$.

(6) Repeat steps (2), (3), (4), and (5) until the ΔT required converges within a desired accuracy.

(7) Enter the q and τ versus ΔT curves established for M_o and λ_o and get proper q and τ values.

(8) Correct the q and τ values for proper x and U_e values according to the relationships:

$$q_{corr.} = q(282.843)\sqrt{U_e/x}$$

$$\tau_{corr.} = \tau(0.0056569)\, U_e\sqrt{U_e/x} \quad . \tag{14}$$

For the maximum heat case the somewhat different procedure is as follows:

(1) Assume H=2.29. This corresponds approximately to the point where $R_{\delta}*_{crit}$ reaches its maximum. Adding heat beyond the value that produces the maximum $R_{\delta}*_{crit}$ will result in $R_{\delta}*_{crit}$ becoming smaller (see Reference 4) and thus be counterproductive.

(2) Enter the curve of H_o versus ΔT, determined in step (1) of the minimum heat procedure, and extract the ΔT required for H_o=2.29.

(3) Extract q and τ for the ΔT of step (2) from curves of q and τ versus ΔT also determined in step (1) of the minimum heat procedure.

Again, the same corrections for U_e and x shown in Equations (14) must be made.

In addition to determining the local values of q and τ, one can multiply these by the corresponding local area elements and numerically sum the results to give a running total of heating power and the laminar skin friction drag in kilowatts and pounds respectively. The formulas used in this summation are:

$$Q = \sum_{n=0}^{N} \frac{\pi(r_n+r_{n+1})(x_{n+1}-x_n)}{144} \left[\frac{q_n+q_{n+1}}{2 \times 10^3}\right] \quad . \quad (15)$$

$$D_{lam} = \sum_{n=0}^{N} \frac{\pi(r_n+r_{n+1})(x_{n+1}-x_n)}{144} \left[\frac{\tau_n \sqrt{1-(\frac{dr}{dx})_n^2}+\tau_{n+1}\sqrt{1-(\frac{dr}{dx})_{n+1}^2}}{2}\right]$$

Laminar Separation

An attempt was made to obtain some limits with regard to the M, λ, and ΔT parameters beyond which laminar separation would occur. Using the criterion that skin friction goes to zero at the point of separation, curves of the type shown in Figures 8-11 were extrapolated to obtain the desired limits. Figure 31 shows one representation of limit lines so obtained. If the operating values of M and λ fall below and to the left of the appropriate ΔT line, laminar separation should occur. As can be seen, temperature difference has relatively little effect on laminar separation.

Another presentation of this same information is given in Figure 32. This is the kind of plot presented in Reference 8 for the two-dimensional (λ=0.0) flow case. The curve from Reference 8 is designated by "RAND" and is compared with the λ=0 case from the present study. Although

showing slightly more effect of temperature, the Rand calculations also indicate the minor roll of heating in the prevention of laminar separation.

Transition

The prediction of transition is dependent on many factors, making it difficult to develop any simplified approach to such predictions. Free-stream turbulence level, surface roughness, body vibrations, etc., can all influence the location of transition. In addition, body shape, which creates the body pressure distribution, and the distribution of heat added to the body wall can materially affect the location of transition. The work reported here concerns only the effect of body shape and heat addition on transition and ignores the other effects. In the present scheme the transition location can be found without resorting to boundary layer or stability calculations. Assuming the body shape is known, one would, of course, have to generate the Falkner-Skan and radius-gradient parameters.

Through the courtesy of A.M.O. Smith, a plot of the results of e^9 stability calculations that were performed on a variety of heated and unheated wedges was obtained. The plot appears as a band of data when $R_{x_{trans}}$ values are plotted against values of shape factor, H. (See Figure 33). $R_{x_{trans}}$ is defined as $R_{x_{trans}} = \frac{U_e \, x_{trans}}{\nu}$. It would be logical to choose the lower bound of this band as the transition criterion. This curve is reproduced in Figure 34 as a plot of $\log_{10} [R_{x_{trans}}]$ versus H and values corresponding to points on the curve are presented in Table 6.

Because the shape factor is known as a function of the parameters, M, λ, and ΔT (see Figures 1-4 and Table 3), the transition Reynolds

number can likewise be plotted as a function of these parameters as shown in Figures 35-38. One can thus interpolate between the values of the parameters and know what the transition Reynolds number should be. The interpolation can be performed by computer using procedures previously outlined and the curve of Figure 34.

Some transition test data for unheated bodies was examined and a correlation with the curve of Figure 34 was attempted. Most of these data are from Reference 12 and appear in Figure 34. The H values for these points were determined from the data of Table 3. Compared with these data, it is obvious that the curve is optimistic, that is, it predicts transition at a higher Reynolds number and thus, at a point farther back on a body.

The prediction of the ΔT distribution and transition location for a specific body is not being reported in this memorandum. This will be left to a later memorandum in which that kind of result will be correlated with the output of TAPS (References 13-14). Without going into details of this correlation, it is sufficient to say that the H's calculated by TAPS for a given temperature distribution have been consistantly higher by a factor of about 1.03, than those used in obtaining the temperature distribution. If one then reduces the H's employed in the determination of the temperature distribution by this factor, one would expect that the TAPS calculations with the new temperatures would produce the desired H values. Using this idea in reverse, if the H values of the data points in Figure 34 were increased by the factor, practically all of them would be located in a band above the curve. This fact helps substantiate the validity of the criterion curve. As a suggested methodology for the use of the curve in Figure 34, one could replot the curve with values of H reduced by 1.03 and then, using

the calculated data of Table 3 in establishing the boundary layer characteristics, one would have a curve consistent with TAPS and experimental transition information.

Of the various simplified criteria for transition developed by others, the correlation line presented by Granville in Reference 15 comes closest to the criteria presented here. He plots a momentum thickness Reynolds number difference between the transition and critical values against a type of radius gradient parameter. He uses no pressure gradient parameter but merely collapses all the data to a single curve depending only on his radius gradient parameter. It would appear that, for the bodies studied, the variation in M was relatively small for most of the transition locations, leading to the use of a single correlation line.

Conclusions

Techniques have been developed and data have been generated that permit one to estimate in a relatively easy manner the temperature distribution necessary to stabilize the flow over an axisymmetric body. Additionally, these techniques and data provide a means for determining the local heat flux, skin friction, the laminar separation point, and the point of transition for a heated axisymmetric body.

All these estimates can be made by using the values of the various quantities presented in the tables and by following the interpolative procedures and criteria that have been outlined. A simple computer program to do this can be easily written or one can interpolate between the curves that are also included in this memorandum.

References

1. Smith, A. M. O. and Clutter, D. W., "Solution of the Incompressible Laminar Boundary Layer Equations," Engineering Paper 1525, Douglas Aircraft Company, Inc., Aircraft Division, Long Beach, California, 1 January 1963.

2. Hill, M. J. and Wirz, H. J., "A Numerical Method for the Solution of the Two-Dimensional Steady Laminar Boundary Layer Equations," von Karman Institute for Fluid Dynamics, Technical Note 103, November 1974.

3. Sheridan, R. E., Jr., "Laminar Boundary Layers on Bodies of Revolution: Computer Programs and Vorticity Budgets," M.S. Thesis, The Pennsylvania State University, September 1968.

4. Lowell, R. L., Jr. and Reshotko, E., "Numberical Study of the Stability of a Heated, Water Boundary Layer," Case Western Reserve University, FTAS TR 73-93, January 1974.

5. Nachtsheim, P. R. and Swigert, P., "Satisfaction of Asymptotic Boundary Conditions in Numerical Solution of Systems of Nonlinear Equations of Boundary-Layer Type," NASA TN D-3004, 1965.

6. Schlichting, H., "Boundary-Layer Theory," McGraw-Hill Book Company, 1968.

7. King, William S., "The Effect of Wall Temperature and Suction on Laminar Boundary-Layer Stability," Rand Report R-1863-ARPA, April 1976.

8. Aroesty, J. and Berger, S. A., "Controlling the Separation of Laminar Boundary Layers in Water: Heating and Suction," Rand Report R-1789-ARPA, September 1975.

9. Touloukian, Y. S. and Makita, T., "Thermophysical Properties of Matter, Volume 6," New York: IFI/Plenum Data Corp., 1970.

10. Touloukian, Y. S., Liley, P. E., and Saxena, S. C., "Thermophysical Properties of Matter, Volume 3," New York: IFI/Plenum Data Corp., 1970.

11. Kaups, K and Smith, A. M. O., "The Laminar Boundary Layer in Water with Variable Properties," ASME-AIChE Heat Transfer Conference, Seattle, Wash., Paper 67-HT-69, August 1967.

12. Groth, E. E. and Pfenninger, W., "Boundary Layer Transition on Bodies of Revolution," Northrop Aircraft Report NAI-57-1162 (BLC-100), July 1957.

13. Gentry, A. E., "The Transition Analysis Program System Volume I - User's Manual," McDonnell Douglas Report No. MDC J 7255/01, June 1976.

14. Gentry, A. E. and Wazzan, A. R., "The Transition Analysis Program System Volume II - Program Formulation and Listings," McDonnell Douglas Report MDC J 7255/02, June 1976.

15. Granville, P. S., "The Prediction of Transition from Laminar to Turbulent Flow in Boundary Layers on Bodies of Revolution," Proceedings of the Tenth Symposium on Naval Hydrodynamics, Session VII, ACR-204, June 1974, pp. 705-729.

22 February 1978
JJE:jep

TABLE 1

Comparison of Quantities Calculated by ARL Code and Those of Reference 4

	Reference 4	ARL Calculations
(T_w = 60, T_∞ = 60)		
f"(0)	0.33205733	0.33205734
θ"(0)	----------	----------
η_δ*	1.72078760	1.72078700
(T_w = 90, T_∞ = 60)		
f"(0)	0.46639971	0.46639956
θ "(0)	-0.71321360	-0.71321537
η_δ*	1.51454910	1.51454380
(T_w = 150, T_∞ = 60)		
f"(0)	0.74319378	0.74319466
θ"(0)	-0.78381642	-0.78381826
η_δ*	1.21124000	1.21123790

22 February 1978
JJE:jep

TABLE 2

Comparison with Blasius' Results

	Blasius	ARL Calculations
$\delta^* \left(\frac{U_e}{\nu_\infty x}\right)^{1/2}$	1.7208	1.72078678
$\theta \left(\frac{U_e}{\nu_\infty x}\right)^{1/2}$	0.664	0.66740880

22 February 1978
JJE:jep

TABLE 3

Laminar Boundary Layer Data

	λ	M	H	q (watts/ft^2)	τ (lb/ft^2)	η_δ*
DATA FOR DELTA T =			0.0			
1	-0.50	-0.0440	3.55605	0.00	0.039180	4.32630
2	-0.50	-0.0400	3.21105	0.00	0.085520	3.77832
3	-0.50	-0.0300	2.89515	0.00	0.153740	3.17978
4	-0.50	-0.0200	2.74414	0.00	0.203040	2.84531
5	-0.50	-0.0100	2.64908	0.00	0.243920	2.61182
6	-0.50	0.0000	2.58210	0.00	0.279640	2.43356
7	-0.50	0.0500	2.41156	0.00	0.418180	1.90616
8	-0.50	0.1000	2.33728	0.00	0.523240	1.62523
9	-0.50	0.2000	2.26732	0.00	0.688260	1.30985
10	-0.50	0.5000	2.19865	0.00	1.038010	0.91627
11	-0.50	0.7500	2.17739	0.00	1.257630	0.76767
12	-0.50	0.9000	2.16921	0.00	1.372690	0.70708
13	0.00	-0.0900	3.79906	0.00	0.022480	3.30322
14	0.00	-0.0800	3.20730	0.00	0.120950	2.67167
15	0.00	-0.0700	3.01196	0.00	0.174650	2.41957
16	0.00	-0.0600	2.89151	0.00	0.217420	2.24844
17	0.00	-0.0553	2.84808	0.00	0.235320	2.18320
18	0.00	-0.0500	2.80588	0.00	0.254250	2.11774
19	0.00	-0.0400	2.74051	0.00	0.287100	2.01193
20	0.00	-0.0300	2.68832	0.00	0.317160	1.92315
21	0.00	-0.0200	2.64538	0.00	0.344950	1.84683
22	0.00	-0.0100	2.60925	0.00	0.370950	1.78004
23	0.00	0.0000	2.57831	0.00	0.395500	1.72079
24	0.00	0.0500	2.47148	0.00	0.502200	1.49894
25	0.00	0.1000	2.40735	0.00	0.591400	1.34786
26	0.00	0.2000	2.33267	0.00	0.740000	1.14920
27	0.00	0.3000	2.28990	0.00	0.864300	1.01960
28	0.00	0.5000	2.24200	0.00	1.071500	0.85468
29	0.00	0.7500	2.21033	0.00	1.285000	0.73010
30	0.00	1.0000	2.19130	0.00	1.468000	0.64790
31	0.50	-0.1300	3.45903	0.00	0.085580	2.42005
32	0.50	-0.1200	3.20442	0.00	0.148130	2.18141
33	0.50	-0.1100	3.06227	0.00	0.193990	2.03390
34	0.50	-0.1000	2.96361	0.00	0.232420	1.92404
35	0.50	-0.0900	2.88873	0.00	0.266290	1.83585
36	0.50	-0.0800	2.82890	0.00	0.296980	1.76201
37	0.50	-0.0600	2.73771	0.00	0.351670	1.64274
38	0.50	-0.0553	2.72016	0.00	0.363530	1.61874
39	0.50	-0.0400	2.67031	0.00	0.400060	1.54848
40	0.50	-0.0200	2.61779	0.00	0.443920	1.47082
41	0.50	0.0000	2.57541	0.00	0.484350	1.40502
42	0.50	0.0500	2.49752	0.00	0.574420	1.27532
43	0.50	0.1000	2.44378	0.00	0.653310	1.17777
44	0.50	0.2000	2.37352	0.00	0.789370	1.03719
45	0.50	0.5000	2.27541	0.00	1.104830	0.80455

	λ	M	H	q (watts/ft^2)	τ (lb/ft^2)	η_δ*
46	0.50	0.7500	2.23753	0.00	1.312350	0.69784
47	0.50	0.9000	2.22232	0.00	1.422630	0.65124
48	1.00	-0.0800	2.73535	0.00	0.406080	1.42265
49	1.00	-0.0600	2.68313	0.00	0.448530	1.35987
50	1.00	-0.0553	2.67231	0.00	0.458020	1.34649
51	1.00	-0.0400	2.64014	0.00	0.487830	1.30591
52	1.00	-0.0200	2.60398	0.00	0.524600	1.25868
53	1.00	0.0000	2.57299	0.00	0.559300	1.21678
54	1.00	0.0500	2.51165	0.00	0.638700	1.12936
55	1.00	0.1000	2.46566	0.00	0.710200	1.05953
56	1.00	0.2000	2.40142	0.00	0.836400	0.95308
57	1.00	0.5000	2.30192	0.00	1.137700	0.76262
58	1.00	0.7500	2.26041	0.00	1.339600	0.66971
59	1.00	0.9000	2.24327	0.00	1.447600	0.62810
60	2.00	-0.0800	2.66394	0.00	0.565760	1.09494
61	2.00	-0.0600	2.63615	0.00	0.597470	1.06627
62	2.00	-0.0400	2.61137	0.00	0.627800	1.04003
63	2.00	-0.0200	2.58907	0.00	0.656930	1.01587
64	2.00	0.0000	2.56890	0.00	0.685000	0.99350
65	2.00	0.0500	2.52584	0.00	0.751100	0.94401
66	2.00	0.1000	2.49077	0.00	0.812400	0.90179
67	2.00	0.2000	2.43677	0.00	0.923900	0.83281
68	2.00	0.5000	2.34131	0.00	1.201700	0.69576
69	2.00	0.7500	2.29669	0.00	1.393400	0.62268
70	2.00	0.9000	2.27734	0.00	1.497100	0.58667
71	3.00	-0.0800	2.63278	0.00	0.689900	0.92342
72	3.00	-0.0600	2.61393	0.00	0.716310	0.90619
73	3.00	-0.0400	2.59653	0.00	0.741900	0.89002
74	3.00	-0.0200	2.58043	0.00	0.766760	0.87479
75	3.00	0.0000	2.56546	0.00	0.790900	0.86039
76	3.00	0.0500	2.53224	0.00	0.848700	0.82759
77	3.00	0.1000	2.50388	0.00	0.903200	0.79858
78	3.00	0.2000	2.45788	0.00	1.004300	0.74921
79	3.00	0.5000	2.36912	0.00	1.263300	0.64419
80	3.00	0.7500	2.32411	0.00	1.446000	0.58460
81	3.00	0.9000	2.30387	0.00	1.545700	0.55607
82	3.00	1.1000	2.28210	0.00	1.669799	0.52390
83	4.00	-0.0800	2.61455	0.00	0.795030	0.81353
84	4.00	-0.0600	2.60029	0.00	0.818130	0.80174
85	4.00	-0.0400	2.58691	0.00	0.840680	0.79051
86	4.00	-0.0200	2.57430	0.00	0.862730	0.77980
87	4.00	0.0000	2.56241	0.00	0.884300	0.76956
88	4.00	0.0500	2.53539	0.00	0.936300	0.74579
89	4.00	0.1000	2.51164	0.00	0.985900	0.72429
90	4.00	0.2000	2.47171	0.00	1.079000	0.68670
91	4.00	0.5000	2.38969	0.00	1.322000	0.60278
92	4.00	0.7500	2.34551	0.00	1.497000	0.55292
93	4.00	0.9000	2.32507	0.00	1.593000	0.52849

	λ	M	H	q (watts/ft^2)	τ (lb/ft^2)	η_δ*
94	4.00	0.9600	2.31782	0.00	1.630420	0.91961
95	4.00	1.1200	2.30062	0.00	1.725300	0.49800
96	4.00	1.2800	2.28592	0.00	1.815420	0.47891
97	5.00	-0.0800	2.60227	0.00	0.887850	0.73541
98	5.00	-0.0600	2.59082	0.00	0.908640	0.72670
99	5.00	-0.0400	2.57993	0.00	0.929030	0.71833
100	5.00	-0.0200	2.56957	0.00	0.949050	0.71027
101	5.00	0.0000	2.55970	0.00	0.968700	0.70251
102	5.00	0.0500	2.53691	0.00	1.016400	0.68428
103	5.00	0.1000	2.51648	0.00	1.062100	0.66752
104	5.00	0.2000	2.48125	0.00	1.148800	0.63766
105	5.00	0.5000	2.40543	0.00	1.379300	0.56854
106	5.00	0.7500	2.36263	0.00	1.547200	0.52598
107	5.00	0.9000	2.34235	0.00	1.640200	0.50474
108	5.00	0.9600	2.33510	0.00	1.675980	0.49696
109	5.00	1.1200	2.31773	0.00	1.768150	0.47789
110	5.00	1.2800	2.30270	0.00	1.855950	0.46090
111	5.00	1.4400	2.28958	0.00	1.939940	0.44564
DATA FOR DELTA T = 30.0						
112	-0.50	-0.0400	2.87276	1237.00	0.100700	3.25866
113	-0.50	-0.0200	2.52498	1469.71	0.199140	2.50159
114	-0.50	0.0000	2.39277	1605.00	0.265550	2.14189
115	-0.50	0.0500	2.25160	1834.00	0.386130	1.67379
116	-0.50	0.1000	2.19045	2003.99	0.477550	1.42349
117	-0.50	0.2000	2.13379	2273.00	0.621040	1.14311
118	-0.50	0.5000	2.07987	2878.19	0.925300	0.79553
119	0.00	-0.0900	3.13521	1570.00	0.081500	2.63566
120	0.00	-0.0800	2.86927	1749.00	0.142420	2.30422
121	0.00	-0.0700	2.73210	1860.00	0.185880	2.11028
122	0.00	-0.0600	2.64085	1946.14	0.221870	1.96995
123	0.00	-0.0553	2.60701	1980.93	0.237110	1.91517
124	0.00	-0.0400	2.52147	2078.50	0.281630	1.76888
125	0.00	-0.0200	2.44421	2182.52	0.331660	1.62532
126	0.00	0.0000	2.38908	2270.00	0.375500	1.51455
127	0.00	0.0500	2.30061	2449.00	0.468400	1.31755
128	0.00	0.1000	2.24743	2594.00	0.546100	1.18355
129	0.00	0.2000	2.18581	2834.00	0.675300	1.00655
130	0.00	0.5000	2.11235	3379.00	0.963650	0.74492
131	0.50	-0.1200	2.86660	2142.00	0.174420	1.88139
132	0.50	-0.1000	2.69544	2316.00	0.243130	1.68129
133	0.50	-0.0900	2.63820	2384.00	0.271730	1.60846
134	0.50	-0.0800	2.59147	2443.00	0.297900	1.54633
135	0.50	-0.0600	2.51877	2545.63	0.344920	1.44429
136	0.50	-0.0553	2.50461	2567.35	0.355160	1.42355
137	0.50	-0.0400	2.46414	2633.27	0.386760	1.36250
138	0.50	-0.0200	2.42115	2710.62	0.424810	1.29454
139	0.50	0.0000	2.38626	2780.00	0.459940	1.23662

	λ	M	H	q (watts/ft^2)	(lb/ft^2)	η_{δ^*}
140	0.50	0.0500	2.32177	2932.00	0.538310	1.12185
141	0.50	0.1000	2.27714	3062.00	0.606990	1.03515
142	0.50	0.2000	2.21888	3282.00	0.725420	0.90993
143	0.50	0.5000	2.13835	3793.19	0.999780	0.70285
144	1.00	-0.0800	2.51652	2939.39	0.398280	1.25079
145	1.00	-0.0600	2.47423	3016.60	0.434970	1.19638
146	1.00	-0.0553	2.46542	3033.64	0.443190	1.18473
147	1.00	-0.0400	2.43915	3086.60	0.469040	1.14928
148	1.00	-0.0200	2.40943	3150.79	0.500960	1.10784
149	1.00	0.0000	2.38387	3211.00	0.531100	1.07095
150	1.00	0.0500	2.33310	3345.00	0.600200	0.99363
151	1.00	0.1000	2.29508	3463.00	0.662400	0.93165
152	1.00	0.2000	2.24154	3668.00	0.772300	0.83689
153	1.00	0.5000	2.15933	4154.70	1.034420	0.66724
154	1.00	0.9000	2.11165	4664.75	1.303860	0.54778
155	2.00	-0.0800	2.45799	3724.00	0.546960	0.96343
156	2.00	-0.0600	2.43530	3780.23	0.574450	0.93838
157	2.00	-0.0400	2.41491	3833.39	0.600780	0.91538
158	2.00	-0.0200	2.39656	3883.89	0.626080	0.89413
159	2.00	0.0000	2.37991	3932.00	0.650500	0.87442
160	2.00	0.0500	2.34424	4044.00	0.707900	0.83070
161	2.00	0.1000	2.31512	4146.00	0.761300	0.79326
162	2.00	0.2000	2.27015	4330.00	0.858400	0.73196
163	2.00	0.5000	2.19093	4778.79	1.100180	0.60987
164	3.00	0.0000	2.37650	4540.00	0.751100	0.75727
165	3.00	0.0500	2.34901	4639.00	0.801400	0.72830
166	3.00	0.1000	2.32548	4730.00	0.848800	0.70260
167	3.00	0.2000	2.28722	4897.00	0.936800	0.65877
168	3.00	0.5000	2.21333	5317.79	1.162180	0.56528
169	4.00	0.0000	2.37358	5076.00	0.839700	0.67733
170	4.00	0.0500	2.35119	5165.00	0.885000	0.65634
171	4.00	0.1000	2.33148	5248.00	0.928100	0.63731
172	4.00	0.2000	2.29826	5403.00	1.009000	0.60396
173	4.00	0.5000	2.22991	5800.29	1.221060	0.52930
174	5.00	0.0000	2.37093	5561.00	0.919900	0.61831
175	5.00	0.0500	2.35206	5642.00	0.961300	0.60221
176	5.00	0.1000	2.33509	5719.00	1.001200	0.58739
177	5.00	0.2000	2.30578	5864.00	1.076600	0.56092
178	5.00	0.5000	2.24256	6241.59	1.277270	0.49946
179	5.00	0.9000	2.18999	6662.80	1.504290	0.44262
DATA FOR DELTA T = 60.0						
180	-0.50	-0.0400	2.53442	2756.00	0.108640	2.85912
181	-0.50	-0.0200	2.36421	3200.68	0.192570	2.22318
182	-0.50	0.0000	2.25545	3473.00	0.250550	1.90540
183	-0.50	0.0500	2.13895	3941.00	0.356270	1.48659

	λ	M	H	q (watts/ft^2)	τ (lb/ft^2)	η_{δ}*
184	-0.50	0.1000	2.08935	4290.00	0.436470	1.26198
185	-0.50	0.2000	2.04470	4851.00	0.562420	1.01080
186	-0.50	0.5000	2.00433	6117.92	0.829970	0.70095
187	0.00	-0.0900	2.80413	3603.00	0.106700	2.26039
188	0.00	-0.0800	2.63106	3897.00	0.153640	2.02170
189	0.00	-0.0700	2.52847	4103.00	0.189900	1.86443
190	0.00	-0.0600	2.45699	4266.68	0.220630	1.74603
191	0.00	-0.0553	2.42999	4334.33	0.233750	1.69906
192	0.00	-0.0400	2.36075	4526.45	0.272330	1.57202
193	0.00	-0.0200	2.29735	4734.30	0.315960	1.44564
194	0.00	0.0000	2.25178	4911.00	0.354300	1.34731
195	0.00	0.0500	2.17853	5275.00	0.435700	1.17133
196	0.00	0.1000	2.13470	5573.00	0.503800	1.05118
197	0.00	0.2000	2.08457	6067.00	0.617300	0.89235
198	0.00	0.5000	2.02663	7203.29	0.870370	0.65811
199	0.50	-0.1200	2.62851	4773.00	0.188170	1.65071
200	0.50	-0.1000	2.49952	5096.00	0.245720	1.48738
201	0.50	-0.0900	2.45440	5226.00	0.270210	1.42563
202	0.50	-0.0800	2.41703	5341.00	0.292800	1.37228
203	0.50	-0.0600	2.35809	5543.75	0.333540	1.28355
204	0.50	-0.0553	2.34653	5586.94	0.342440	1.26538
205	0.50	-0.0400	2.31330	5718.54	0.369990	1.21166
206	0.50	-0.0200	2.27785	5873.96	0.403240	1.15154
207	0.50	0.0000	2.24896	6015.00	0.433970	1.10008
208	0.50	0.0500	2.19549	6323.00	0.502630	0.99763
209	0.50	0.1000	2.15857	6588.00	0.562850	0.91998
210	0.50	0.2000	2.11068	7042.00	0.666740	0.80765
211	0.50	0.5000	2.04579	8102.00	0.907530	0.62195
212	1.00	-0.0800	2.35586	6401.40	0.385140	1.11159
213	1.00	-0.0600	2.32121	6555.09	0.417090	1.06381
214	1.00	-0.0553	2.31396	6589.18	0.424270	1.05354
215	1.00	-0.0400	2.29231	6695.29	0.446830	1.02222
216	1.00	-0.0200	2.26775	6824.79	0.474740	0.98550
217	1.00	0.0000	2.24659	6945.00	0.501100	0.95269
218	1.00	0.0500	2.20447	7218.00	0.561600	0.88372
219	1.00	0.1000	2.17293	7459.00	0.616200	0.82826
220	1.00	0.2000	2.12871	7881.00	0.712500	0.74330
221	1.00	0.5000	2.06178	8886.96	0.942550	0.59108
222	1.00	0.9000	2.02397	9949.09	1.179110	0.48414
223	2.00	-0.0800	2.30720	8087.29	0.523250	0.85678
224	2.00	-0.0600	2.28845	8200.10	0.547250	0.83464
225	2.00	-0.0400	2.27163	8307.09	0.570260	0.81426
226	2.00	-0.0200	2.25643	8409.00	0.592390	0.79540
227	2.00	0.0000	2.24261	8506.00	0.613700	0.77787
228	2.00	0.0500	2.21299	8734.00	0.664100	0.73888
229	2.00	0.1000	2.18876	8942.00	0.710800	0.70543
230	2.00	0.2000	2.15152	9317.00	0.796000	0.65052
231	2.00	0.5000	2.08629	10242.50	1.008090	0.54099

	λ	M	H	q (watts/ft^2)	τ (lb/ft^2)	η_δ*
232	3.00	0.0000	2.23922	9822.00	0.708700	0.67366
233	3.00	0.0500	2.21638	10022.00	0.752700	0.64783
234	3.00	0.1000	2.19683	10208.00	0.794300	0.62488
235	3.00	0.2000	2.16503	10549.00	0.871400	0.58567
236	3.00	0.5000	2.10388	11413.30	1.069110	0.50181
237	4.00	0.0000	2.23631	10982.00	0.792300	0.60254
238	4.00	0.0500	2.21770	11161.00	0.831900	0.58384
239	4.00	0.1000	2.20130	11331.00	0.869700	0.56685
240	4.00	0.2000	2.17366	11646.00	0.940700	0.53703
241	4.00	0.5000	2.11693	12461.19	1.126610	0.47010
242	5.00	0.0000	2.23367	12030.00	0.867900	0.55004
243	5.00	0.0500	2.21797	12194.00	0.904200	0.53570
244	5.00	0.1000	2.20385	12351.00	0.939100	0.52247
245	5.00	0.2000	2.17945	12646.00	1.005300	0.49881
246	5.00	0.5000	2.12686	13420.00	1.181210	0.44375
247	5.00	0.9000	2.08338	14287.59	1.380370	0.39274
DATA FOR DELTA T = 90.0						
248	-0.50	-0.0400	2.46339	4500.00	0.111780	2.54460
249	-0.50	-0.0200	2.24701	5141.33	0.184410	1.99676
250	-0.50	0.0000	2.15691	5548.00	0.235480	1.71296
251	-0.50	0.0500	2.06114	6259.00	0.328980	1.33522
252	-0.50	0.1000	2.02165	6796.00	0.400040	1.13212
253	-0.50	0.2000	1.98775	7661.00	0.511790	0.90528
254	0.00	-0.0900	2.58584	5976.00	0.119670	1.98775
255	0.00	-0.0800	2.46010	6364.00	0.158080	1.79930
256	0.00	-0.0700	2.37993	6653.00	0.189000	1.66708
257	0.00	-0.0600	2.32242	6889.29	0.215590	1.56490
258	0.00	-0.0553	2.30043	6987.94	0.227030	1.52388
259	0.00	-0.0400	2.24353	7270.94	0.260800	1.41192
260	0.00	-0.0200	2.19101	7580.66	0.299170	1.29937
261	0.00	0.0000	2.15317	7846.00	0.333000	1.21124
262	0.00	0.0500	2.09258	8397.00	0.404900	1.05271
263	0.00	0.1000	2.05676	8851.00	0.465200	0.94414
264	0.00	0.2000	2.01666	9610.00	0.565700	0.80053
265	0.00	0.5000	1.97261	11365.39	0.790390	0.58906
266	0.50	-0.1200	2.45758	7794.00	0.193610	1.46913
267	0.50	-0.1000	2.35628	8250.00	0.242810	1.33120
268	0.50	-0.0900	2.31985	8438.00	0.264000	1.27773
269	0.50	-0.0800	2.28935	8607.00	0.283700	1.23110
270	0.50	-0.0600	2.24086	8905.03	0.319410	1.15283
271	0.50	-0.0553	2.23130	8969.09	0.327230	1.13671
272	0.50	-0.0400	2.20375	9165.09	0.351460	1.08890
273	0.50	-0.0200	2.17431	9397.77	0.380750	1.03514
274	0.50	0.0000	2.15030	9610.00	0.407860	0.98697
275	0.50	0.0500	2.10597	10076.00	0.468530	0.89675

	λ	M	H	w (watts/ft^2)	τ (lb/ft^2)	η_δ*
276	0.50	0.1000	2.07555	10479.00	0.521810	0.82665
277	0.50	0.2000	2.03658	11172.00	0.613800	0.72510
278	0.50	0.5000	1.98556	12804.60	0.827310	0.55728
279	1.00	-0.0800	2.23861	10282.70	0.368820	0.99838
280	1.00	-0.0600	2.20991	10511.20	0.396910	0.95592
281	1.00	-0.0553	2.20389	10561.99	0.403220	0.94676
282	1.00	-0.0400	2.18589	10720.70	0.423090	0.91880
283	1.00	-0.0200	2.16549	10914.79	0.447690	0.88591
284	1.00	0.0000	2.14789	11096.00	0.471000	0.85647
285	1.00	0.0500	2.11291	11508.00	0.524400	0.79441
286	1.00	0.1000	2.08683	11875.00	0.572700	0.74438
287	1.00	0.2000	2.05053	12518.00	0.658000	0.66761
288	1.00	0.5000	1.99699	14062.50	0.861810	0.52999
289	2.00	-0.0600	2.18199	13130.09	0.518170	0.75019
290	2.00	-0.0400	2.16799	13290.40	0.538460	0.73195
291	2.00	-0.0200	2.15532	13443.60	0.557970	0.71505
292	2.00	0.0000	2.14381	13590.00	0.576800	0.69931
293	2.00	0.0500	2.11916	13934.00	0.621300	0.66424
294	2.00	0.1000	2.09908	14249.00	0.662600	0.63410
295	2.00	0.2000	2.06830	14820.00	0.738000	0.58453
296	2.00	0.5000	2.01516	16235.39	0.925790	0.48550
297	3.00	0.0000	2.14041	15693.00	0.666000	0.60562
298	3.00	0.0500	2.12138	15993.00	0.704900	0.58240
299	3.00	0.1000	2.10600	16267.00	0.740600	0.56240
300	3.00	0.2000	2.07873	16793.00	0.809900	0.52635
301	3.00	0.5000	2.02847	18112.39	0.984910	0.45057
302	4.00	0.0000	2.13744	17545.00	0.744700	0.54168
303	4.00	0.0500	2.12192	17816.00	0.779600	0.52487
304	4.00	0.1000	2.10826	18072.00	0.813000	0.50958
305	4.00	0.2000	2.08528	18551.00	0.875800	0.48270
306	4.00	0.5000	2.03839	19792.39	1.040320	0.42223
307	5.00	0.0000	2.13477	19220.00	0.815700	0.49449
308	5.00	0.0500	2.12166	19468.00	0.847800	0.48159
309	5.00	0.1000	2.10988	19705.00	0.878600	0.46969
310	5.00	0.2000	2.08955	20152.00	0.937100	0.44837
311	5.00	0.5000	2.04595	21328.79	1.092750	0.39865

TABLE 4

Laminar Boundary Layer Data for Various Ambient Temperatures

	ΔT	M	H	q (watts/ft^2)	τ (lb/ft^2)	η_{δ^*}
DATA FOR LAMBDA = 0.0, T AT INFINITY = 60.0						
1	0.0	0.0000	2.57831	0.00	0.395500	1.72079
2	0.0	0.0500	2.47148	0.00	0.502200	1.49841
3	0.0	0.1000	2.40735	0.00	0.591400	1.34786
4	0.0	0.2000	2.33267	0.00	0.740000	1.14920
5	30.0	0.0000	2.38908	2270.00	0.375500	1.51455
6	30.0	0.0500	2.30061	2449.00	0.468400	1.31755
7	30.0	0.1000	2.24743	2594.00	0.546100	1.18355
8	30.0	0.2000	2.18581	2834.00	0.675300	1.00655
9	60.0	0.0000	2.25178	4911.00	0.354300	1.34731
10	60.0	0.0500	2.17853	5275.00	0.435700	1.17133
11	60.0	0.1000	2.13470	5573.00	0.503800	1.05118
12	60.0	0.2000	2.08457	6067.00	0.617300	0.89235
13	90.0	0.0000	2.15317	7846.00	0.333000	1.21124
14	90.0	0.0500	2.09258	8397.00	0.404900	1.05271
15	90.0	0.1000	2.05676	8851.00	0.465200	0.94414
16	90.0	0.2000	2.01666	9610.00	0.565700	0.80053
DATA FOR LAMBDA = 0.0, T AT INFINITY = 90.0						
17	0.0	0.0000	2.57831	0.00	0.325200	1.72079
18	0.0	0.0500	2.47148	0.00	0.412900	1.49841
19	0.0	0.1000	2.40735	0.00	0.486300	1.34786
20	0.0	0.2000	2.33267	0.00	0.608400	1.14920
21	30.0	0.0000	2.43051	2429.00	0.309600	1.54479
22	30.0	0.0500	2.33984	2617.00	0.387500	1.34442
23	30.0	0.1000	2.28544	2769.00	0.452700	1.20821
24	30.0	0.2000	2.22251	3022.00	0.561300	1.02828
25	60.0	0.0000	2.32214	5165.00	0.293600	1.40009
26	60.0	0.0500	2.24502	5544.00	0.363300	1.21811
27	60.0	0.1000	2.19901	5855.00	0.421700	1.09401
28	60.0	0.2000	2.14645	6371.00	0.519000	0.92994
29	90.0	0.0000	2.24388	8141.99	0.277800	1.28059
30	90.0	0.0500	2.17820	8714.00	0.340700	1.11406
31	90.0	0.1000	2.13947	9187.00	0.393400	1.00018
32	90.0	0.2000	2.09609	9974.00	0.481300	0.84953
DATA FOR LAMBDA = 0.0, T AT INFINITY = 120.0						
33	0.0	0.0000	2.57831	0.00	0.277300	1.72079
34	0.0	0.0500	2.47148	0.00	0.352000	1.49841
35	0.0	0.1000	2.40735	0.00	0.414600	1.34786

22 February 1978
JJE:jep

	ΔT	M	H	q (watts/ft^2)	τ (lb/ft^2)	η_δ*
36	C.0	C.2000	2.33267	0.CC	0.518800	1.14920
37	30.0	0.0000	2.46277	2565.CC	0.264700	1.56982
38	30.0	0.0500	2.37008	2759.00	0.332300	1.36651
39	30.0	0.1000	2.31457	2918.CC	0.388800	1.22840
40	30.0	0.2000	2.25040	3180.CC	0.482900	1.04600
41	60.0	0.0000	2.37774	5383.CC	0.252200	1.44408
42	60.0	0.1000	2.24912	6096.00	0.365000	1.12939
43	60.0	0.2000	2.19435	6629.CC	0.450700	0.96086
44	90.0	0.0000	2.31655	8400.CC	0.239900	1.33893
45	90.0	0.1000	2.20496	9475.00	0.343300	1.04695
46	90.0	0.2000	2.15871	10284.00	0.421900	0.89027

TABLE 5

Critical Reynolds Number Variation with Shape Factor

	$R_{\delta^*_{crit}}$	H
1	105.000	3.80000
2	115.000	3.50000
3	130.000	3.20000
4	150.000	3.00000
5	180.000	2.90000
6	232.000	2.80000
7	326.000	2.70000
8	485.000	2.60000
9	675.000	2.55000
10	1000.000	2.51800
11	1500.000	2.48750
12	2000.000	2.46600
13	3000.000	2.43750
14	4000.000	2.41800
15	5000.000	2.40250
16	6000.000	2.38950
17	7000.000	2.37550
18	8000.000	2.36050
19	9000.000	2.34400
20	10000.000	2.32540
21	10500.000	2.31500
22	11000.000	2.29750
23	11210.000	2.28000

TABLE 6

Transition Reynolds Number Variation with Shape Factor

H	$R_{x_{trans}}$	$\log_{10}[R_{x_{trans}}]$
2.20000	8.51732	0.32909E 09
2.25000	8.28045	0.19074E 09
2.30000	8.04405	0.11067E 09
2.35000	7.80882	0.64390E 08
2.40000	7.57548	0.37625E 08
2.45000	7.34473	0.22117E 08
2.50000	7.11730	0.13100E 08
2.55000	6.89390	0.78324E 07
2.60000	6.67524	0.47341E 07
2.65000	6.46204	0.28976E 07
2.70000	6.25501	0.17989E 07
2.75000	6.05486	0.11346E 07
2.80000	5.86231	0.72829E 06
2.84999	5.67808	0.47651E 06
2.90000	5.50287	0.31832E 06
2.95000	5.33741	0.21747E 06

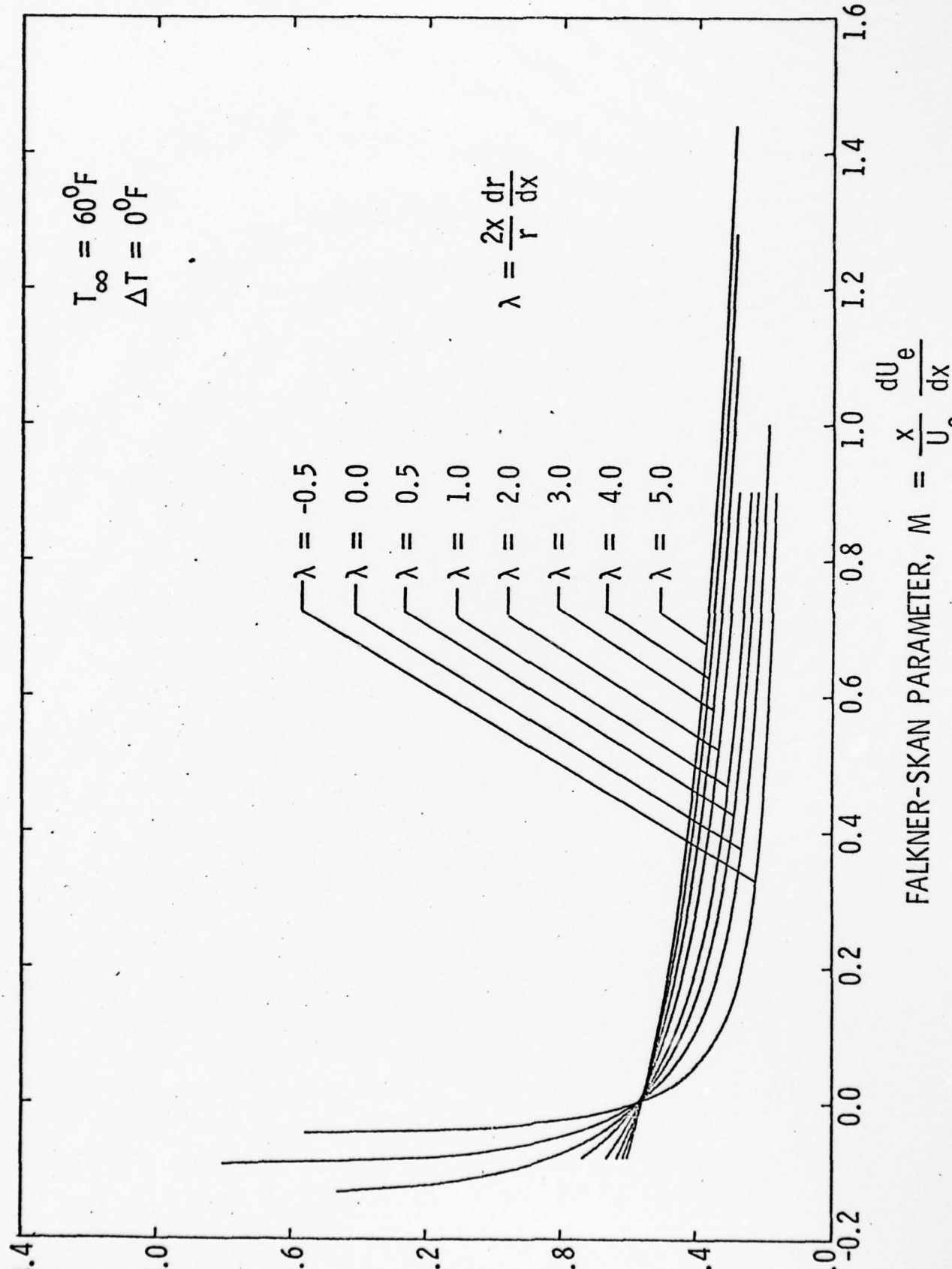

Figure 1 - Shape Factor Variation with M for $\Delta T=0$

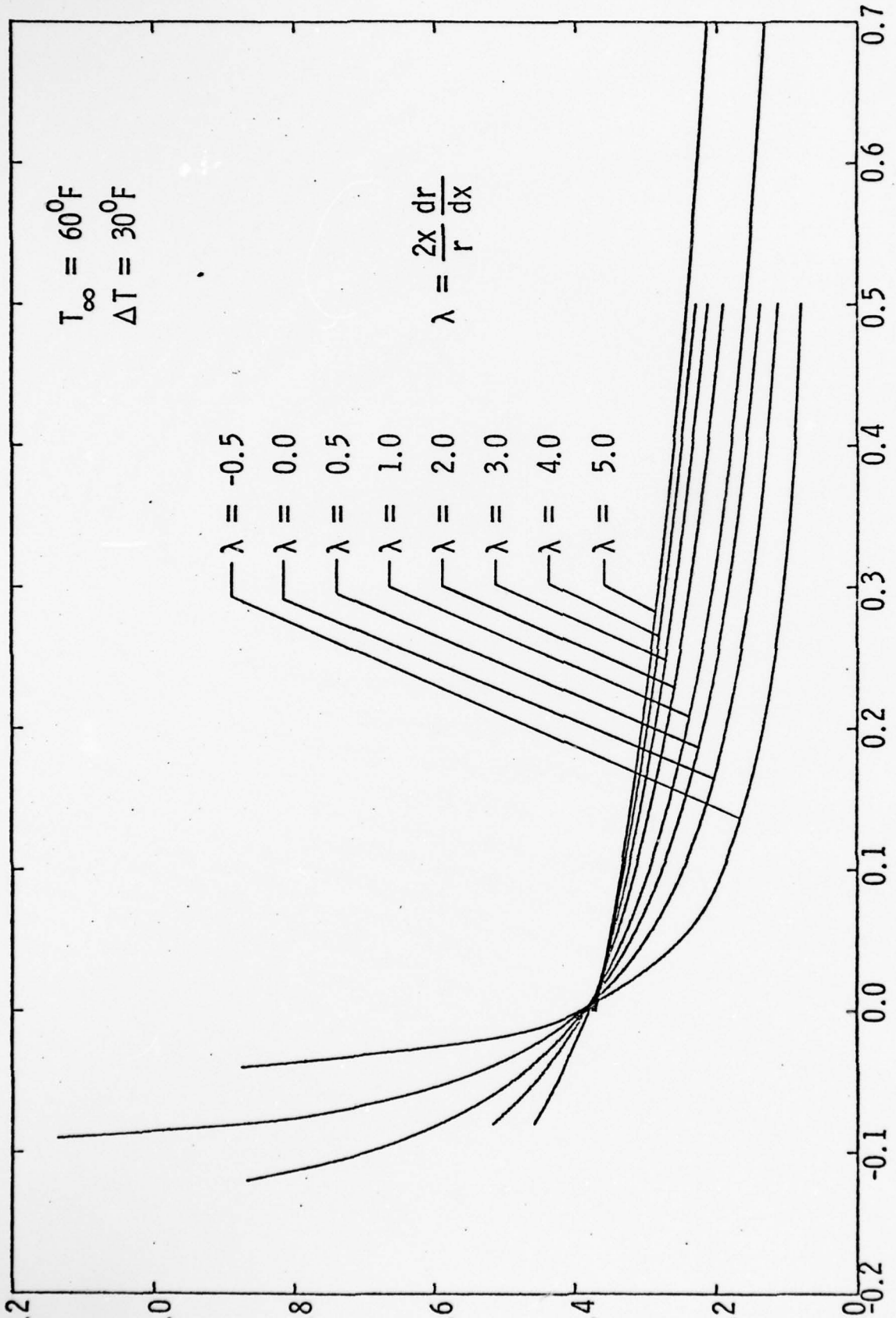

Figure 2 - Shape Factor Variation with M for $\Delta T=30°F$

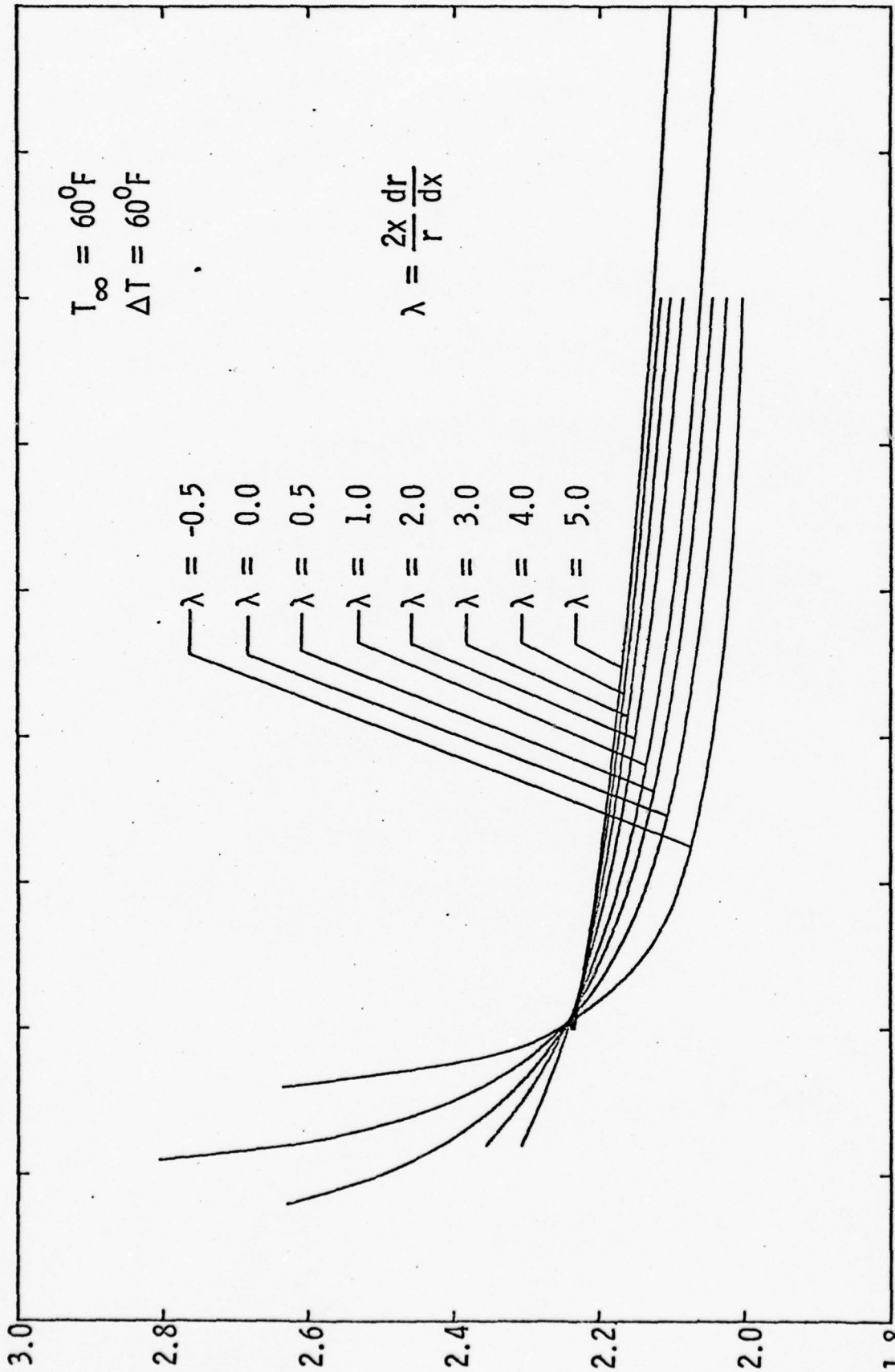

Figure 3 - Shape Factor Variation with M for $\Delta T=60°F$

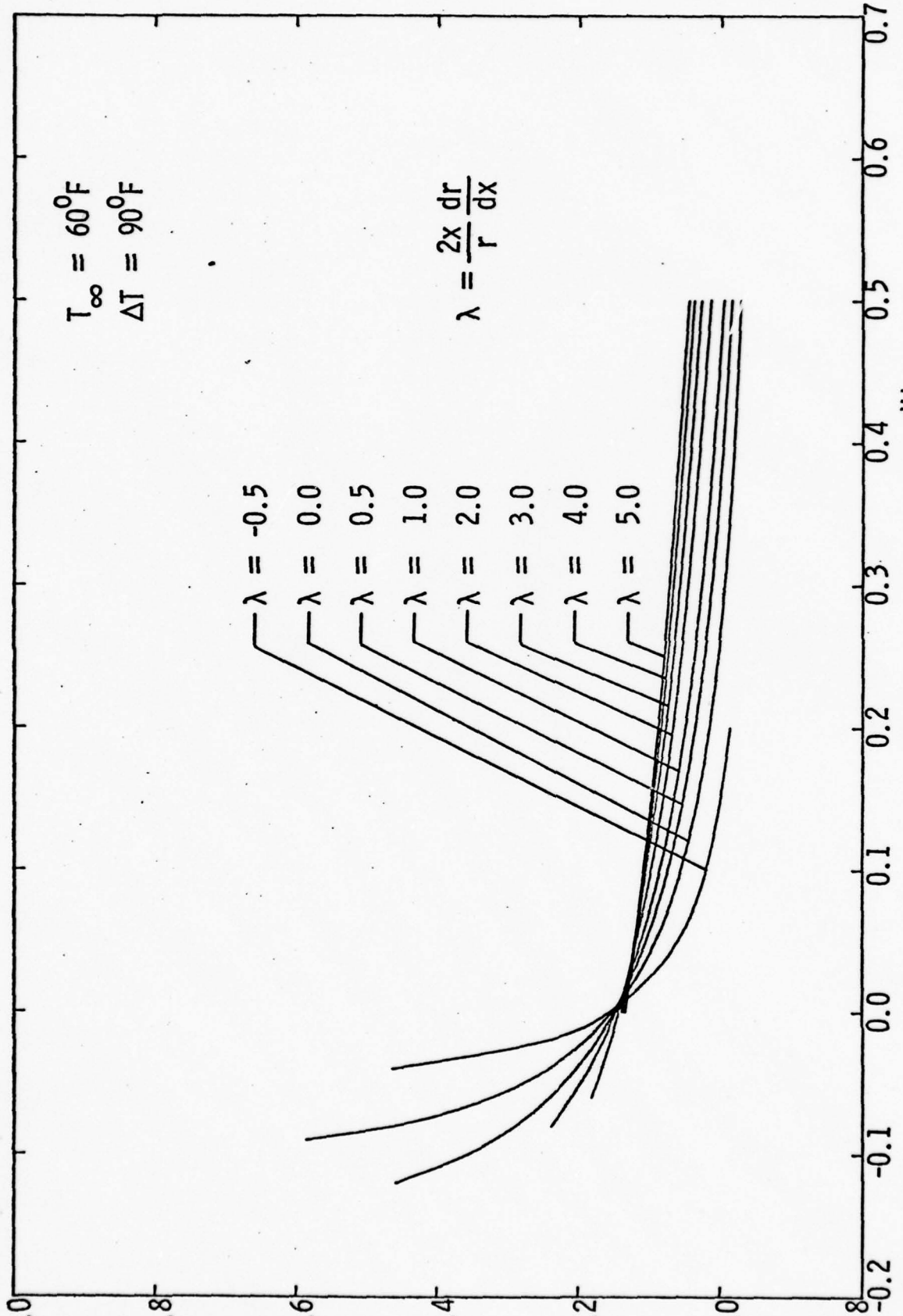

Figure 4 - Shape Factor Variation with M for $\Delta T=90°F$

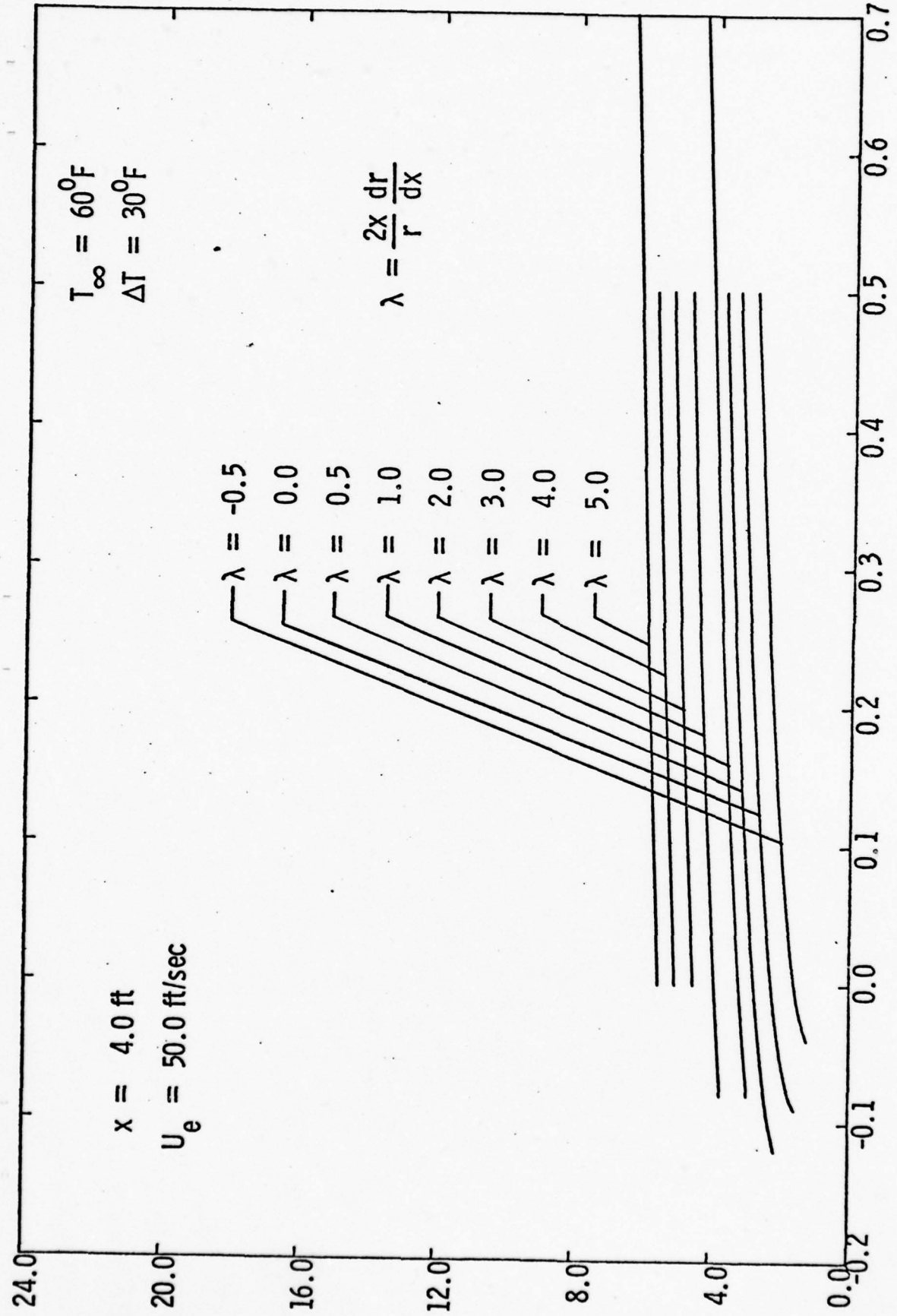

Figure 5 - Local Heat Flux Variation with M for ΔT=30°F

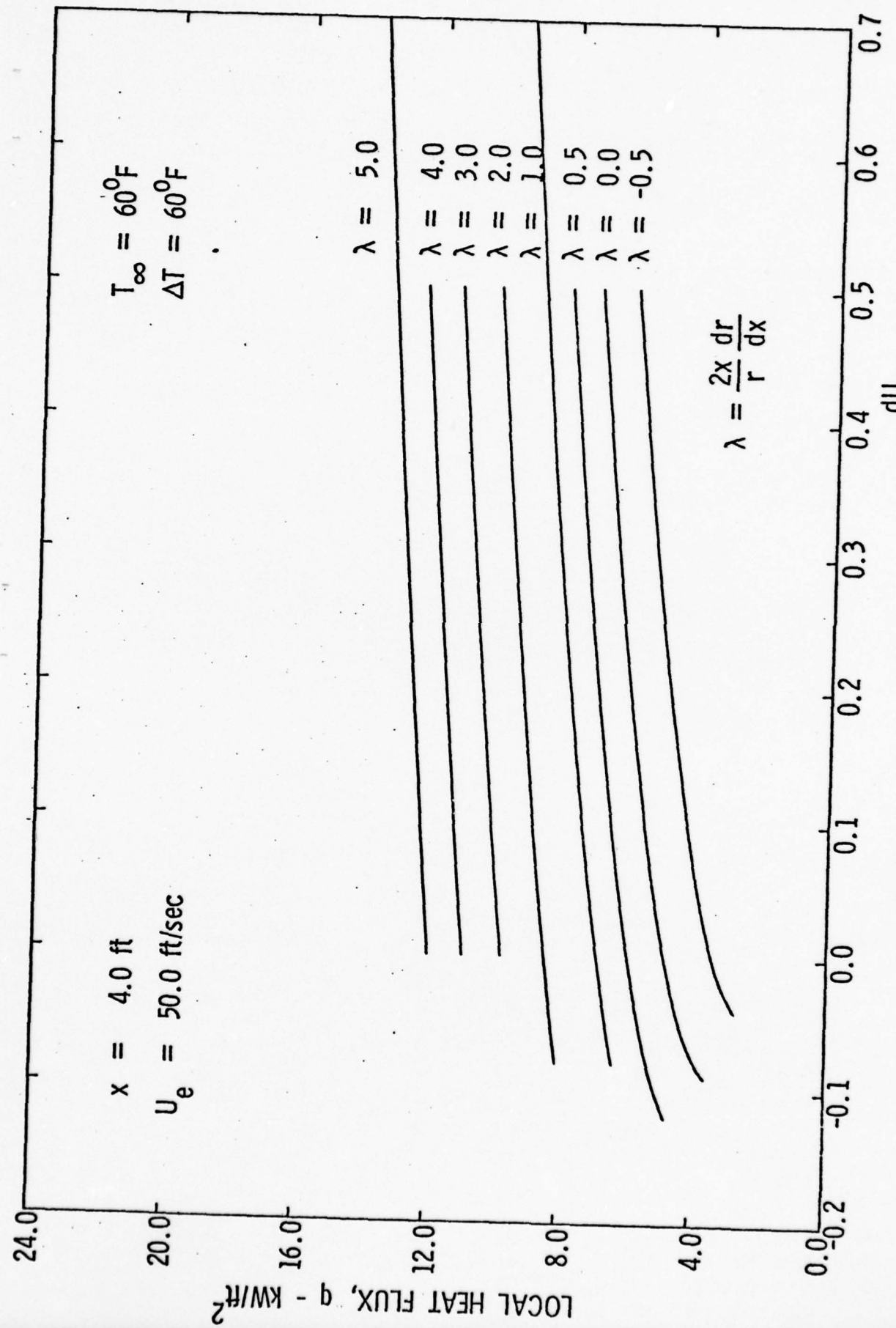

Figure 6 - Local Heat Flux Variation with M for ΔT=60°F

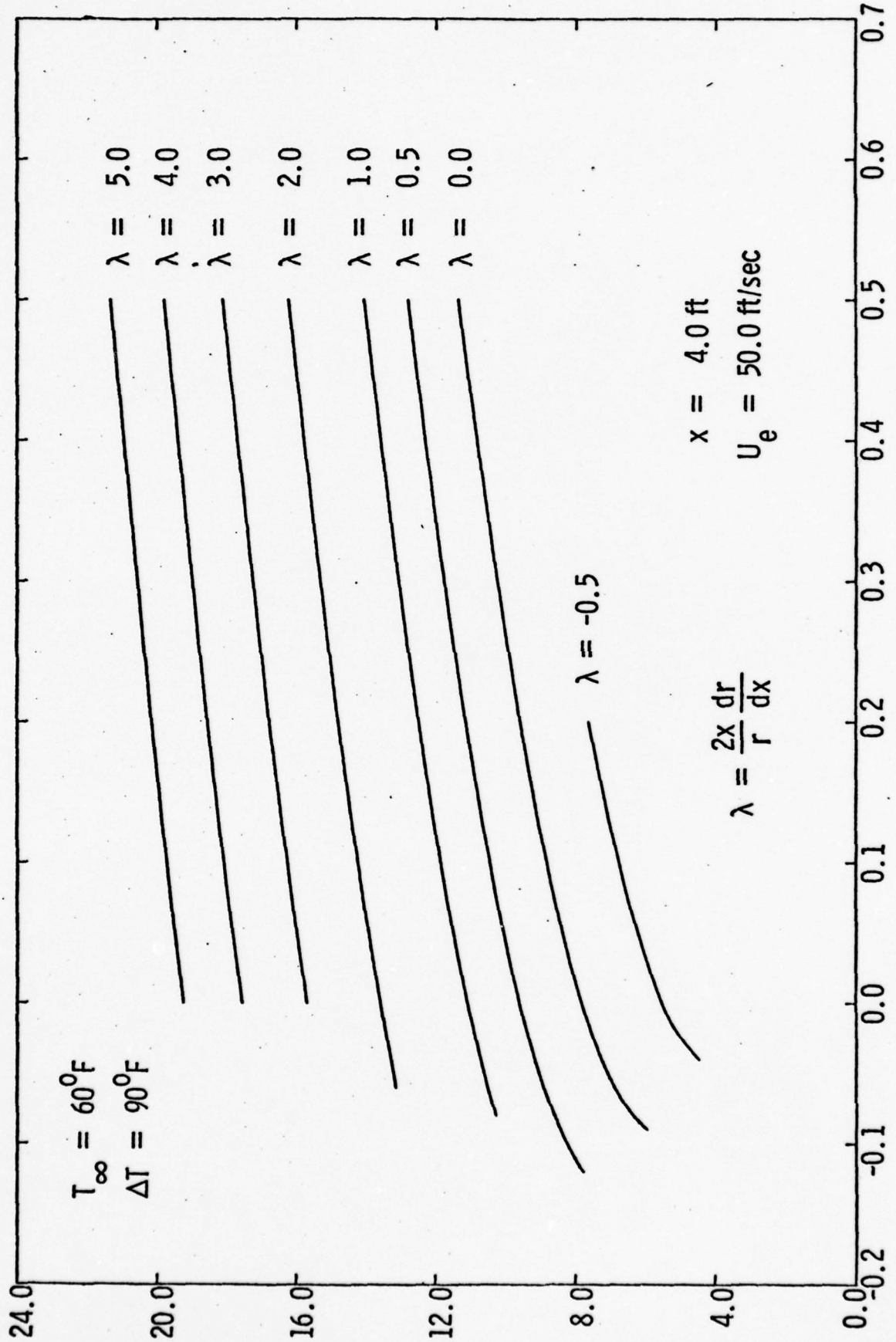

Figure 7 - Local Heat Flux Variation with M for ΔT=90°F

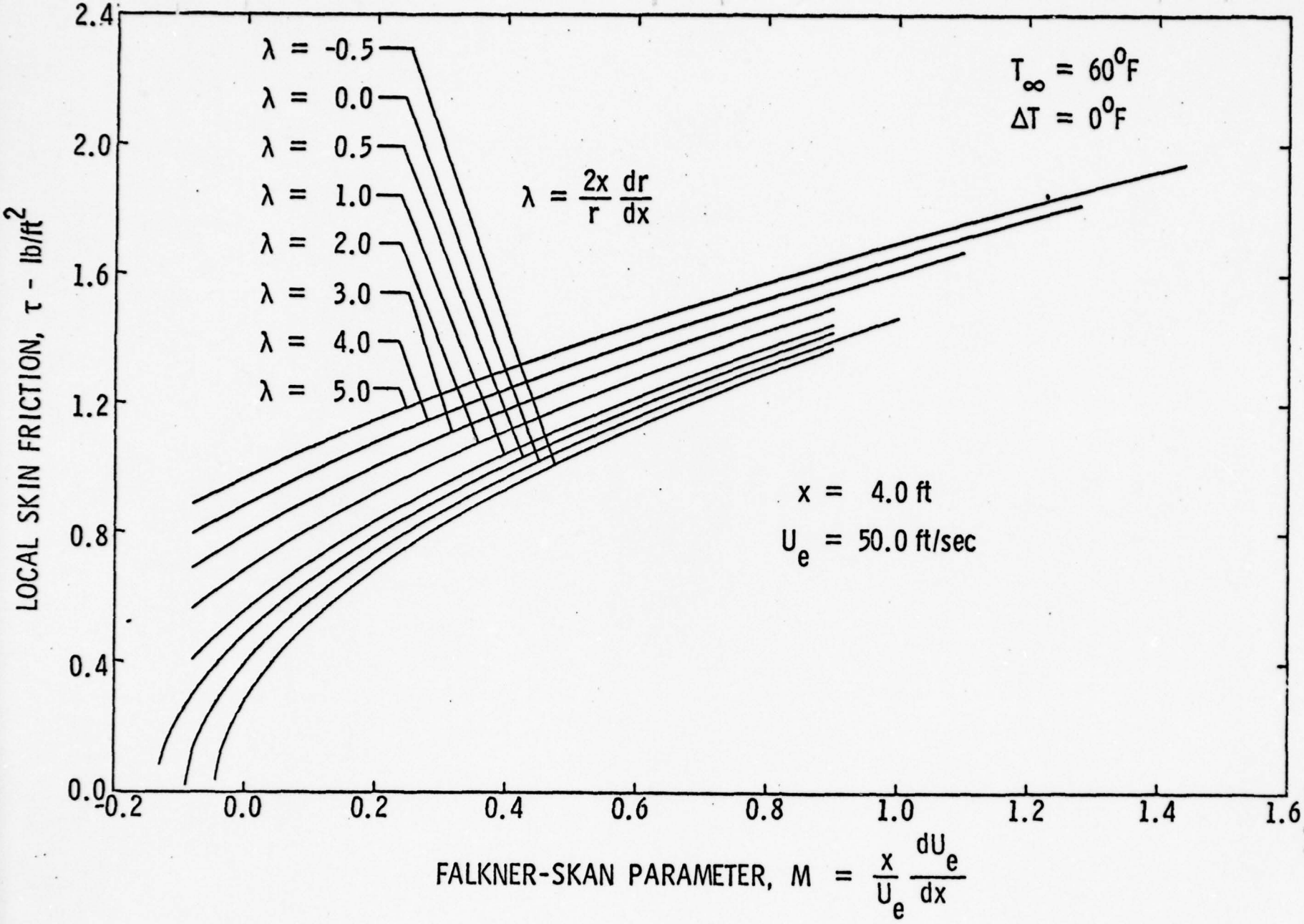

Figure 8 - Local Skin Friction Variation with M for ΔT=0

22 February 1978
JJE:jep

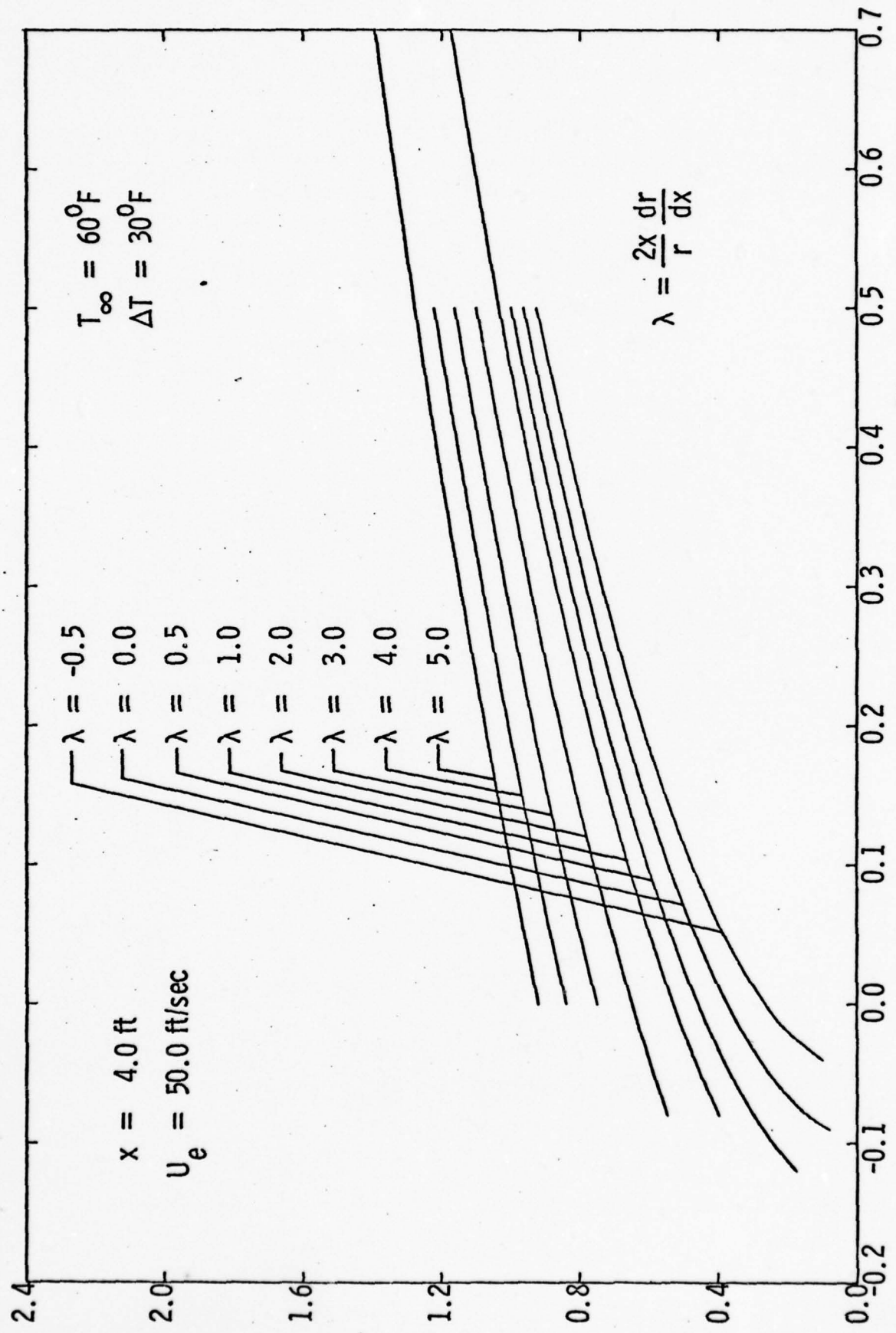

Figure 9 - Local Skin Friction Variation with M for ΔT=30°F

22 February 1978
JJE:jep

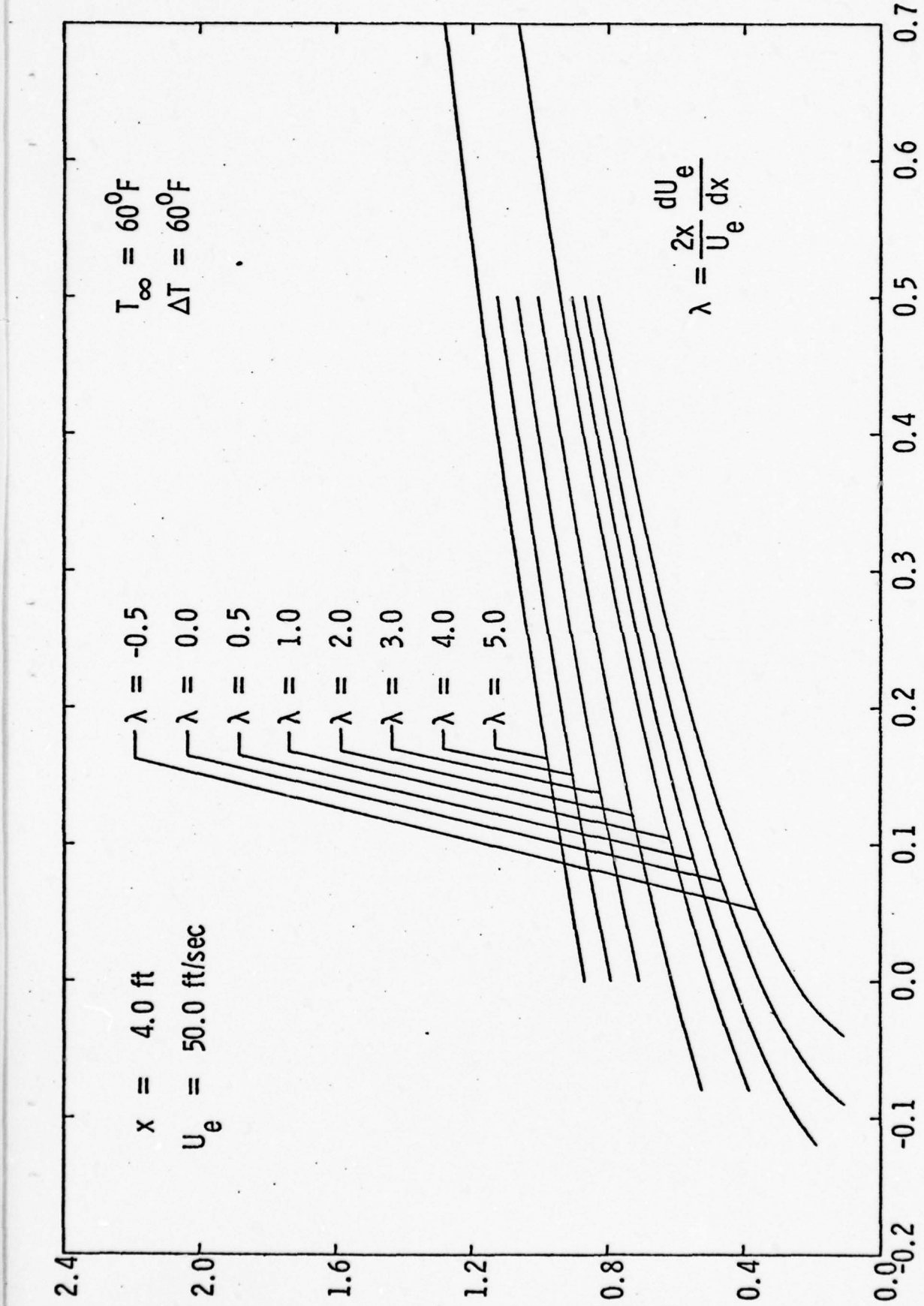

Figure 10 - Local Skin Friction Variation with M for ΔT=60°F

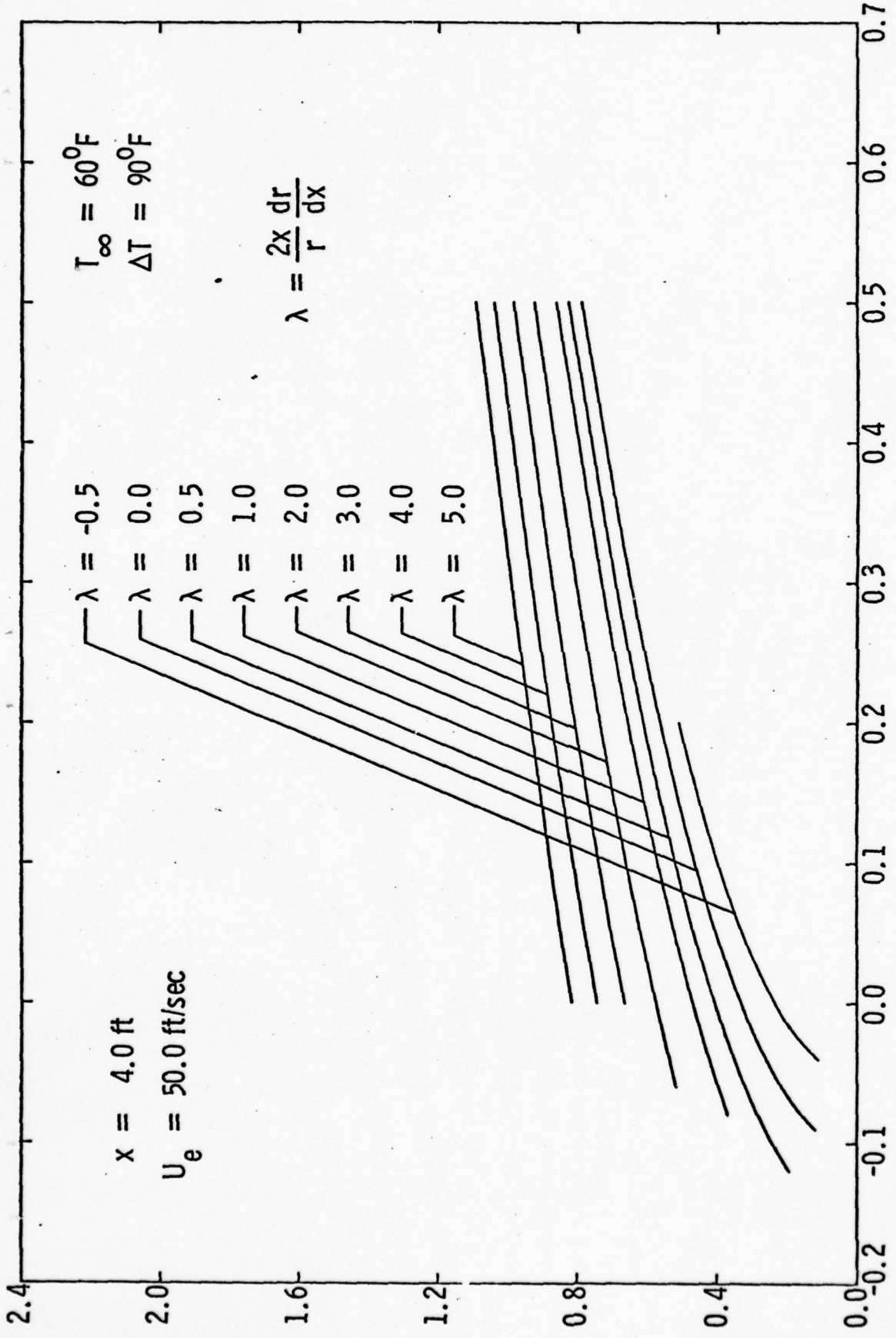

Figure 11 - Local Skin Friction Variation with M for ΔT=90°F

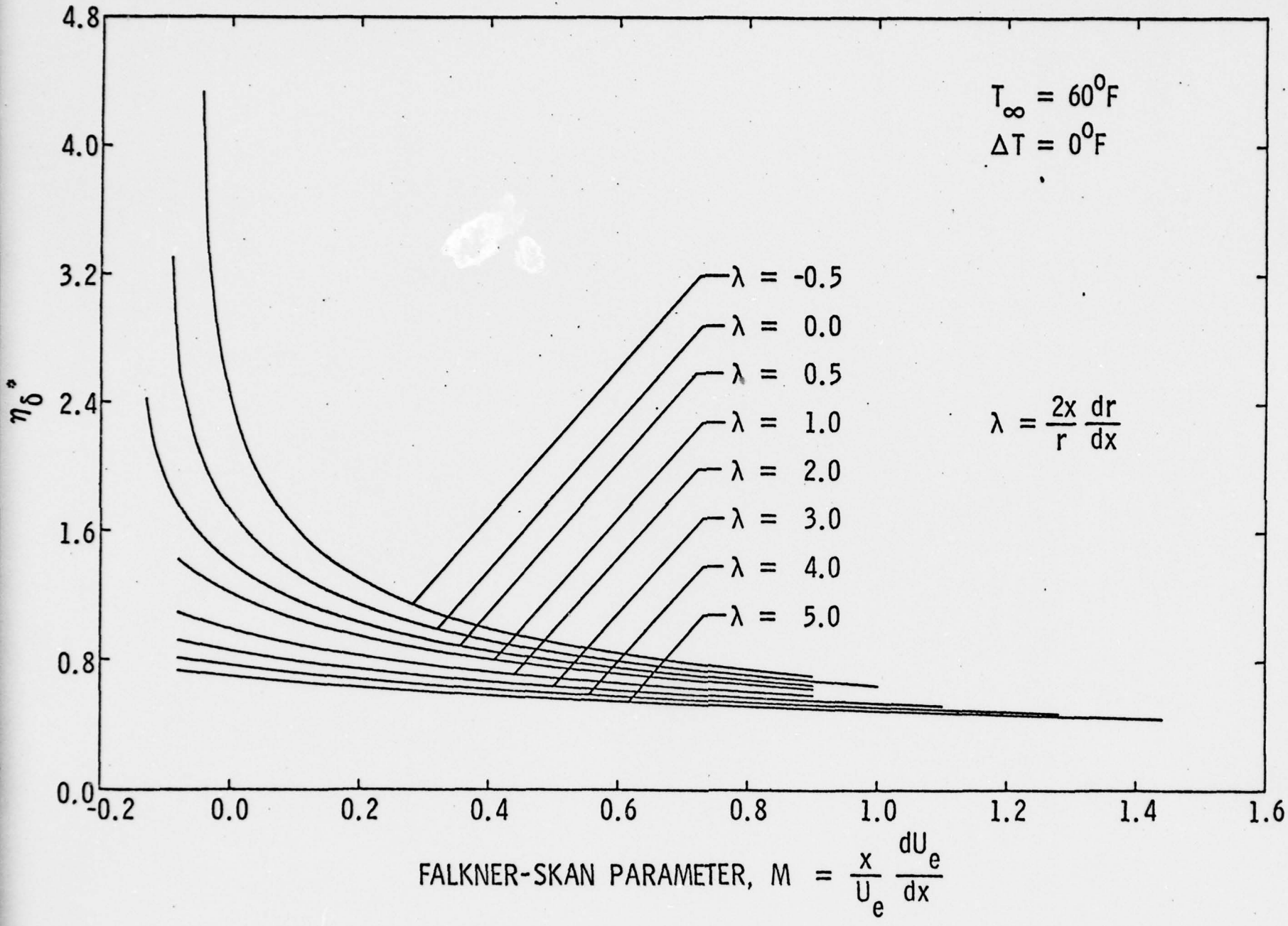

Figure 12 - η_{δ^*} Variation with M for $\Delta T=0$

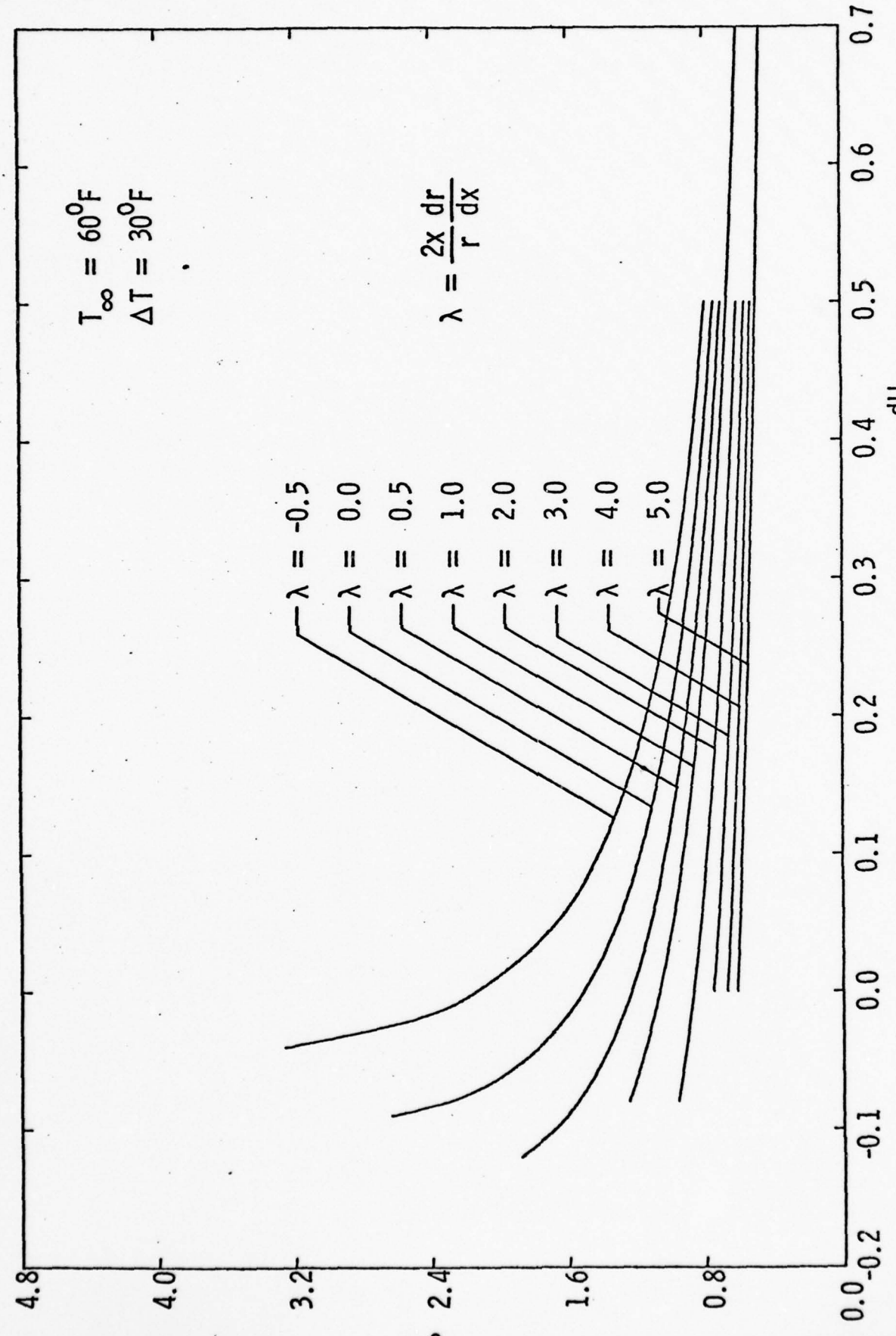

Figure 13 - η_δ^* Variation with M for $\Delta T=30°F$

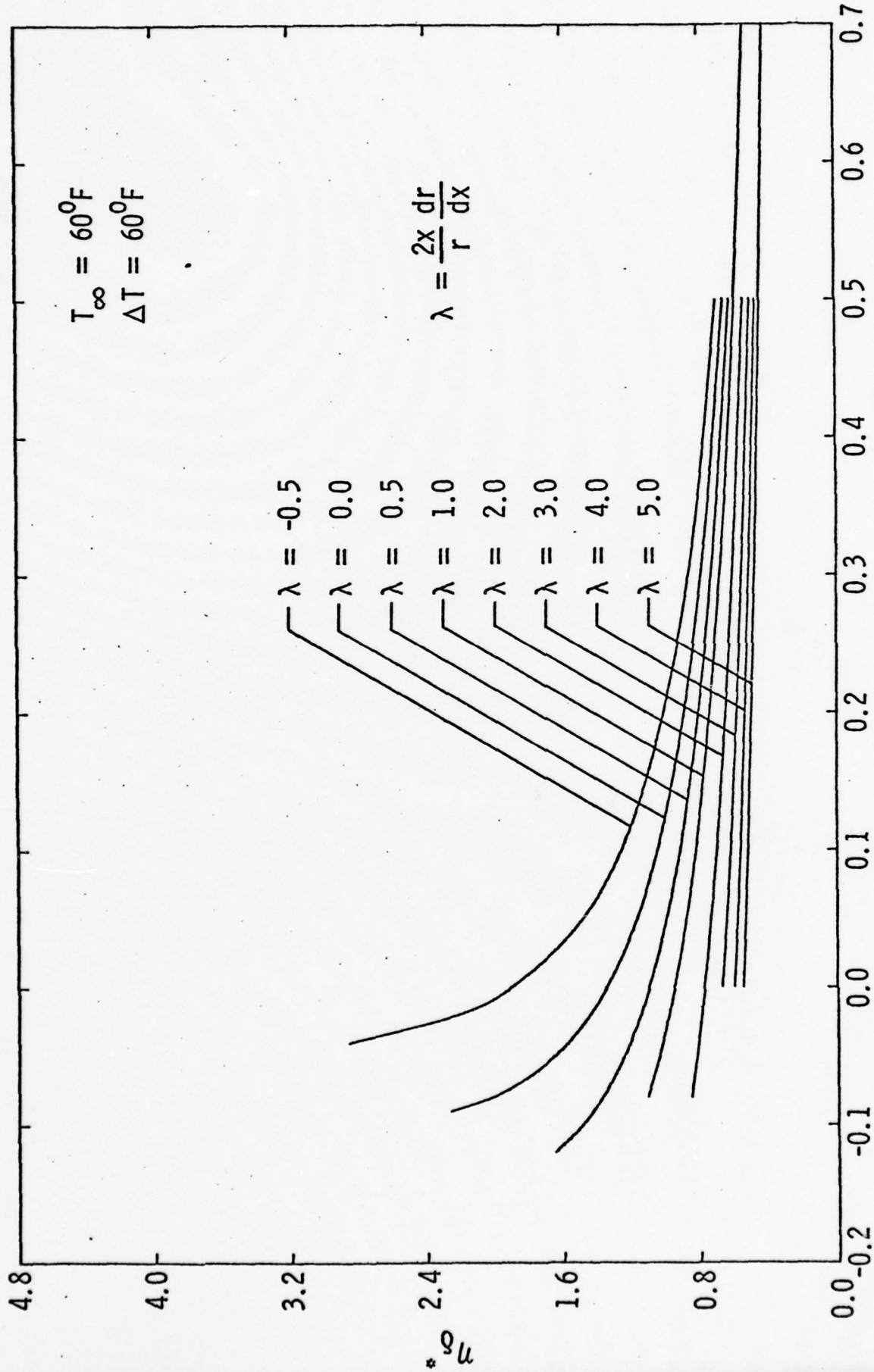

Figure 14 - η_{δ^*} Variation with M for $\Delta T=60°F$

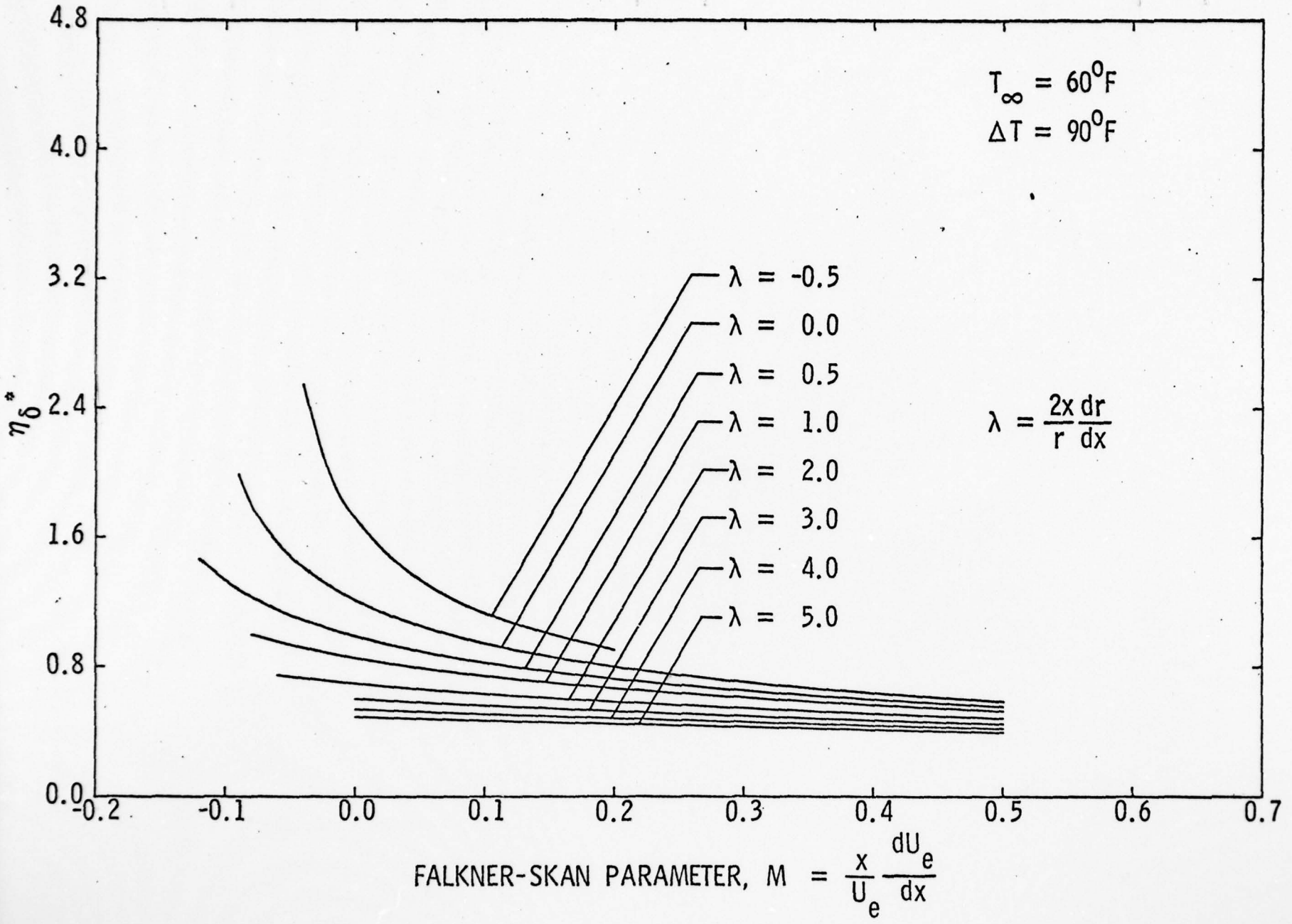

Figure 15 - η_{δ^*} Variation with M for $\Delta T=90°F$

22 February 1978
JJE:jep

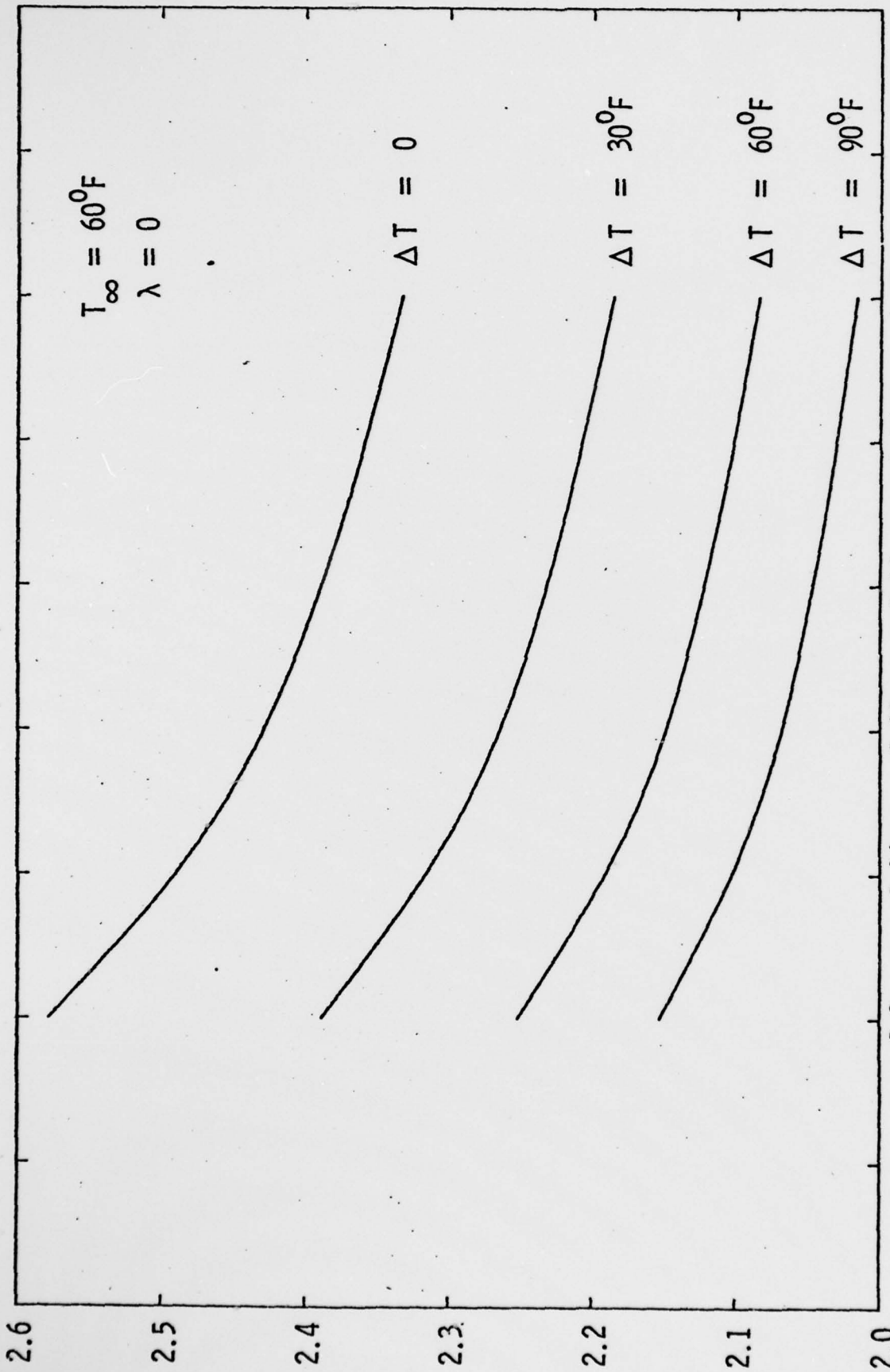

Figure 16 - Shape Factor Variation with M for T_∞=60°F

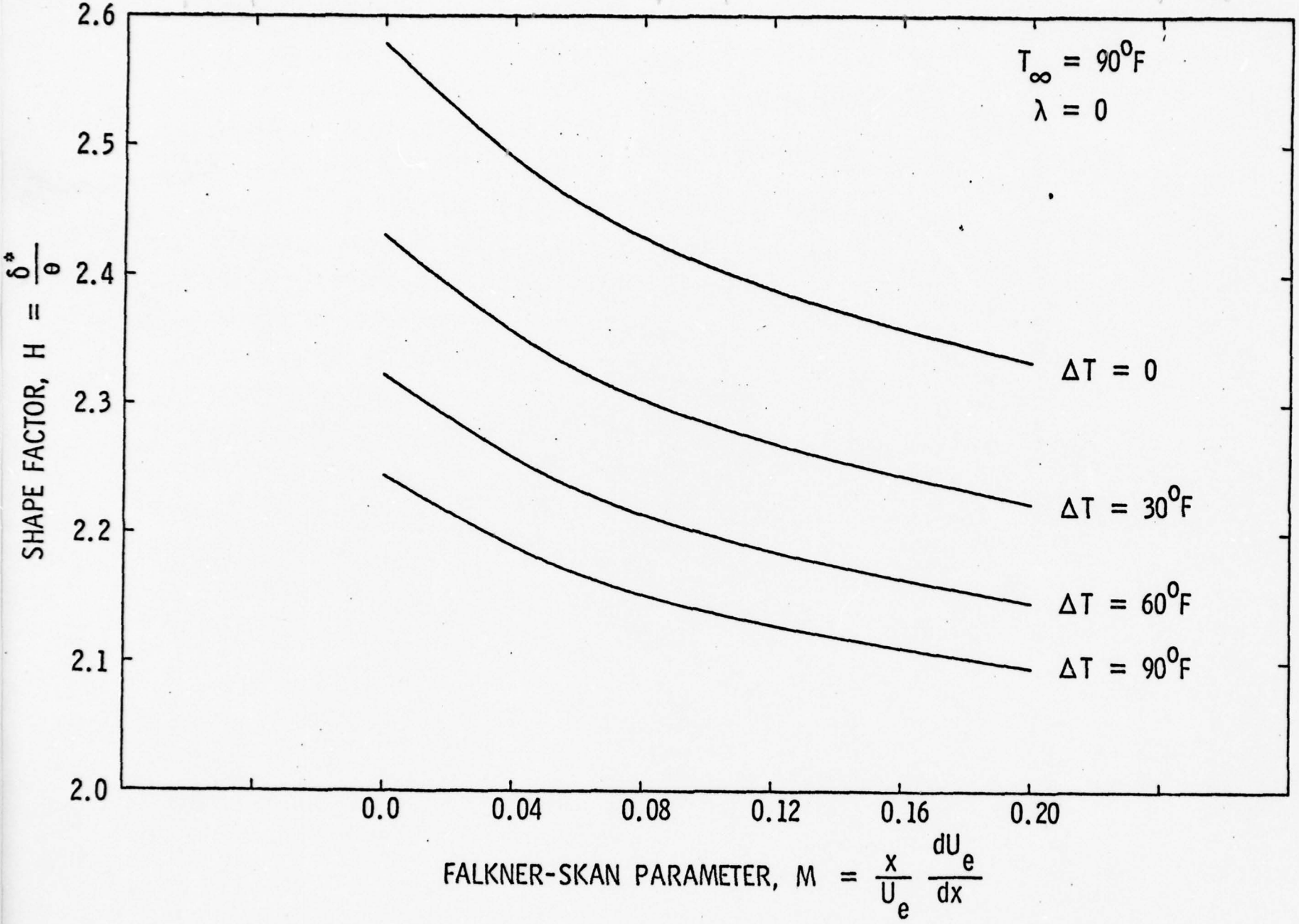

Figure 17 - Shape Factor Variation with M for T_∞=90°F

22 February 1978
JJE:jep

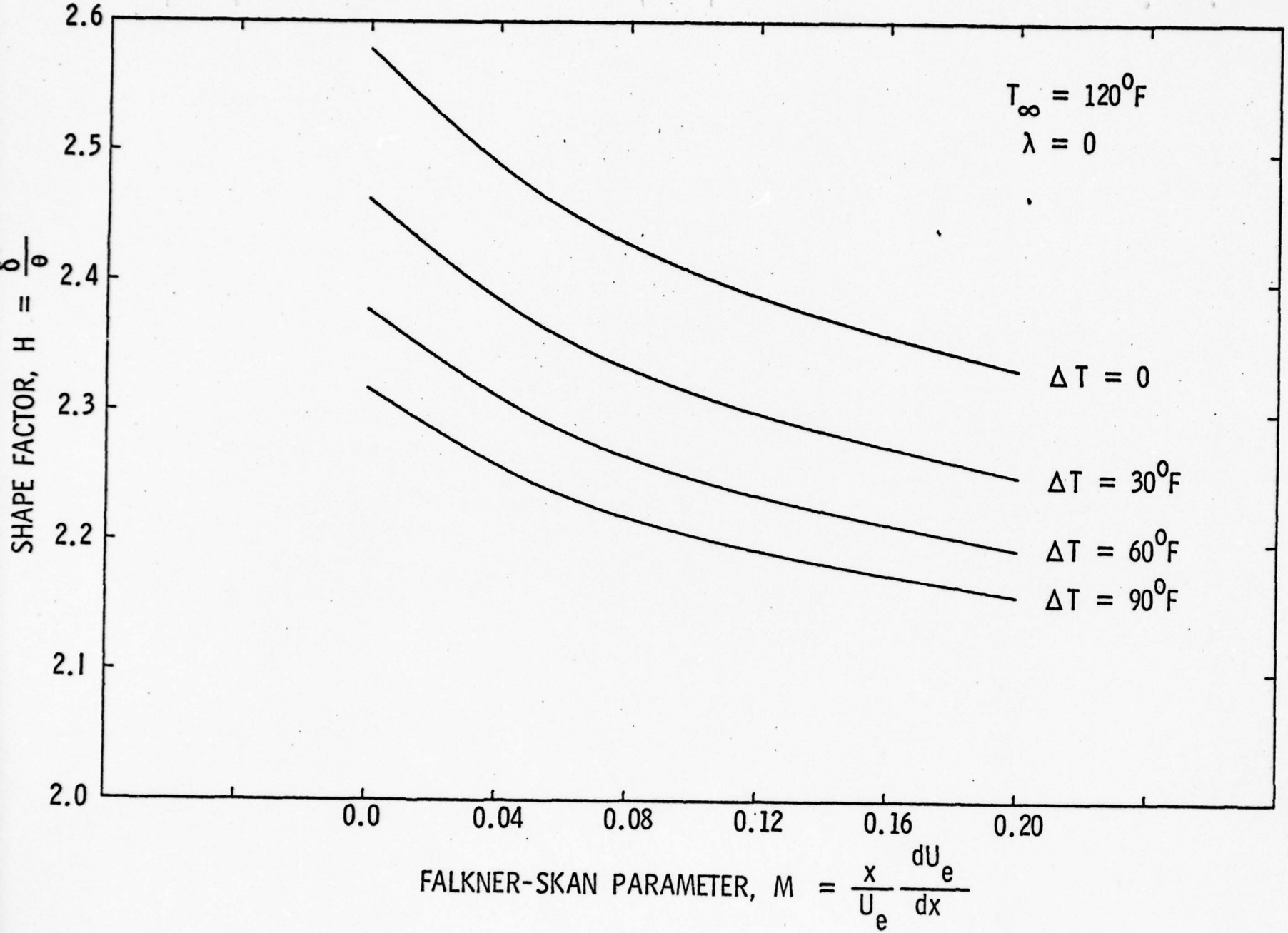

Figure 18 - Shape Factor Variation with M for T_∞=120°F

22 February 1978
JJE:jep

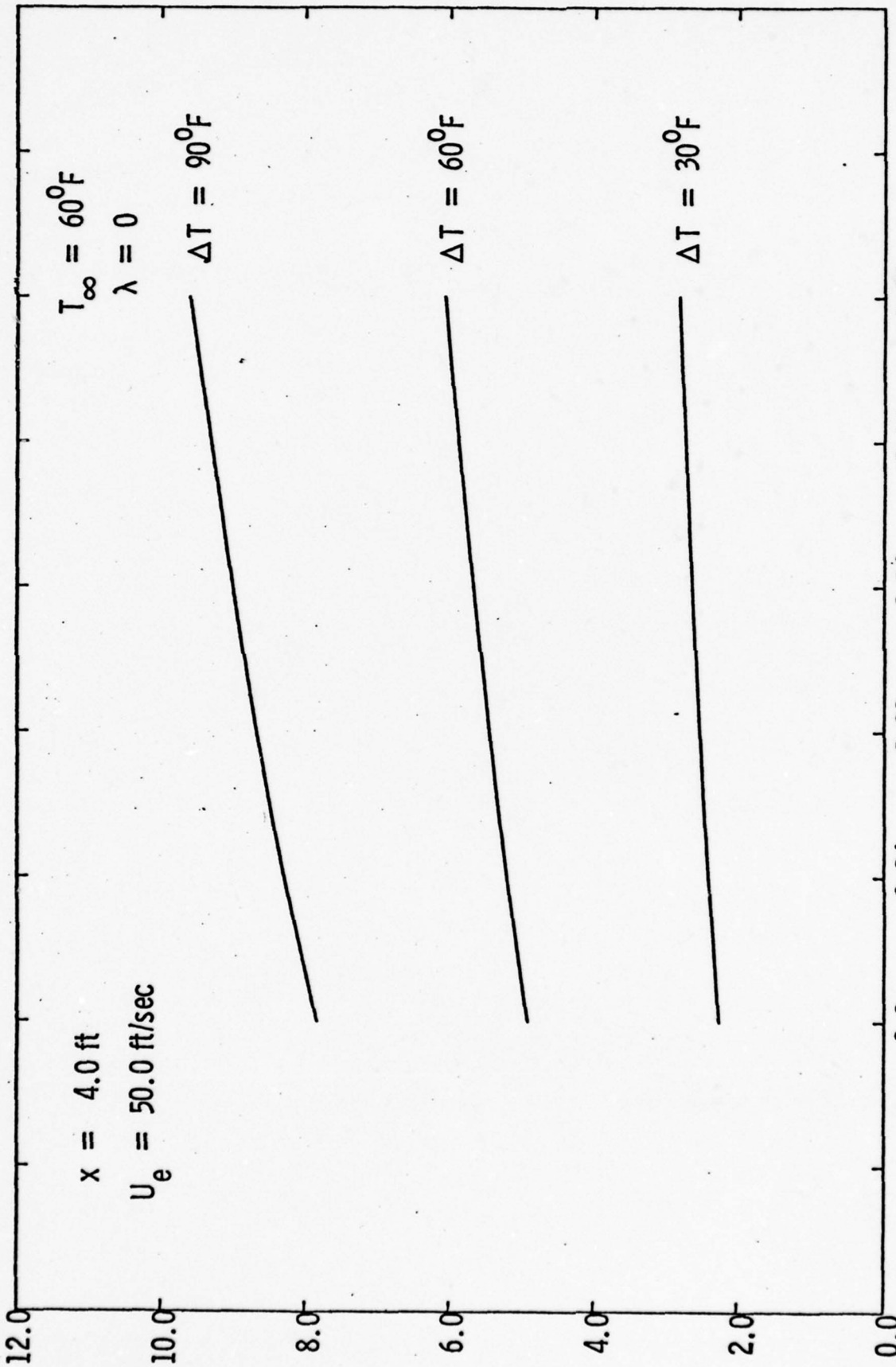

Figure 19. - Local Heat Flux Variation with M for T_∞=60°F

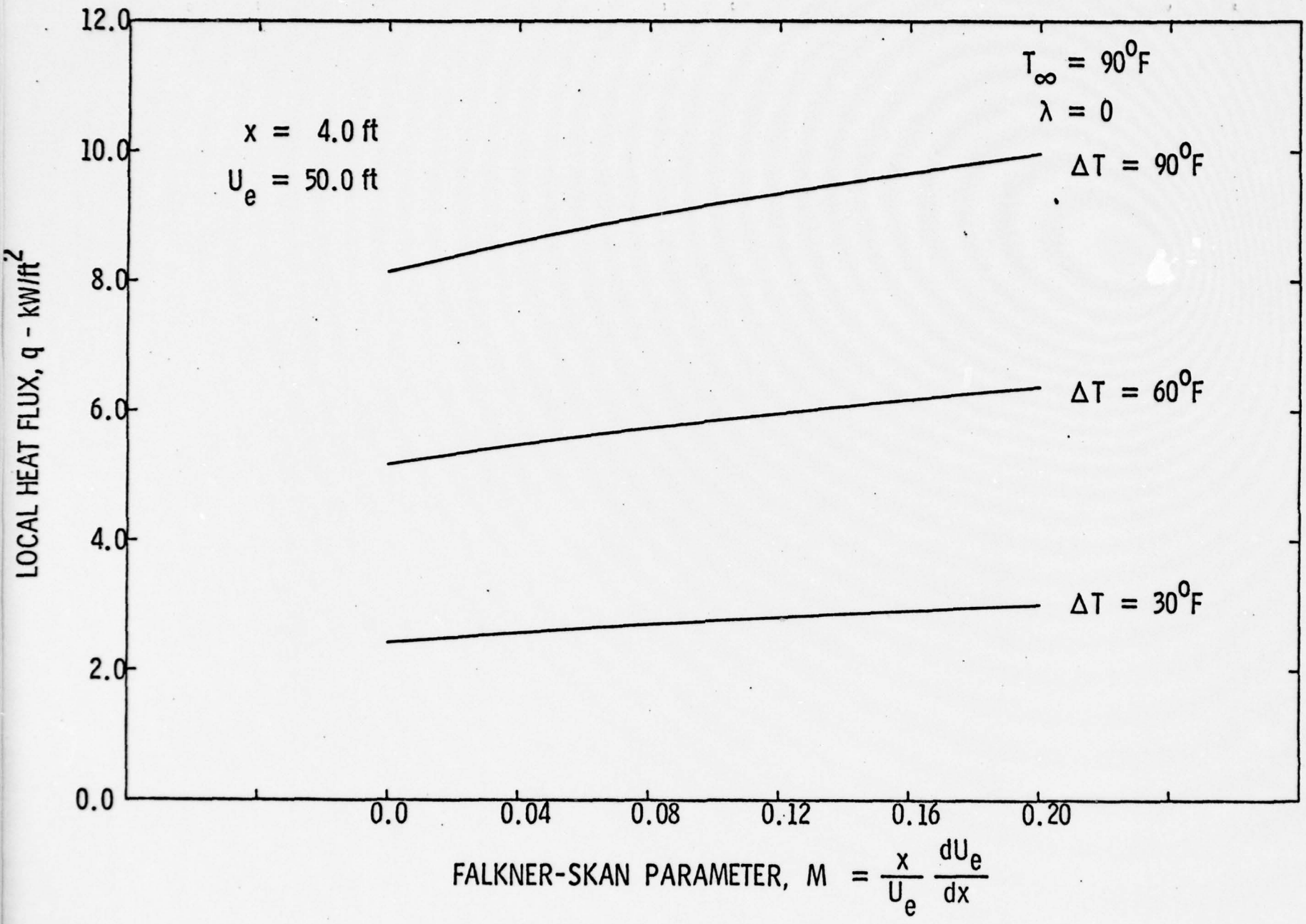

Figure 20 - Local Heat Flux Variation with M for T_∞=90°F

22 February 1978
JJE:jep

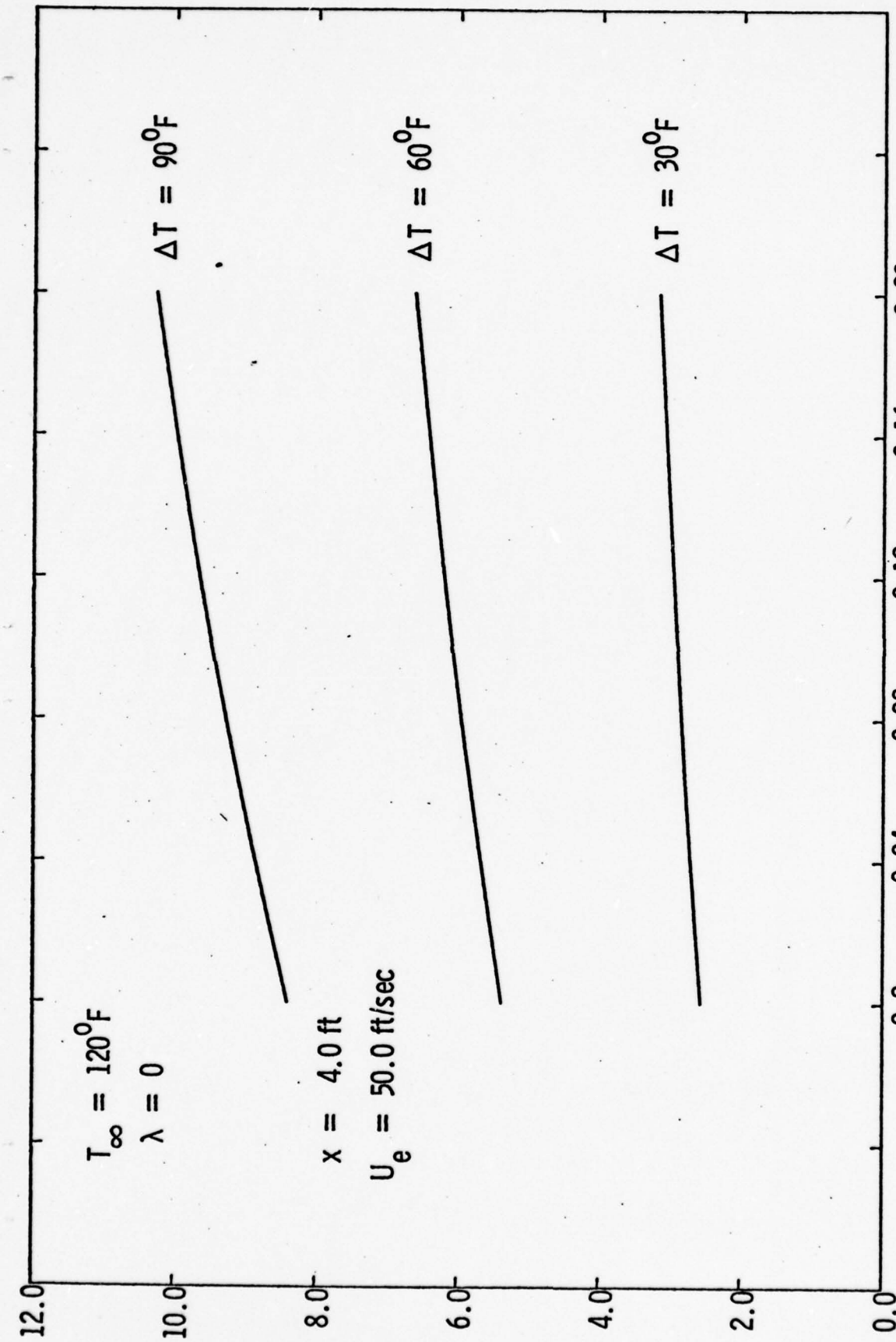

Figure 21 - Local Heat Flux Variation with M for T_∞=120°F

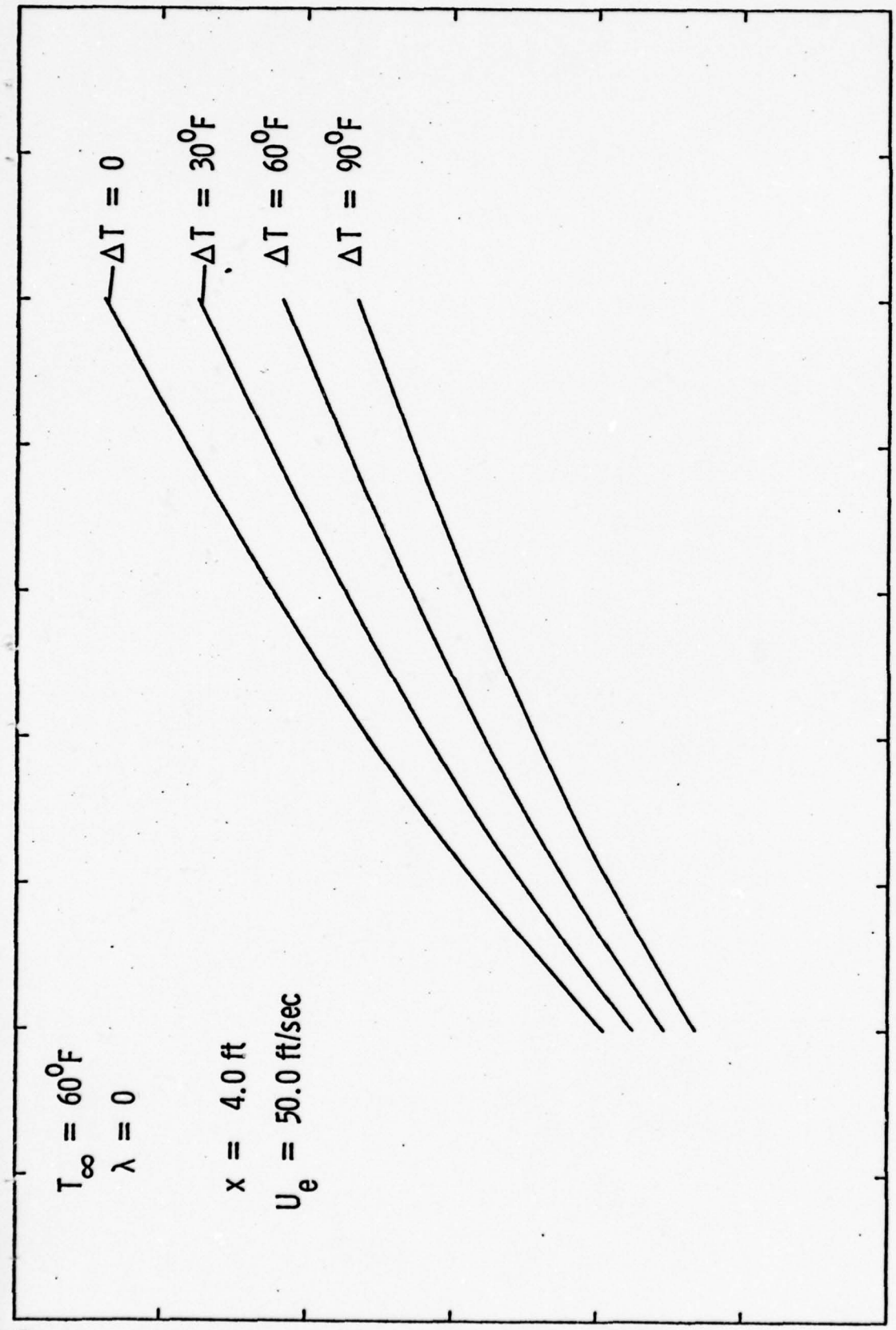

Figure 22 - Local Skin Friction Variation with M for T_∞=60°F

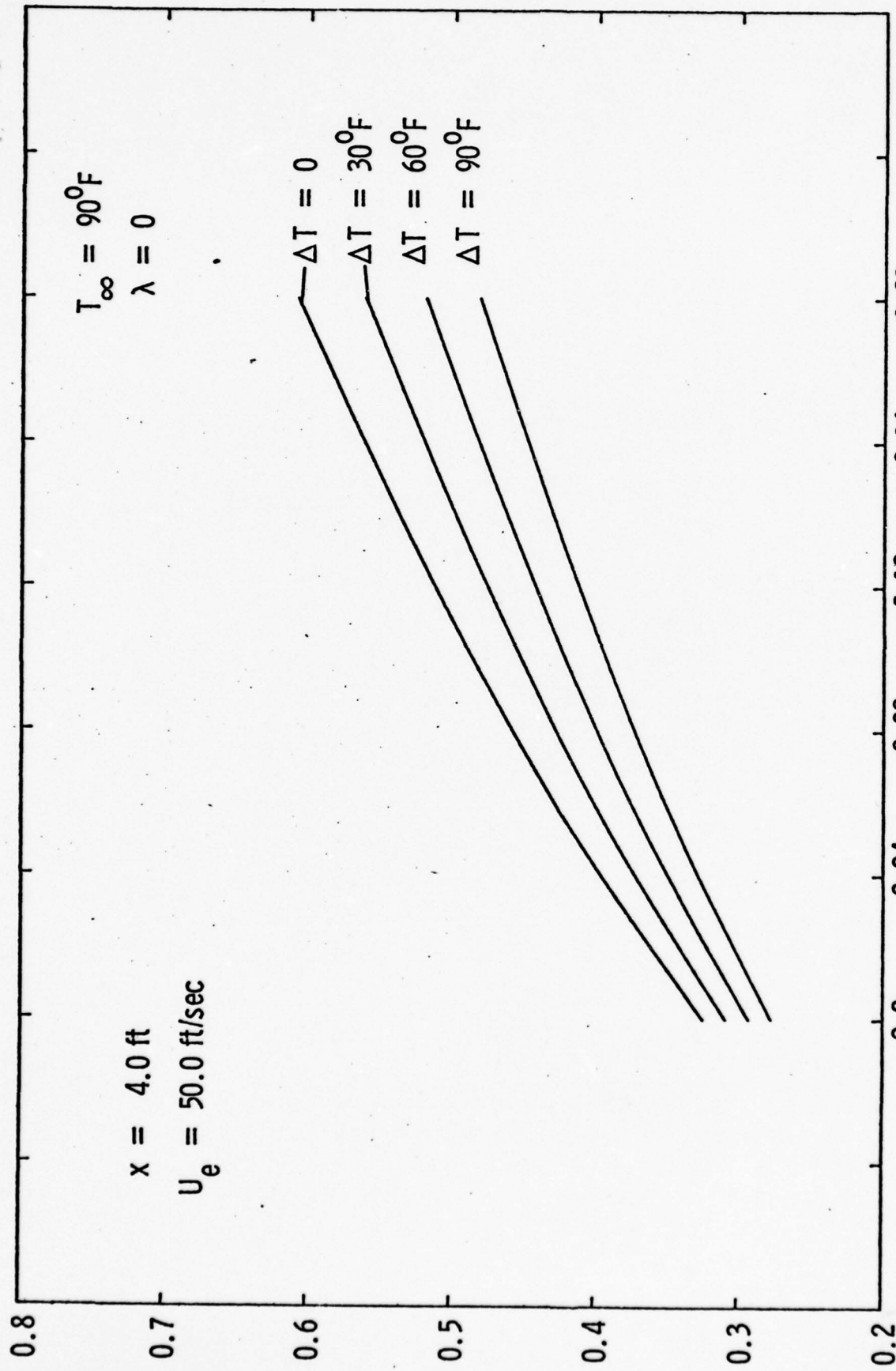

Figure 23 - Local Skin Friction Variation with M for T_∞=90°F

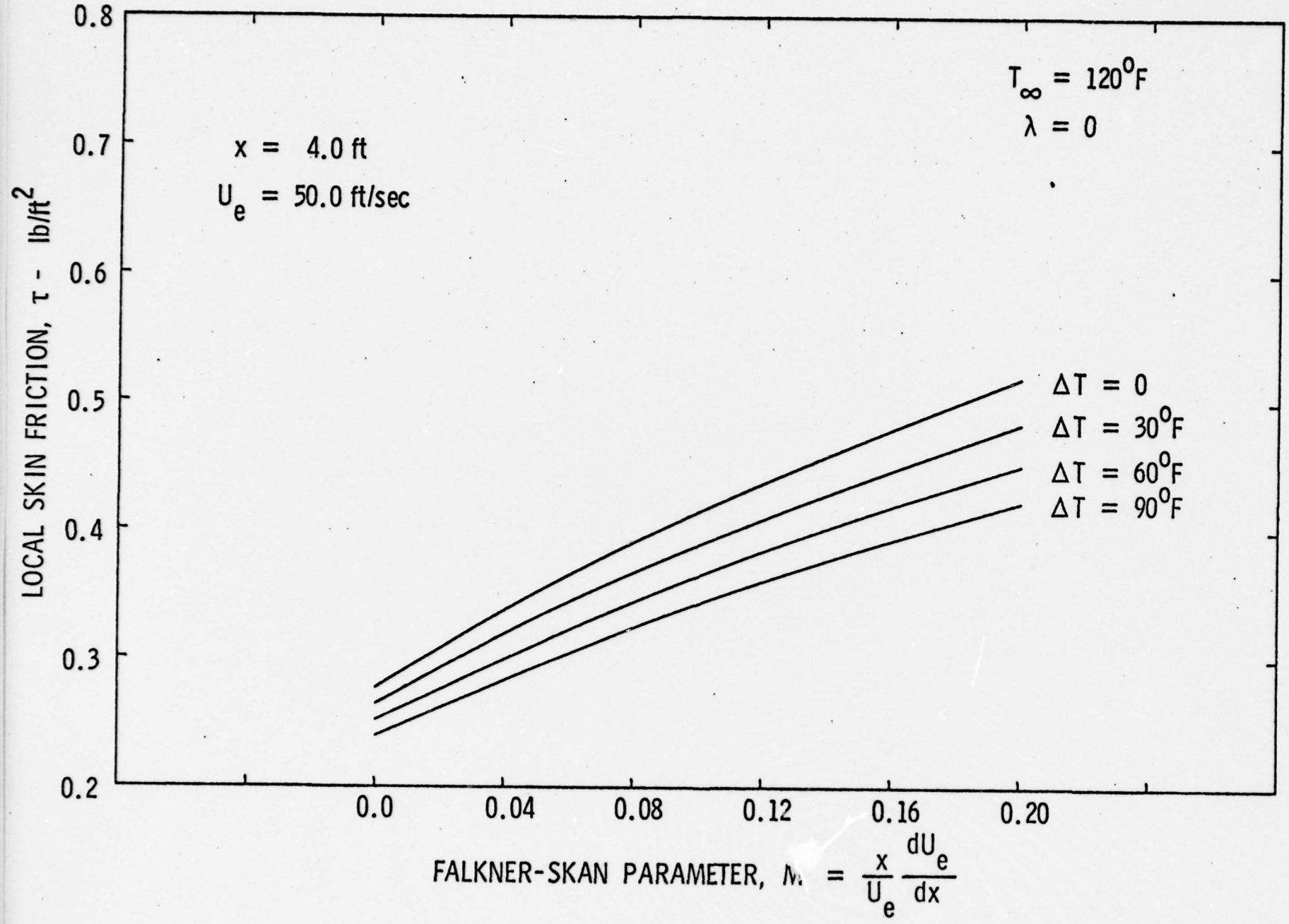

Figure 24 - Local Skin Friction Variation with M for T_∞=120°F

22 February 1978
JJE:jep

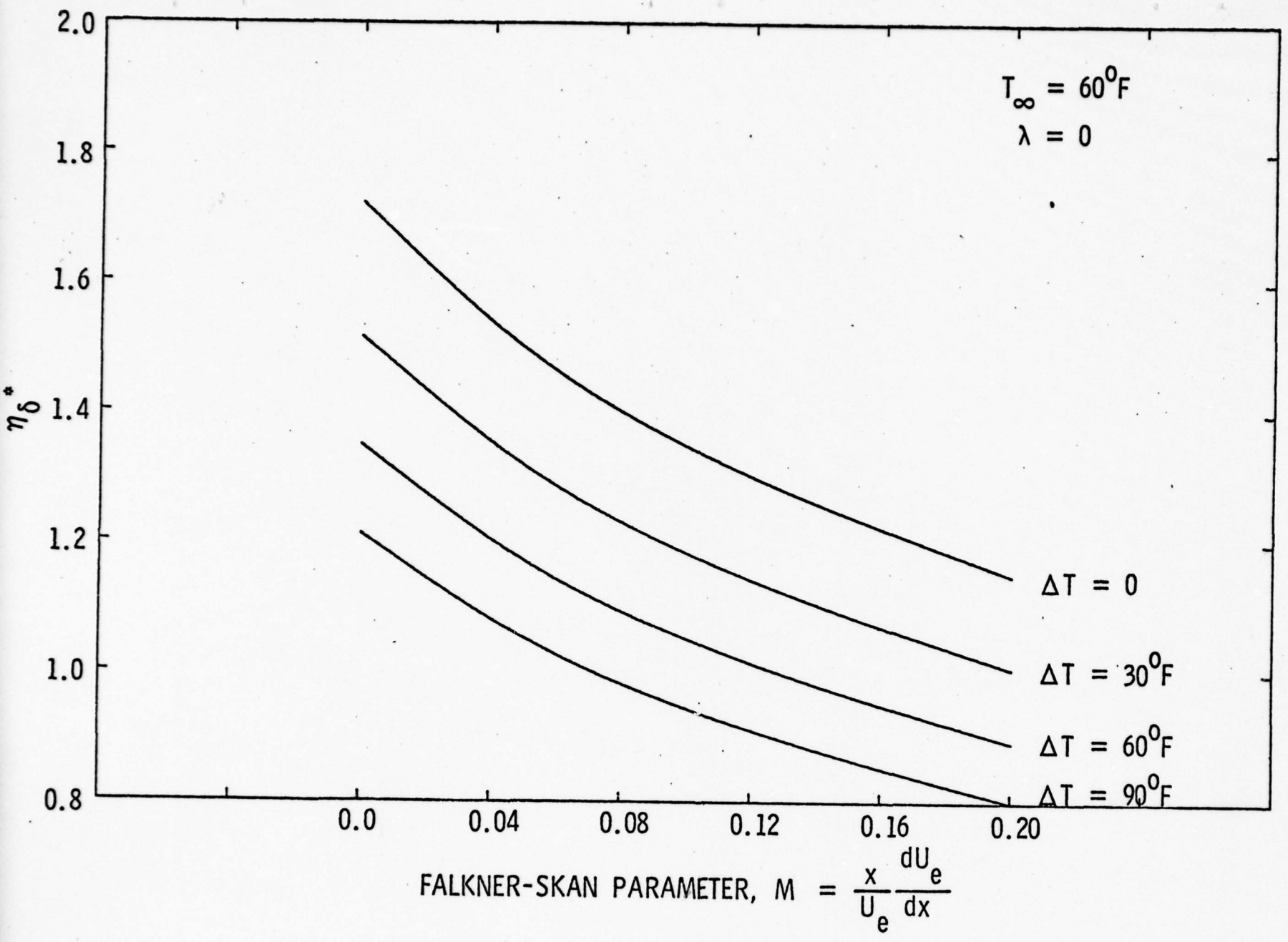

Figure 25 - η_δ* Variation with M for T_∞=60°F

22 February 1978
JJE:jep

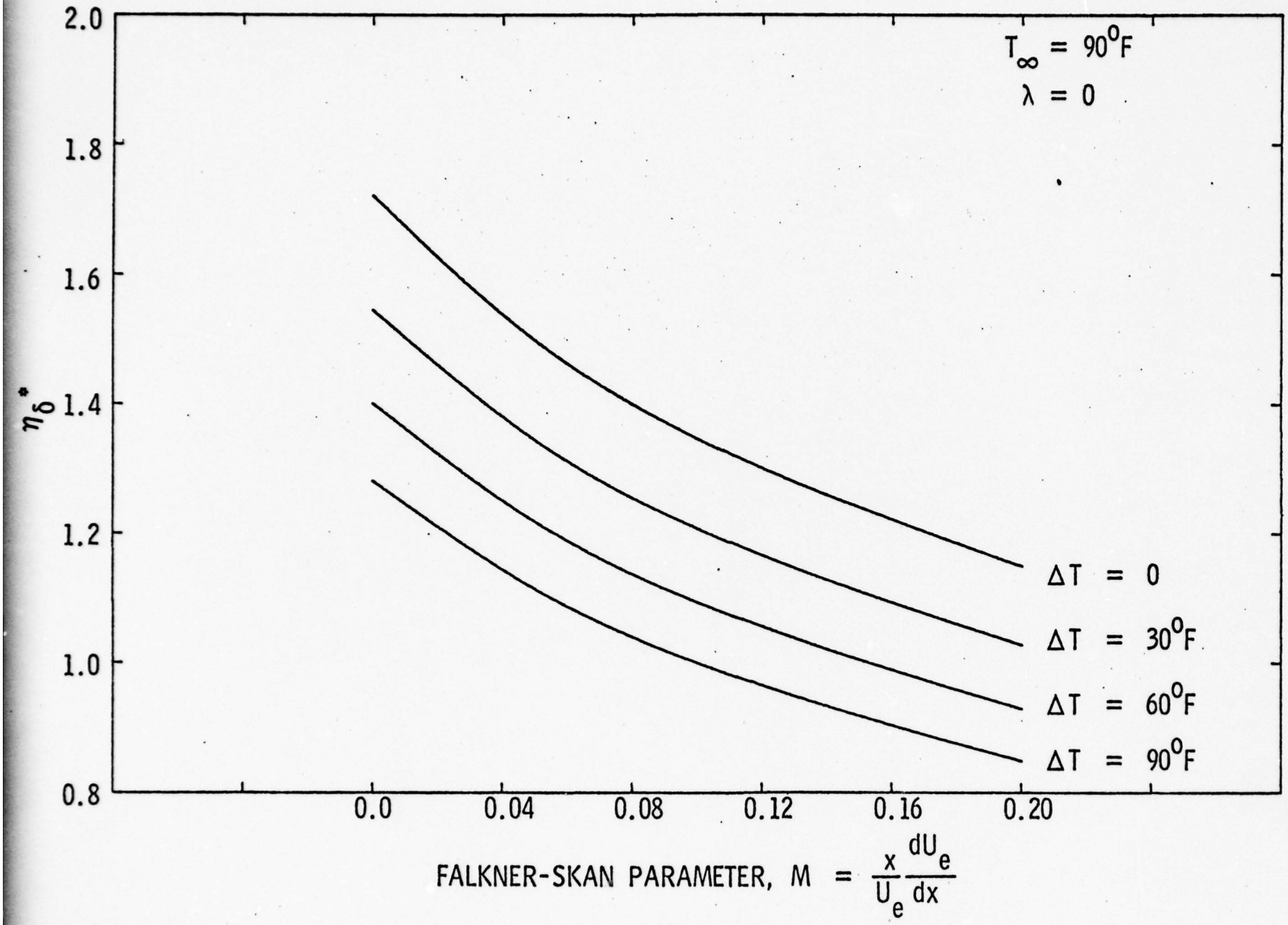

Figure 26 - $\eta_{\delta}*$ Variation with M for T_∞=90°F

22 February 1978
JJE:jep

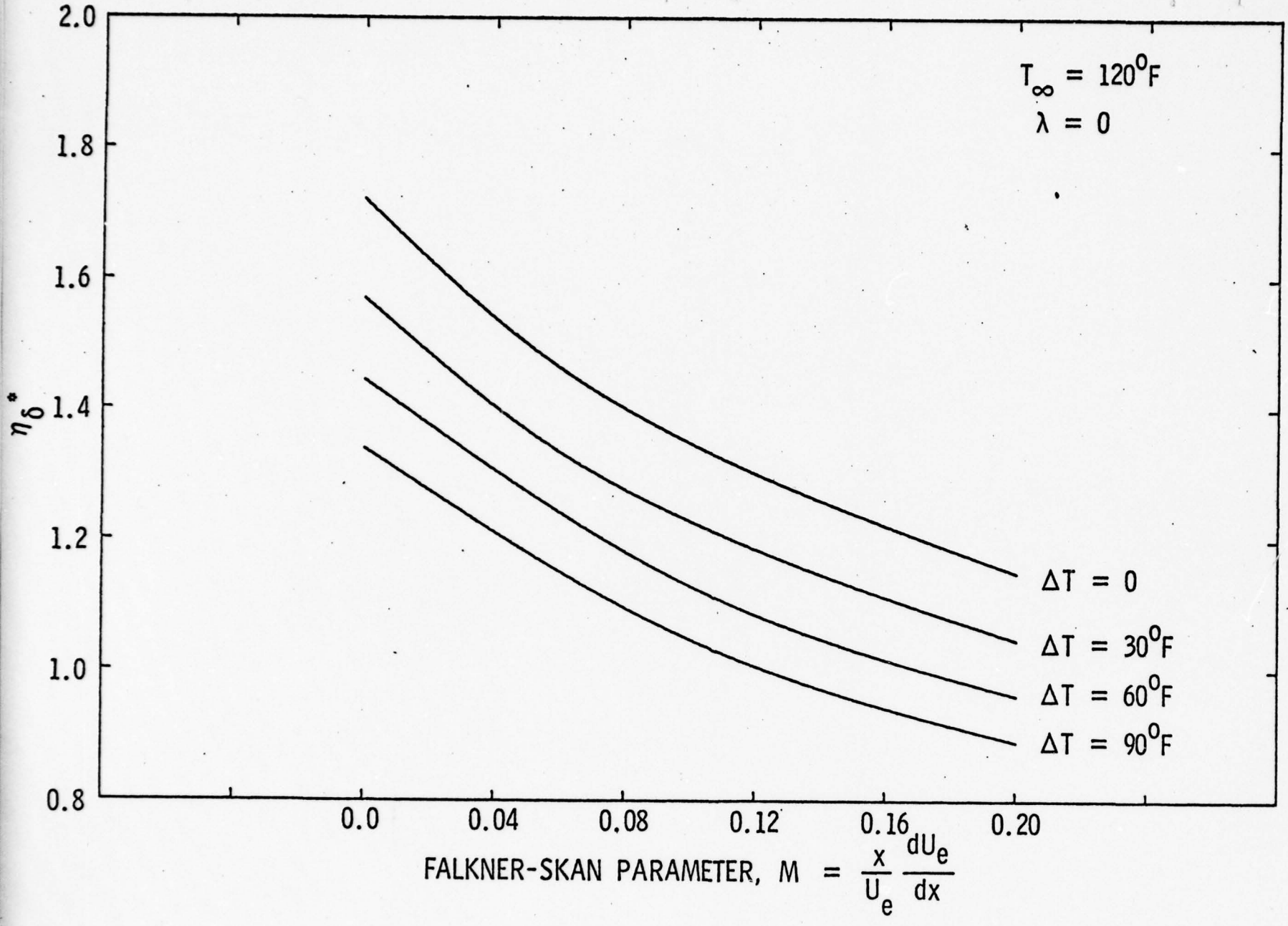

Figure 27 - η_δ^* Variation with M for T_∞=120°F

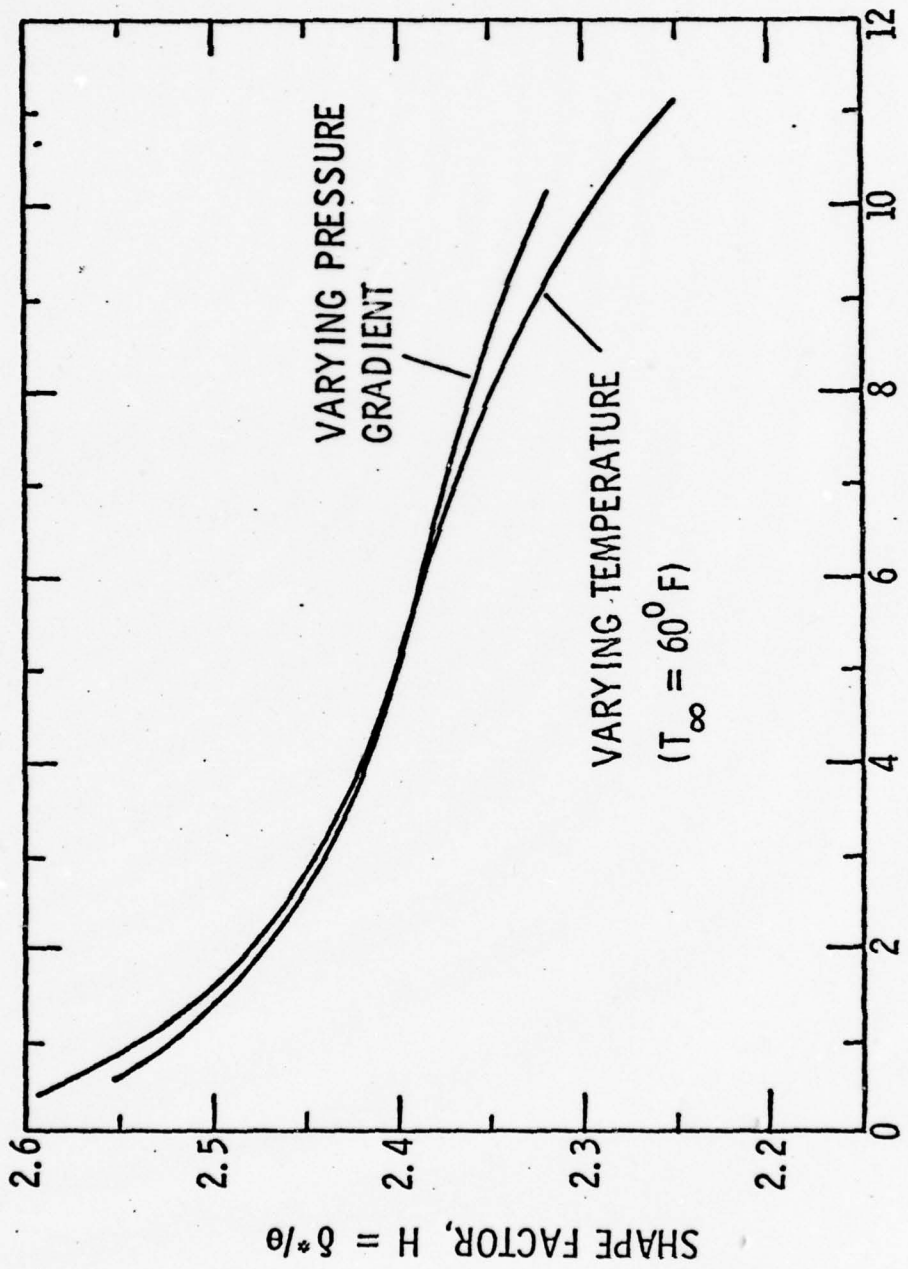

Figure 28 - Correlation of Shape Factor with Critical Reynolds Number

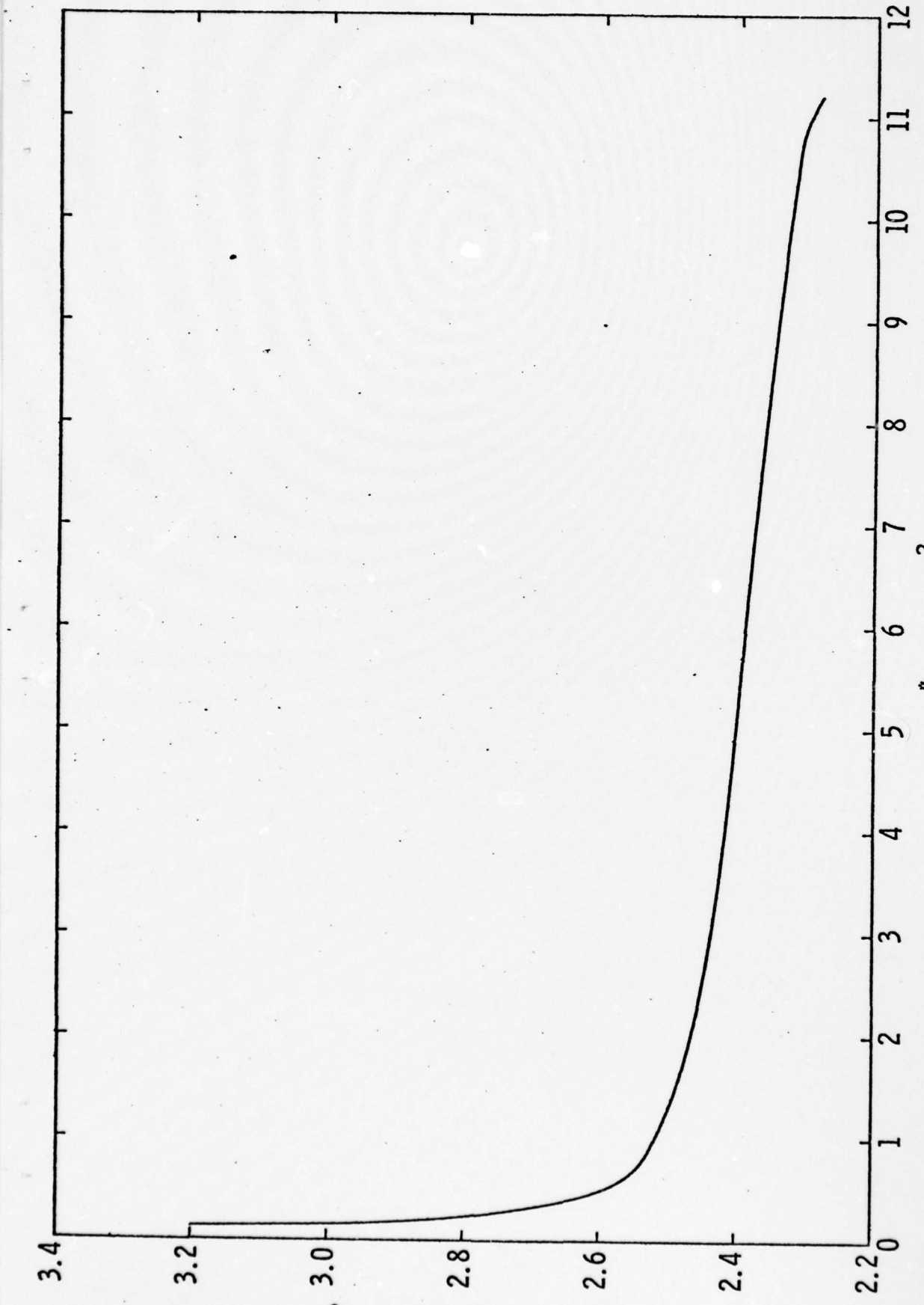

Figure 29 - Shape Factor vs Critical Reynolds Number

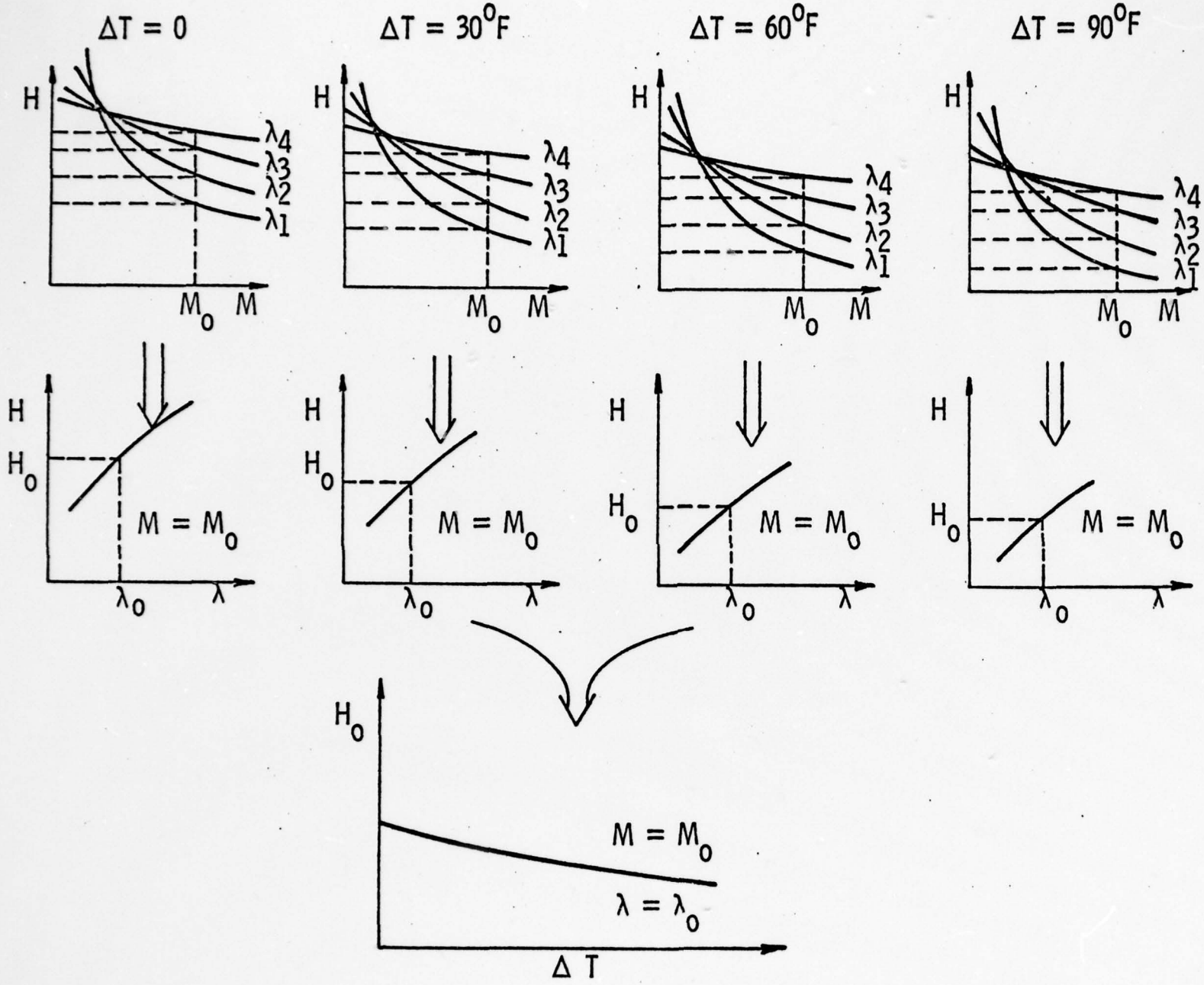

Figure 30 - Interpolation Procedure for Boundary Layer Data

22 February 1978
JJE:jep

22 February 1978
JJE:jep

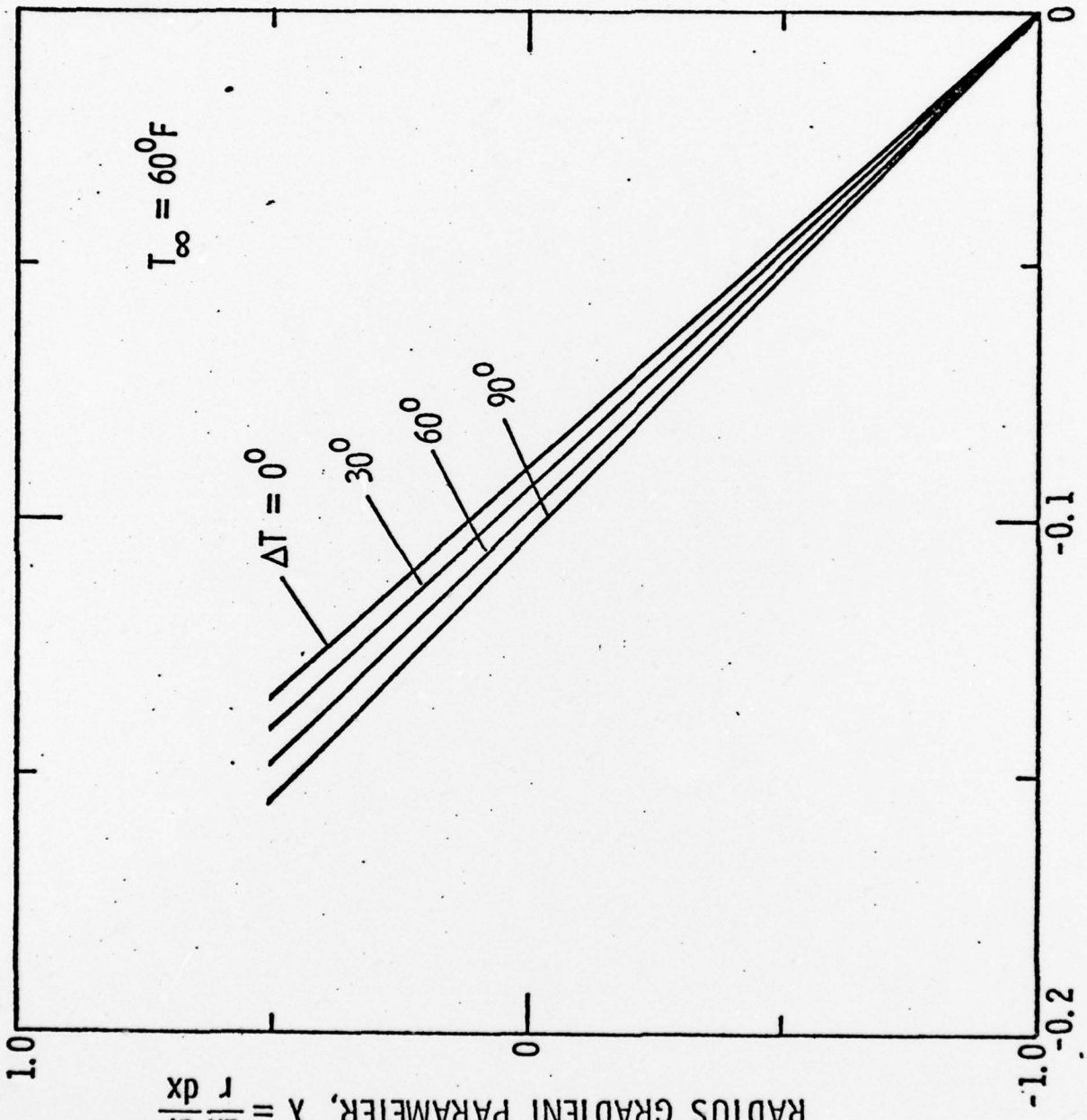

Figure 31 - Laminar Separation Limits

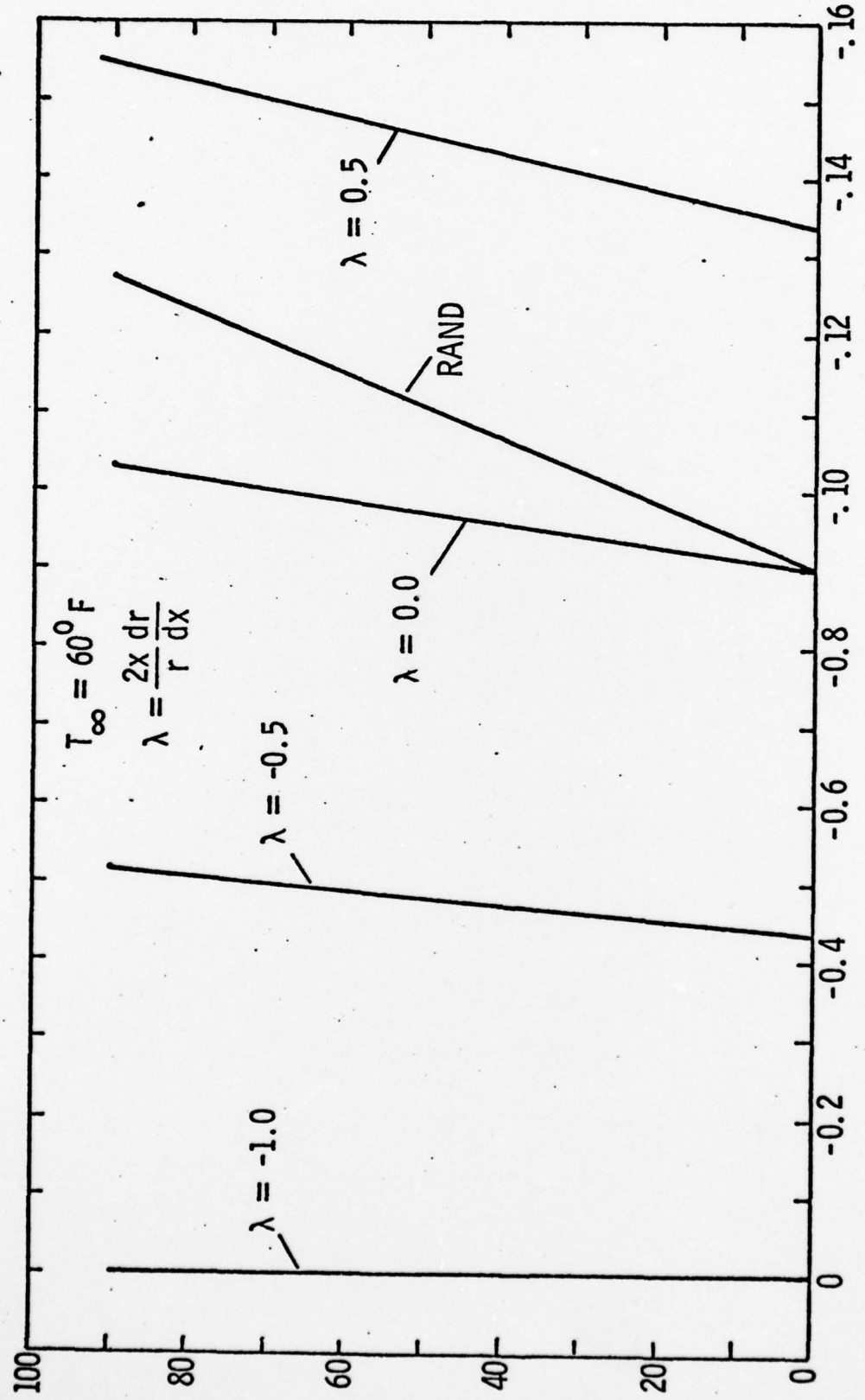

Figure 32 - Alternate Display of Laminar Separation Limits

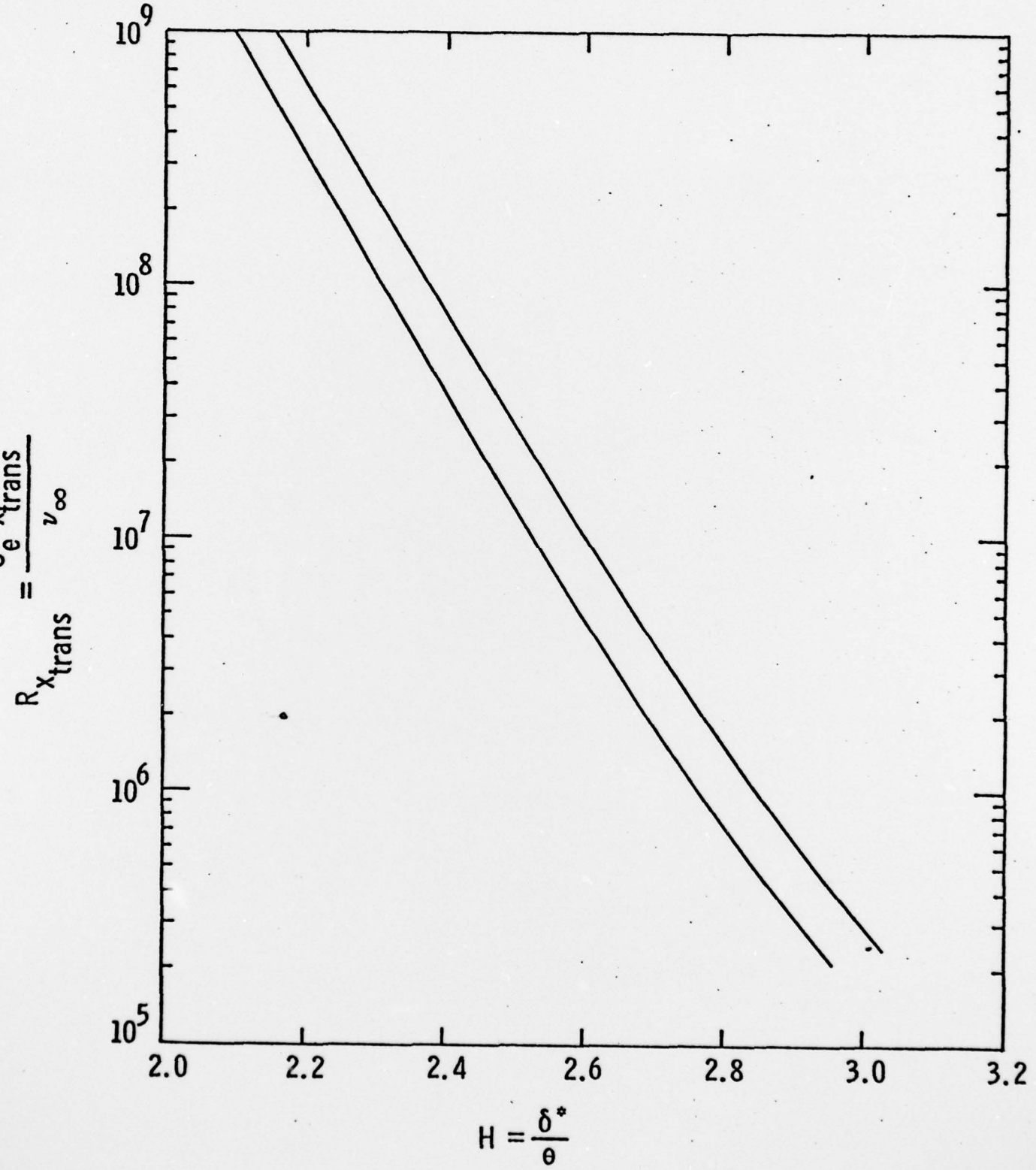

Figure 33 - Transition Reynolds Number Variation with H from e^9 Stability Calculations

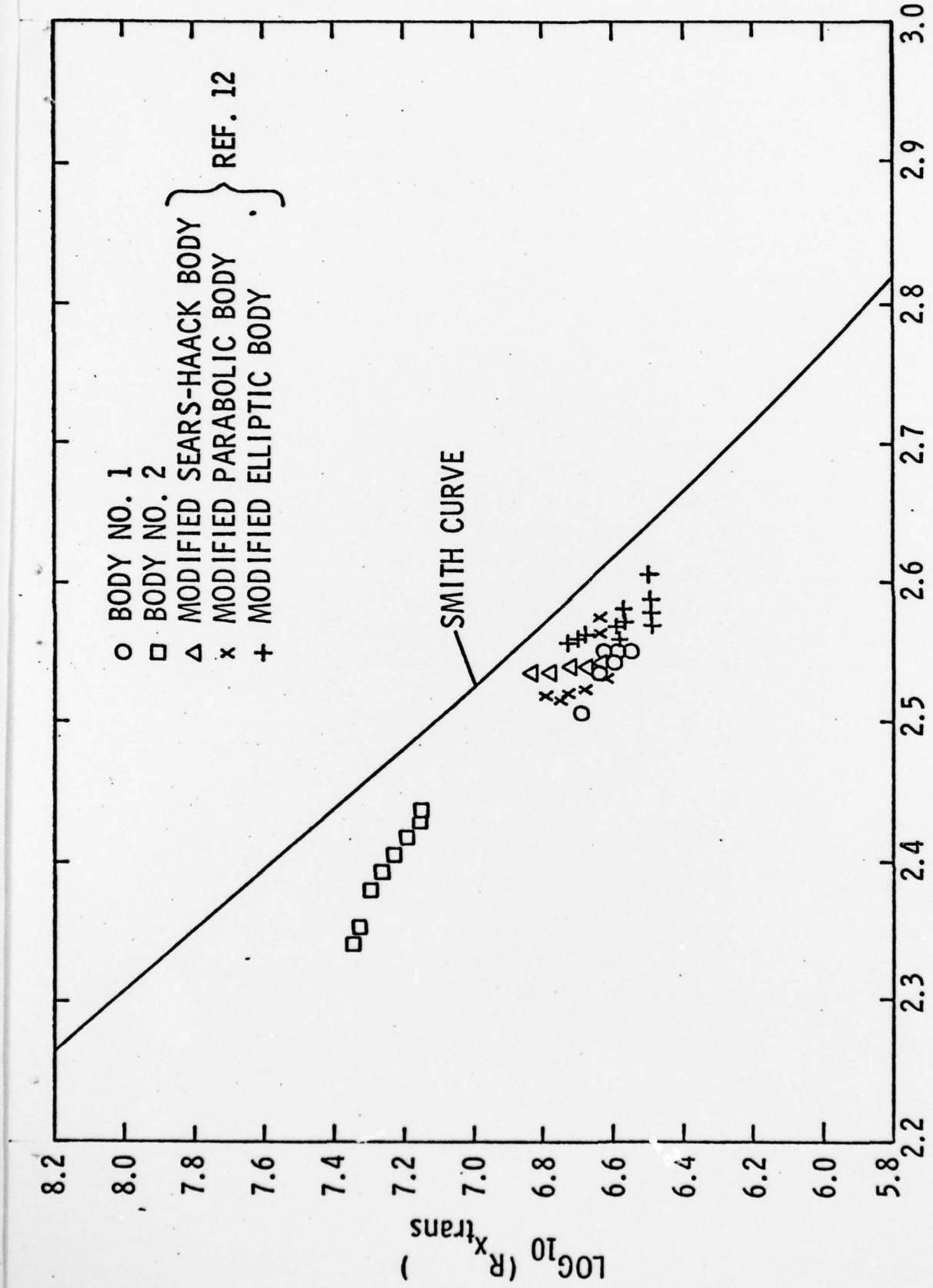

Figure 34 - Log Plot of Transition Reynolds Number Variation with Shape Factor

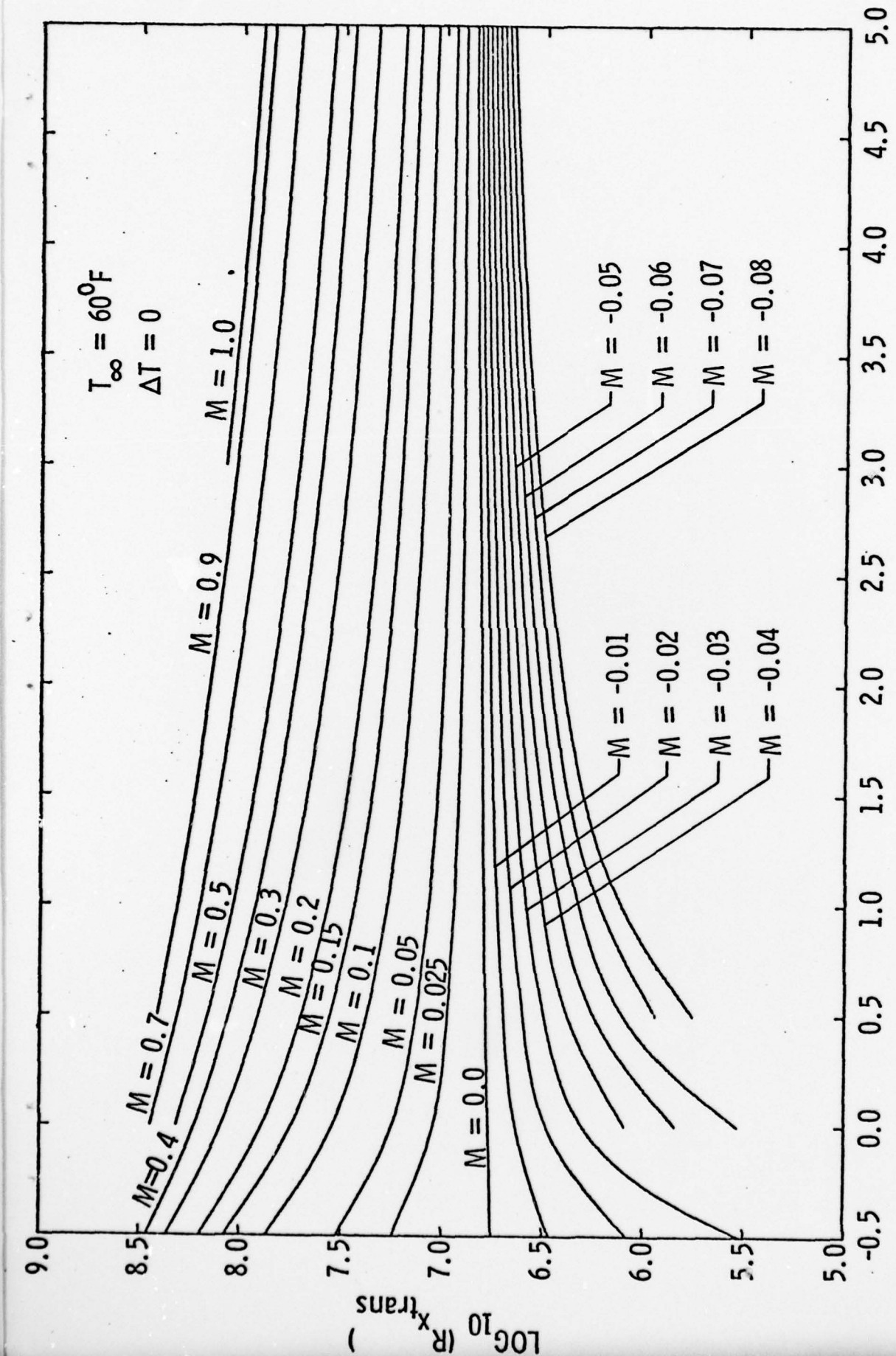

Figure 35 - Transition Reynolds Number Information for $\Delta T=0$

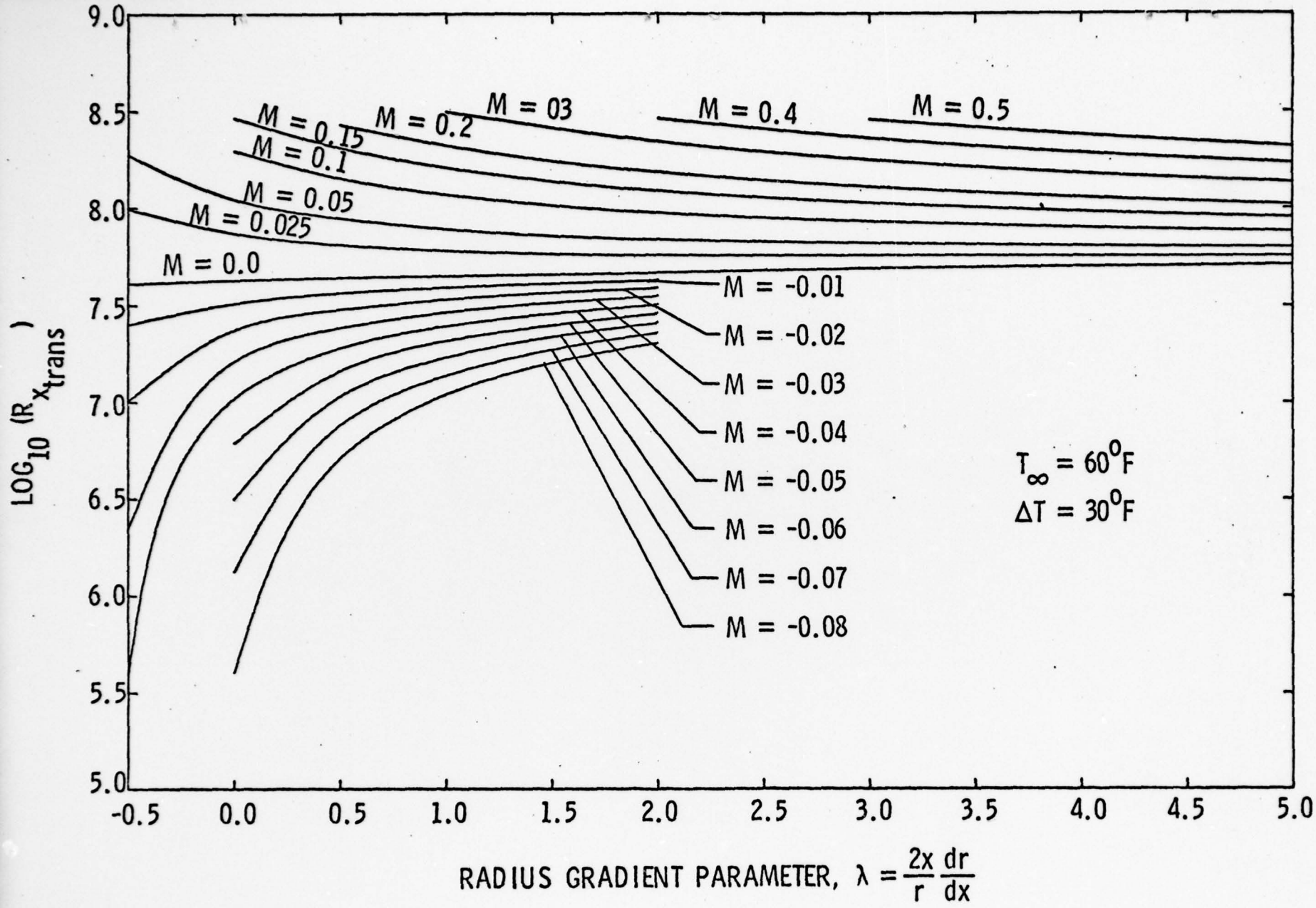

Figure 36 - Transition Reynolds Number Information for ΔT=30°F

22 February 1978
JJE:jep

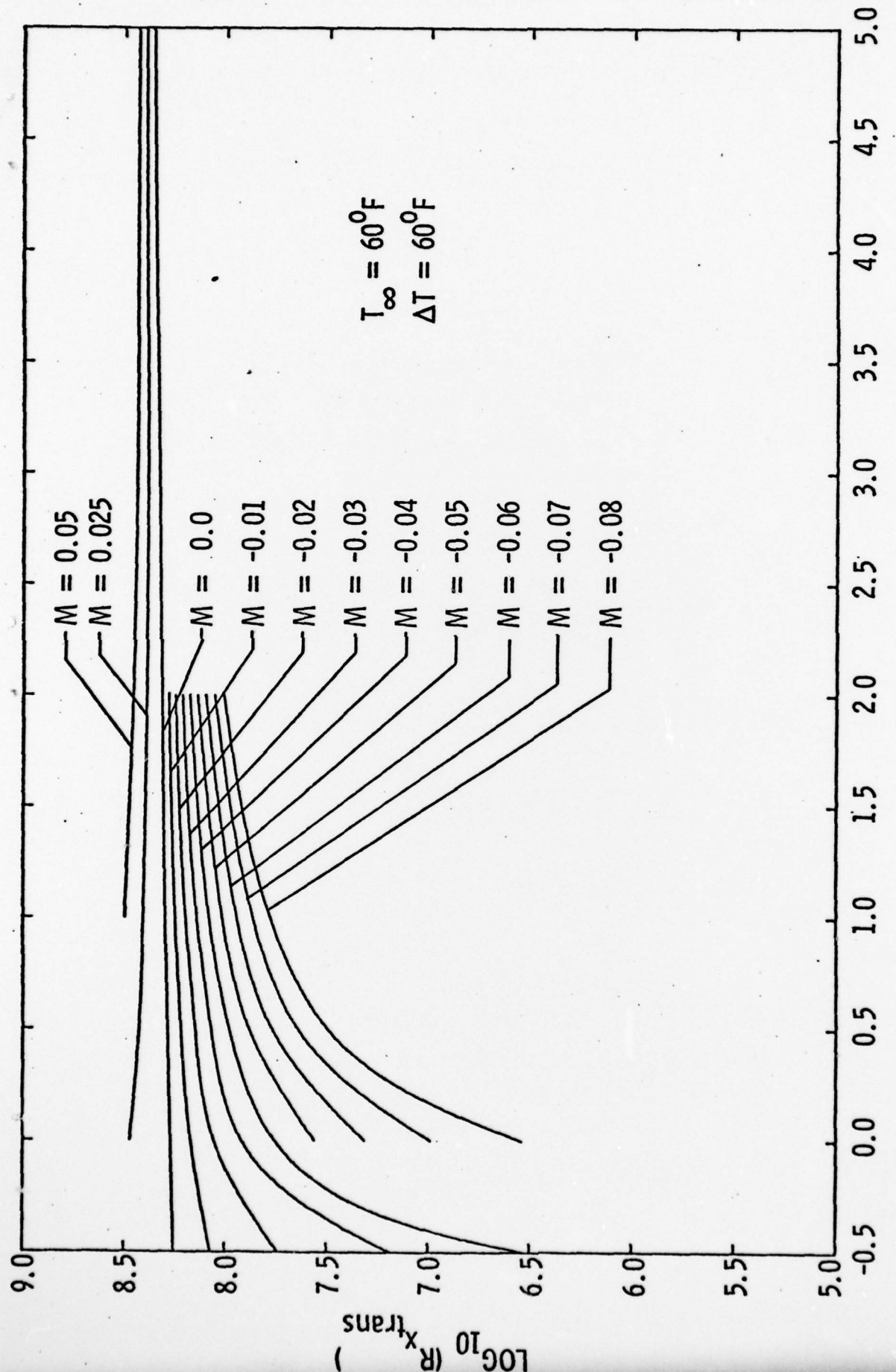

Figure 37 - Transition Reynolds Number Information for $\Delta T=60°F$

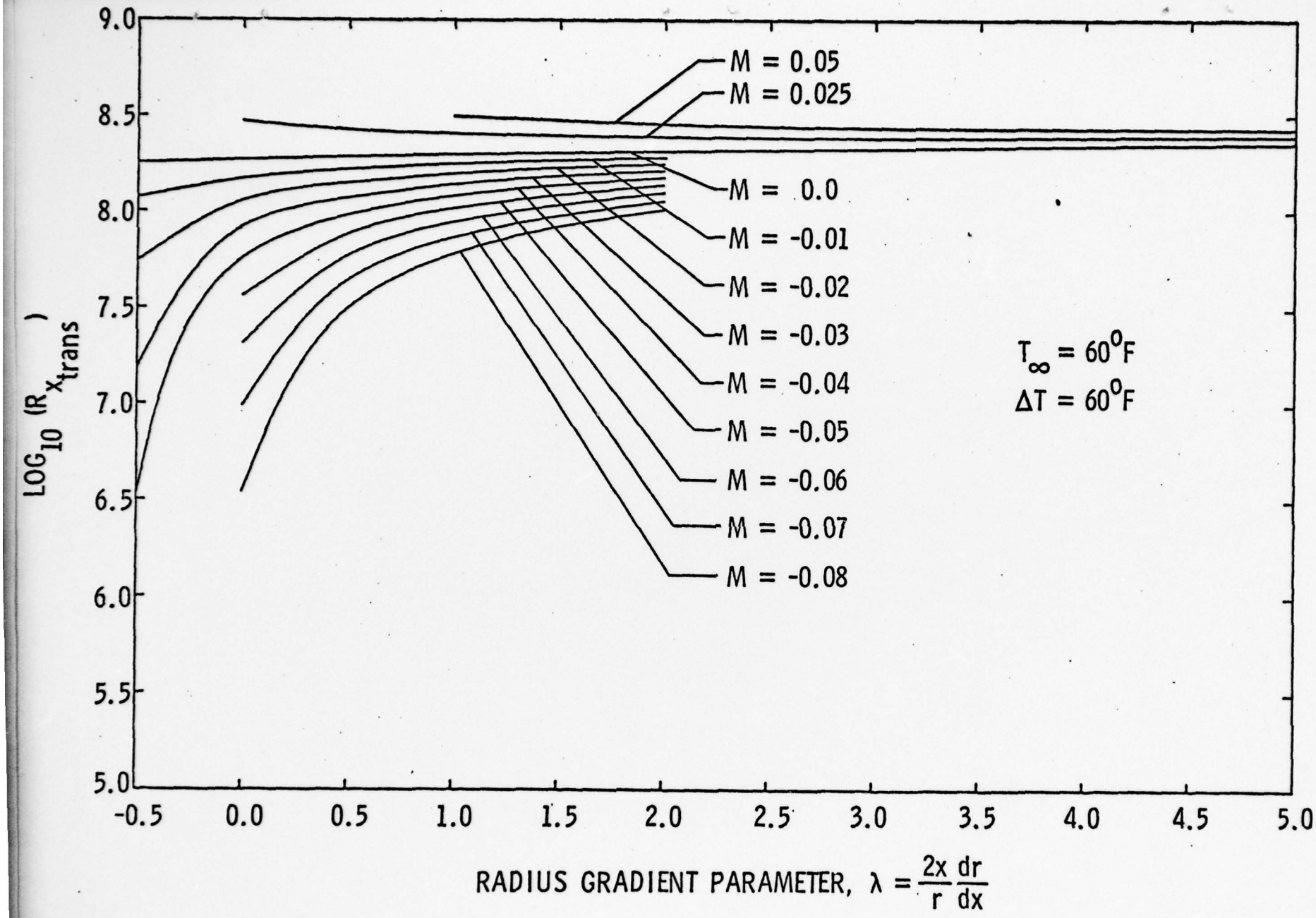

Figure 37 - Transition Reynolds Number Information for ΔT=60°F

22 February 1978
JJE:jep

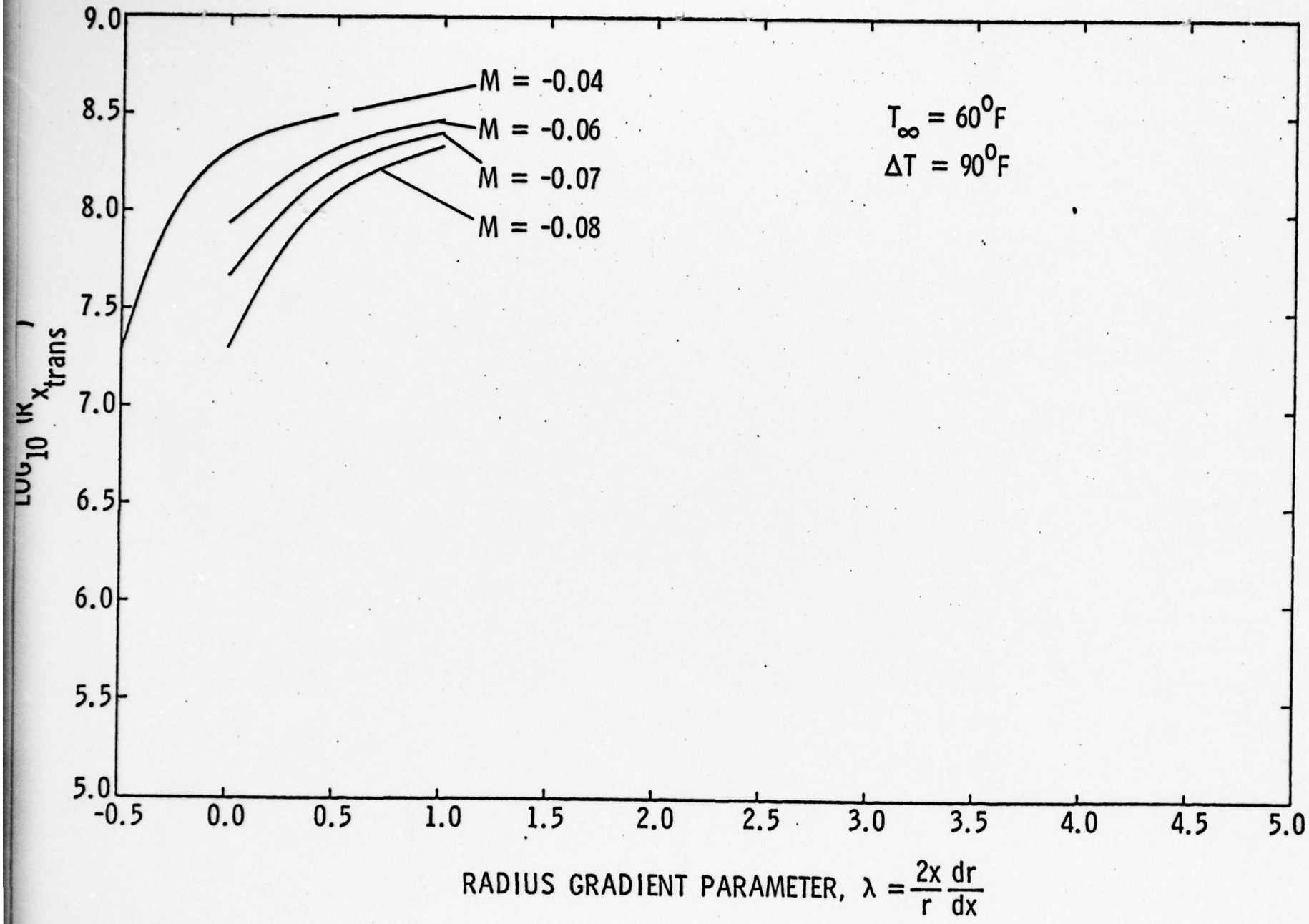

Figure 38 - Transition Reynolds Number Information for ΔT=90°F

22 February 1978
JJE:jep

APPENDIX A

Property Variation with Temperture for Water

Without getting into all the details of why, the formulation of the variation of the water properties with temperature by Touloukian and others (References 9 and 10) was used in Reference 4. It was judged the "best" from the standpoint of derivatives of these properties. Actually, for the free-stream properties, the fomulations by Kaups and Smith (Reference 11) were used. The option to use either of the above within the boundary layer is open in the program, but the equations of Touloukian and Makita were the ones used. The following are these formulations:

Specific Heat, C_p

$$C_p = 2.13974 - 9.68137 \times 10^{-3}\, T + 2.68536 \times 10^{-5}\, T^2 - 2.42139 \times 10^{-8}\, T^3 \qquad (1\text{-A})$$

C_p is in cal. g^{-1} $°K^{-1}$

T is in °K .

Density, ρ

$$\rho = 1 - \frac{(T-3.9863)^2\,(T+288.9414)}{508929.2\,(T+68.12963)} + 0.011445 \exp\left[-\frac{374.3}{T}\right] \qquad (2\text{-A})$$

ρ is in g/ml

T is in °C .

Dynamic Viscosity, μ

$$\log \mu = -1.64779 + \frac{262.37}{T-133.98} \qquad (3\text{-A})$$

μ is in cp

T is in °K .

Thermal Conductivity, k

$$k = -9.901090 + 0.1001982\ T - 1.873892 \times 10^{-4}\ T^2 + 1.039570 \times 10^{-7}\ T^3 \qquad (4\text{-A})$$

k is in m watts cm^{-1} $°K^{-1}$

T is in °K .

Unit Conversions

The following conversions are made so that the end quantities are in commonly used units:

$\rho \times 1.9409$ to get ρ in $slugs/ft^3$

$\mu \times (2.088 \times 10^{-5})$ to get μ in $lb/sec/ft^2$

$k \times (0.16933)$ to get k in watts/ft/°R .

DISTRIBUTION LIST FOR UNCLASSIFIED TM 78-39 by J. J. Eisenhuth, dated 22 February 1978

Commander
Naval Sea Systems Command
Department of the Navy
Washington, DC 20362
Attn: Library
Code NSEA-09G32
(Copy Nos. 1 and 2)

Naval Sea Systems Command
Attn: C. G. McGuigan
Code NSEA-03133
(Copy No. 3)

Naval Sea Systems Command
Attn: L. Benen
Code NSEA-0322
(Copy No. 4)

Naval Sea Systems Command
Attn: E. G. Liszka
Code NSEA-0342
(Copy No. 5)

Naval Sea Systems Command
Attn: G. Sorkin
Code NSEA-035
(Copy No. 6)

Naval Sea Systems Command
Attn: T. E. Peirce
Code NSEA-0351
(Copy No. 7)

Commanding Officer
Naval Underwater Systems Center
Newport, RI 02840
Attn: D. Goodrich
Code SB323
(Copy No. 8)

Naval Underwater Systems Center
Attn: R. Nadolink
Code SB323
(Copy No. 9)

Naval Underwater Systems Center
Attn: R. Trainor
Code SB323
(Copy No. 10)

Naval Underwater Systems Center
Attn: Library
Code LA15
(Copy No. 11)

Commanding Officer
Naval Ocean Systems Center
San Diego, CA 92152
Attn: J. W. Hoyt
Code 2501
(Copy No. 12)

Naval Ocean Systems Center
Attn: D. Nelson
Code 2542
(Copy No. 13)

Naval Ocean Systems Center
Attn: A. G. Fabula
Code 5311
(Copy No. 14)

Commander
David W. Taylor Naval Ship R&D Center
Department of the Navy
Bethesda, MD 20084
Attn: Tech. Info. Lib.
(Copy No. 15)

David W. Taylor Naval Ship R&D Center
Attn: W. E. Cummins
Code 15
(Copy No. 16)

David W. Taylor Naval Ship R&D Center
Attn: S. F. Crump
Code 1505
(Copy No. 17)

David W. Taylor Naval Ship R&D Center
Attn: J. McCarthy
Code 1552
(Copy No. 18)

David W. Taylor Naval Ship R&D Center
Attn: M. Sevik
Code 19
(Copy No. 19)

DISTRIBUTION LIST FOR UNCLASSIFIED TM 78-39 by J. J. Eisenhuth, dated 22 February 1978 (continued)

David W. Taylor Naval Ship R&D Center
Attn: P. S. Granville
(Copy No. 20)

Office of Naval Research
Department of the Navy
800 N. Quincy Street
Arlington, VA 22217
Attn: Ralph Cooper
(Copy No. 21)

Defense Documentation Center
5010 Duke Street
Cameron Station
Alexandria, VA 22314
(Copy Nos. 22 - 33)

National Bureau of Standards
Aerodynamics Section
Washington, DC 20234
Attn: P. S. Klebanoff
(Copy No. 34)

Rand Corporation
1700 Main Street
Santa Monica, CA 90406
Attn: R. King
(Copy No. 35)

Rand Corporation
Attn: C. Gazley
(Copy No. 36)

Jet Propulsion Laboratory
Pasadena, CA 01109
Attn: L. Mack
(Copy No. 37)

GTWT Library
The Pennsylvania State University
APPLIED RESEARCH LABORATORY
Post Office Box 30
State College, PA 16801
(Copy No. 38)

J. J. Eisenhuth
The Pennsylvania State University
APPLIED RESEARCH LABORATORY
Post Office Box 30
State College, PA 16801
(Copy No. 39)